DTIC FILE COPY

POR-2053(EX)
(WT-2053)(EX)
EXTRACTED VERSION

# OPERATION DOMINIC

## FISH BOWL AND CHRISTMAS SERIES

### Organizational, Operational, Funding, Logistic, and Scientific Summary

Deputy Chief of Staff
Weapons Effects and Tests
Field Command
Defense Atomic Support Agency
Sandia Base, New Mexico

DTIC
ELECTE
APR 2 9 1987
S D
D

30 December 1963

AD-A995 461

NOTICE:
This is an extracted version of POR-2053 (WT-2053), OPERATION DOMINIC, Fish Bowl and Christmas Series.

Approved for public release;
distribution is unlimited.

Extracted version prepared for
Director
DEFENSE NUCLEAR AGENCY
Washington, DC 20305-1000

1 September 1985

## ABSTRACT

During 1962, the Weapons Effects and Tests Group (WET), Field Command, Defense Atomic Support Agency, executed the Department of Defense (DOD) scientific programs of Operation Dominic, except those for Shot Sword Fish and the operational suitability tests of the Polaris system conducted by the US Navy.

The main WET effort was in the Fish Bowl Series, which consisted of five high-altitude nuclear detonations. The objectives included studies of weapons effects on rader and communications, changes in the ionosphere and the earth's magnetic field, and distribution of debris from the nuclear devices.

A further portion of the DOD effort was directed toward the Atomic Energy Commission tests on Christmas Island.

During the operational period of Operation Dominic, 4 April through 3 November, Task Unit 8.1.3 (the WET portion of Joint Task Force EIGHT) operated scientific stations throughout the Pacific area. Task Unit 8.1.3 was under the operational control of Joint Task Force EIGHT and received technical guidance from the Defense Atomic Support Agency.

The main objective of this report is to discuss the organizational, operational, funding, and logistic aspects of Task Unit 8.1.3 in Operation Dominic. The various scientific experiments are described under the general types of effects and phenomena studied. The results are discussed briefly; detailed discussions are available in the appropriate Project Officers Reports. In general, the data obtained was excellent.

Chapter 1

# INTRODUCTION

## 1.1 SCOPE OF REPORT

This report is a summary of the participation by Field Command, Defense Atomic Support Agency (FCDASA) in Operation Dominic, a joint Department of Defense-Atomic Energy Commission (DOD-AEC) operation held in the Pacific Ocean area during the period 1 May through 3 November 1962.

The operation was conducted by Joint Task Force EIGHT (JTF-8), initially under the command of Major General Alfred D. Starbird, USA, and later by Rear Admiral Lloyd M. Mustin, USN. During the operational period, the DOD scientific element, Task Unit 8.1.3, under the Weapons Effects and Tests Group, FCDASA, was commanded by Colonel Leo A. Kiley, USAF.

Although major portions of Dominic took place in both the Christmas and Johnston Island areas, the events at Johnston Island were the ones of primary interest to the DOD and were called the Fish Bowl Series. The events at Christmas Island were basically AEC events. The AEC also had a series of airdrops in the Johnston Island Danger Area. Two weapons tests by the Navy were included in Dominic; they were conducted in the ocean area between the United States and Christmas Island by JTF-8.

No attempt is made to include in this report detailed results of the DOD scientific effort; complete reports of the various scientific experiments may be found in the Project Officers Reports (POR's) listed in Appendix A.

This summary is written primarily to report the operational, support, and fiscal aspects of the operation, together with summaries of the scientific experiments and their results.

## 1.2 BACKGROUND

The culmination of the DOD-AEC efforts for the resumption of an atmospheric test program occurred on 10 October 1961 when the President approved the recommendations contained in a letter from the Secretary of Defense concerning nuclear testing. The primary recommendation was that approval be given the DOD and the AEC to prepare for atmospheric and high-altitude nuclear tests at suitable locations. Prior to this approval, neither the DOD nor AEC were authorized to plan or to prepare for atmospheric tests during the test moratorium. The Secretary of Defense on 12 October 1961 forwarded a memorandum to the Chairman of the Joint Chiefs of Staff (JCS) authorizing and directing certain actions pertaining to the planning and preparation for nuclear weapons testing in the atmosphere.

On 21 October 1961, the JCS implemented the program for the proposed weapons test plans and preparations and assigned the specific responsfbilities to the respective service organizations.

The specific responsibilities assigned to Chief, Defense Atomic Support Agency (DASA) were: (1) to plan and prepare experimental programs to include delivery means, for high-altitude effects tests, at an overseas location; (2) to plan experimental programs for nuclear weapons effects based on the possibility of continuing test programs; (3) to prepare to provide the necessary support to the AEC; and (4) to activate JTF-8 with the Commander to be designated by JCS.

At the National Security Council (NSC) meeting of 2 November 1961, appropriate decisions were made with regard to an atmospheric nuclear test program, and the implementation action was ordered. The JCS was directed to prepare to execute nuclear weapons tests operations in accordance with the recommended AEC-DOD program at an overseas site to commence in about 6 months (approximately 1 April 1962) and to be completed about 3 months thereafter (1 July). At this time, there was still no authority to conduct or execute an atmospheric test program. This specific authority had to be obtained from the President. On 29 November 1961, the NSC recommended to the President that a series of atmospheric nuclear tests be approved beginning in the spring of 1962. The President approved the NSC proposed list of atmospheric nuclear tests for the purpose of proceeding with preparations, but reserved judgment on the final decision for or against the resumption of atmospheric testing.

## 1.3 OBJECTIVES

As initially approved, the Fish Bowl Series was to be a high-altitude test program to be conducted at Johnston Island in the spring of 1962 (21 April through 1 July). It provided for: (1) Thor system proof test (nonnuclear), 1 May;

and (3) 1.45-Mt test at 400 km (Shot Star Fish), 15 June. The Thor missile was chosen as the carrier (Figure 1.1).

The purpose of the Fish Bowl Series was to satisfy JCS requirements for weapons effects data of the following general categories. The data sought from Shot Blue Gill included: (1) fireball transparency, growth, and rise; (2) intensity of beta and D-region ionization; (3) structural response to thermal radiation; and (4) radiation flux measurements. The data sought from Shot Star Fish included: (1) intensity and duration of ionization layers (fission debris and radiations), (2) radio and radar blackout areas (phenomenology of magnetic conjugate points), and (3) motion of debris pancake.

More specifically, the data sought concerned the following: (1) ICBM kill mechanisms and vulnerability, (2) penetration aids, (3) retaliatory force capabilities, (4) AICBM effectiveness, (5) early warning systems, (6) communications and control, (7) satellites, and (8) biomedical thermal responses.

In addition, information on physical aspects was needed to supplement the above data. This included: (1) debris location; (2) debris charge; (3) production and loss of electrons in the fireball; (4) production and loss of electrons in the ionosphere; (5) electromagnetic (EM) noise; (6) absorption and refraction of EM waves; (7) nuclear, thermal, and X-radiation outputs and damage mechanisms; (8) EM pulse output and damage mechanisms; and (9) ultraviolet through infrared radiation output, damage, and attenuation.

As explained in Section 1.4, the original shot schedule was changed.

TABLE 1.2 RECORDED STATISTICS FOR FISH BOWL EVENTS .

| Characteristics | Star Fish | Check Mate | King Fish | Blue Gill | Tight Rope |
|---|---|---|---|---|---|
| Altitude, km | 400.09 | | | | |
| Yield, fission/fusion, kt | | | | | |
| Shot Date, GMT | 9 July 1962<br>0900:09.0290Z | 20 October 1962<br>0830:00.0031Z | 1 November 1962<br>1210:06.1263Z | 26 October 1962<br>0959:48.4753Z | 4 November 1962<br>0730:00.0678Z |
| Geographic Coordinates * | 16° 28′ 06.32″ N<br>169° 37′ 48.27″ W | 16° 04′ 20.57″ N<br>169° 36′ 35.95″ W | 16° 06′ 48.61″ N<br>169° 40′ 56.02″ W | 16° 24′ 57.03″ N<br>169° 36′ 11.18″ W | 16° 42′ 26.71″ N<br>169° 32′ 32.66″ W |

Chapter 6

# SCIENTIFIC ACTIVITY

## 6.1 COMMUNICATIONS EFFECTS

6.1.1 Background. Shots Teak and Orange during Operation Hardtack, and the Argus shots of 1958, demonstrated that high-altitude nuclear explosions can significantly alter the electrical properties of large volumes of the atmosphere. High-energy radiation, subatomic particles, and high-speed debris particles may partially or completely ionize the air they penetrate. The ionization, in turn, may cause absorption and refraction of electromagnetic (EM) waves. Consequently, high-altitude nuclear detonations may have profound effects on the performance of radio communications systems.

Military communications systems use frequencies from VLF to UHF in a variety of propagation modes. Long-distance communications between surface stations and satellites or space vehicles must traverse the ionosphere and may be affected by ionization produced by high-altitude nuclear bursts. Even in the absence of nuclear burst induced disturbances, the changing nature of the normal ionosphere requires consideration of a number of factors such as modulation, power, antennas, noise, and operating frequencies to maintain communications efficiency. Artificially created anomalies in the ionosphere need not necessarily be large to have significant effects.

Electron densities in the ionosphere can be altered either because the total number of electrons present is changed, or because electrons already present are redistributed. Both types of changes are produced by nuclear detonations. Electrons are produced by ionizing emanations from the burst. In some cases, molecular species not normally present may be produced by the detonation, which subsequently leads to anomalous electron loss rates. Various types of traveling disturbances redistribute electrons at great distances from the burst point. Alterations in the ionospheric electron density were studied during Operation Dominic by riometers, ionosondes, and Granger sounders at stations throughout the Pacific during each of the events in the Fish Bowl series.

The Fish Bowl instrumentation to determine nuclear effects on communications covered all frequencies of military interest, but the effort was concentrated on the HF band. During Operation Hardtack, limited measurement indicated that severe communications blackouts existed for long periods after the detonation of Teak and Orange, both in the burst and magnetic conjugate areas. The data available consisted primarily of vertical-incidence soundings at a few points, backscatter soundings, riometer measurements, and magnetometer records. The only data of a real communications nature consisted of logs of various operational circuits. Analysis of these logs indicate that the communication circuits failed shortly after the detonations and remained unusable for many hours. Unfortunately, these records were made at only a few frequencies and without any special test instrumentation.

In the period after Hardtack, requirements for more rapid and precise evaluation of the propagation conditions existing on communications circuits led to the full development by Granger Associates of improved sounder equipment. The Granger oblique incidence, step-frequency sounder system employs a transmitter at one end of the communications path to

be studied and a receiver at the other end. The synchronized transmitter and receiver pair are electronically stepped through 160 channels (frequencies) in the band from 4 to 64 Mc in a time as short as 3.2 seconds. Pulses are transmitted on each channel, and the equipment is designed to permit a number of modes of operation by varying the pulses per channel, pulse repetition rate, and pulse width. A program control unit permits a network-type of operation in which a transmitter can serve more than one path, and a receiver can be associated with more than one transmitter.

The use of short pulses allows a determination of such characteristics as mode structure, signal strength, pulse distortion, and multipath propagation. The extremely short scan time permitted a nearly simultaneous study of all the frequencies in the band of interest.

Ionospheric vertical sounding techniques provided a vast amount of information on the structure of the ionosphere. Ionosondes measure the lowest frequency reflected from the ionosphere (f-min) and the critical, or maximum, frequency reflected at vertical incidence. The value of f-min is related to the amount of absorption in the ionosphere; as the absorption increases the minimum observable reflected frequency also increases. The critical, or maximum, frequency reflected at vertical incidence is a function of the electron density, increasing as the square root of the electron density.

The ionosonde is a radar-type instrument which transmits short pulses of RF energy directly overhead and receives echo returns from reflections in the ionosphere. Echoes occur from regions where electron densities are great enough to reflect the RF energy. Typically, the frequency is swept through the range of 1 to 25 Mc in about 15 seconds. Data is obtained by photographing the oscilloscope display of echo returns. This yields virtual height of the reflecting layer as a function of frequency.

6.1.2 Objectives. The primary objective of the communications-effects measurement program was to determine the effects of high-altitude nuclear explosions on communications performance at frequencies of military interest. Measurements to determine communications performance included: attenuation of signals, phase shift of signals, noise, propagation mode structure, multipath propagation, distortion, and ionospheric composition.

The secondary objective of the communications-effects measurement program was to obtain data of a scientific nature bearing on problems not yet clearly defined or of unknown military application. Data obtained will help assess the usefulness of various EM phenomena as detection tools and will help assess the high-altitude detonation as an aid in the study of upper atmospheric processes. Measurements made at ELF and sub-ELF (dc to 3 kc) are considered magnetic in nature for the purposes of this report and are covered in a later section. Table 6.1 lists the frequency bands of interest in military communications.

6.1.3 Instrumentation. VLF noise produced at about 5 kc is attributed to motion of particles released by a nuclear detonation. This noise peaks at 4 to 5 kc and is known to be enhanced during periods of magnetic disturbances. AFCRL (Project 6.5a) operated 5-kc receivers on Samoa, Johnston Island, Ship S-5, Palmyra, Kauai, Canton, and Tongatabu (Tonga).

The EM pulse generated by the detonation was measured by broadband receivers on Johnston Island, Hawaii, Palmyra, and Ship S-3. This pulse peaks at a few kilocycles. Instrumentation included two underwater trailing antenna installations on Navy ships operated near Oahu (Shot Star Fish only). The underwater measurements were obtained to provide information on indirect bomb damage assessment (IBDA) useful to submarine commanders. This project (7.1) was primarily interested in the atmospheric shots at Christmas Island but did obtain data during Star Fish.

VLF propagation instrumentation is shown in Table M.1. Much research has been performed to establish VLF for worldwide communications and as a navigational aid. Fish Bowl instrumentation consisted primarily of receivers and on-site frequency standards (stability of a few parts in $10^{10}$ per day) to monitor existing VLF transmitters. Measurements of noise, signal strength, and phase changes yield information on the amount and arrival time of D-layer ionization induced by the high-altitude nuclear bursts. Information on service-sponsored measurements using existing operational circuits is not included in this report.

LF propagation instrumentation is shown in Table M.2.

No special instrumentation was fielded for MF measurements. Military operational circuits in this band include the worldwide Loran navigation system (1800 to 2000 kc).

HF propagation instrumentation is shown in Table M.3.

VHF/UHF propagation measurements were made by Project 7.4 using a KC-135 and a B-47 to form a line-of-sight communications link between Johnston Island and Hickam AFB.

HF sounders used during Fish Bowl are listed in Table M.4. These sounders were operated for several weeks before Star Fish and before the events in October and November 1962, to obtain background data.

6.1.4 VLF Results. The high-altitude events of Fish Bowl were not effective in producing significant degradation of VLF communications. However, all events produced a pronounced change in phase of the received signal and some change in amplitude over certain paths. Both absorption and signal enhancement were noted. The change in phase is associated with the decrease in D-layer height, the decrease generally being limited to a reduction in height from 90 km to about 70 km. Typically, the phase of the received signal advanced several hundred degrees shortly after burst. The effects at VLF from the Fish Bowl type of events are most significant if phase information is being used, such as in certain navigational systems.

6.1.5 LF/MF Results. Significant localized effects on both phase and amplitude were noted on LF and MF bands. MF sky modes were generally lost on propagation paths crossing the burst or conjugate area; ground waves were not affected.

On Star Fish, LF and MF circuits crossing the burst auroral regions were unusable for one to several hours. By H+2 hours about half of the circuits were usable, but none of the circuits were completely back to normal until the following night. The 76-kc circuit from Johnston to Hickam was out from H+0 to H+2 minutes. The 46-kc circuit from an aircraft south of Johnston Island was usable after burst at a somewhat reduced signal strength (antenna arced over at burst time for 1 to 2 seconds, cutting off transmission).

Check Mate produced effects at LF and MF, which were very similar to those produced by Star Fish. Loran-C signals (100 kc) through the burst region and passing as far north as French Frigate Shoals showed immediate loss of signal, which lasted for several minutes. Some phase shift problems existed for about 1 hour.

King Fish and Blue Gill produced outages of the Loran-C signal on north-south paths for several hours with King Fish somewhat more effective than Blue Gill. The effects produced on other LF and MF circuits were less pronounced than for Star Fish.

Tight Rope produced no significant effects in the LF and MF bands.

6.1.6 HF Results. At HF, the ionospheric absorption, traveling disturbances in the F-region, synchrotron noise, and spurious reflections affect communication circuits.

However, actual circuit outages due to the events were less extensive and of shorter duration than had been anticipated. The use of oblique sounder technique, which can rapidly identify usable frequencies and optimum routing, can to a large extent overcome the effects noted after the Fish Bowl types of bursts. Data obtained during Fish Bowl will permit a refinement of ionospheric reaction rates, which may permit better scaling of communications effects from nuclear detonations.

The HF blackout problem, however, has not been resolved by the Fish Bowl tests; changes in weapon orientation, use of multiple bursts, detonations under daytime conditions or at extreme altitudes (above 1,000 km) may well induce alterations to the ionosphere sufficient to blackout HF communications for thousands of miles for many tens of minutes after burst.

Star Fish blacked out HF communications circuits for 1 to 4 minutes through the burst and conjugate regions. Attenuation was noted in both magnetic conjugate areas for 12 hours. One path, Kauai to Midway, was affected for 2 days. Star Fish caused frequency selection problems, but did not seriously degrade communications effectiveness.

Check Mate effects resembled those of Star Fish, but were greatly scaled down in spatial extent. Only paths within 700 km of Johnston Island were significantly affected.

The effects from King Fish were delayed up to 1 hour on some paths. Immediate attenuation was noted on signal paths within 2,500 km of Johnston Island, but severe attenuation was limited to paths within 500 km of the burst point. F-layer depletion in the northern area started at H + 25 minutes and resulted in poor communications for the rest of the night.

Blue Gill and Tight Rope produced significant effects at HF only, on paths through the burst region. Unlike Star Fish, Check Mate, and King Fish, no bomb-created modes of propagation were observed. In summary, from an HF communications standpoint, the effects of Blue Gill and Tight Rope were minor.

6.1.7 VHF/UHF Results. Line-of-sight propagation paths that did not cross the D-layer (or the fireball) were not affected by the Fish Bowl events. The aircraft UHF communications link between Johnston and Hickam AFB suffered no degradation from any of the shots. The DCA Midway to Kauai ionospheric scatter circuit (53 Mc) was adversely affected for 21 minutes by King Fish, 30 seconds by Star Fish, and 20 minutes by Check Mate.

6.1.8 Ionosonde Results. Prompt absorption effects were observed at all ionosonde stations following Star Fish, Check Mate, King Fish, and Blue Gill. These events also caused traveling disturbances in the F-region over a large portion of the Pacific Ocean. Tight Rope produced no noticeable effects except at the ionosonde located at Johnston Island.

The changes in the ionosphere resulting from Star Fish were greatest at stations located near the magnetic meridian passing through the burst point. The greatest duration of total blackout, approximately 85 minutes, occurred at French Frigate Shoals. Following this total blackout, a large amount of absorption persisted for several hours, and only weak echoes from the F-region were observed.

At Tonga and at the north conjugate point near French Frigate Shoals, an extended period of blackout was also observed following Star Fish. At H + 51 minutes, weak returns from high in the F-region were observed. The value of f-min at H + 80 minutes was near 8 Mc, decreasing to 2 Mc at H + 3 hours, a value only 1 Mc above preshot conditions.

At Tutuila (Samoa), very dramatic ionospheric effects were also observed after Star Fish. Total blackout lasted only for a few seconds. The value of f-min, although exceeding 12 Mc for a short time, did not cause a blackout beyond the initial 6 seconds as critical frequencies in the F-region increased concurrently to values greater than the 20 Mc (upper limit of the ionosonde); thus, communications circuits having reflection points in this region would have suffered only temporary interruption. The value of f-min dropped very rapidly from the initial high value to within 1 Mc of its preshot value by H+10 minutes. The critical frequency, however, remained very high. It is interesting to note that the ionization created over Tutuila following Star Fish was on the order of 4 times the maximum value that exists at noon on a normal July day. The increase of F-region critical frequency from 4 Mc to more than 20 Mc indicates a greater than 25-fold increase in electron density.

Star Fish produced perturbations in the ionosphere in the equatorial region over Canton Island which, while significant, were much less than observed at other ionosonde stations along the magnetic meridian. Blackout occurred for only a little over a minute after burst. No F2-layer effect was observed until about H+7 minutes, when the critical frequency began to increase, rising to a value of 11.5 Mc at H+20 minutes. This increase of critical frequency corresponds to an increase in electron density of more than 2.5 times that which existed prior to the detonation.

The effects observed at Maui, Midway, Kwajalein, and Wake were smaller in magnitude than at the stations discussed previously.

At Johnston Island, Star Fish caused complete absorption for several minutes. At H+24 minutes, a new layer formed, which had a critical frequency range of 10 to 15 Mc at heights from 400 to 550 km. A considerable spread effect was noted. The layer density increased with time, and the highest frequency was greater than 25 Mc; f-min was observed to be 5 Mc. At sunrise the following morning, f-min remained at a higher-than-normal value. The F-layer critical frequency was considerably lower than normal.

Check Mate, King Fish, and Blue Gill caused prompt absorption effects at all ionosonde stations. These events also produced traveling disturbances in the F-region over a large portion of the Pacific Ocean. The delayed effects noted were greatest following King Fish, but these were still considerably less than the effects noted after Star Fish. The overall effect of Check Mate and Blue Gill tended to be about equal. However, the principal traveling disturbance was located higher in the ionosphere (mainly above the peak electron density of the F-region) for Check Mate than for Blue Gill. Following King Fish, daytime f-min was higher than normal at Maui, French Frigate Shoals, Tutuila, and Tonga. Blue Gill was followed by abnormally high daytime f-min at French Frigate Shoals, Canton, Tutuila, and Tonga. On Johnston Island, complete blackout was observed for 45 seconds after Check Mate, 2 hours after King Fish, and 3 hours after Blue Gill. Blackout on Johnston Island was followed by abnormally high f-min and critical frequency for the remainder of the nights following these three events.

Tight Rope produced effects detectable only in the Johnston Island area.

## 6.2 RADAR EFFECTS

6.2.1 Background. One of the more significant military effects of nuclear detonations at high altitudes is the degradation of radar system performance. Experimental data is urgently needed to design defense systems which will be effective (in a nuclear environment) against ballistic missiles. Information gained on the defense problem is applicable to the complementary offensive problem of ballistic missile penetration. Present and

proposed defense systems require radar early warning, acquisition, discrimination, and high-precision target tracking on incoming reentry vehicles.

The detonation of nuclear devices at high altitudes produces complex phenomena dependent not only on yield, altitude, and fission-to-fusion yield ratio, but also upon weapon orientation, burst location with respect to the earth's magnetic field, and the time of day. The ionizing radiation and ionizing particles from the detonation produce wide-scale effects. In addition, the fission products are a significant continuing source of ionization that remains effective for many hours.

Typically, radar search systems operate in the UHF band (300 to 3000 Mc) and tracking and guidance radars in the lower part of the SHF band (3000 to 10,000 Mc). Even short periods of degradation of these frequency bands induced by high-altitude nuclear bursts may seriously affect system performance. Degradation of surface and air search radars whose propagation paths do not traverse the ionosphere can result from backscatter and EM noise produced by a nuclear detonation.

6.2.2 Objectives. The general objective of the radar measurements program was to obtain data on the magnitude, duration, and spatial extent of burst-induced EM noise, radar clutter, signal refraction, and attenuation at commonly used radar frequencies.

RF noise is an important parameter in any radar system in that it determines the minimum signal that can be detected, and hence, the maximum range of detection for a given target. The objective of the noise measurement program was to determine the EM energy incident upon radiometer antennas on Johnston Island and on the USAS American Mariner (DAMP ship).

The objective of the clutter measurement program was to assess the military significance of the radar reflection phenomena of high-altitude nuclear detonations. Specifically, the objective was to determine, as a function of time, the strength, position in space, and variation as a function of frequency, of the radar reflections associated with the burst region, auroral display occurring in the magnetic conjugate areas, and tube of ionization passing overhead at the magnetic equator.

Following a high-altitude nuclear explosion, the refractive index of the atmosphere is modified by the sudden increase in air temperature and by the change in the density and distribution of electrons. This may cause the paths followed by EM waves to differ from those in the normal atmosphere. Also, the apparent angle of arrival of the return signal may fluctuate, because the signal crosses regions of time-varying refractive index, so that tracking would be extremely poor or even impossible. Both of these effects were investigated on paths through and near the burst region, and on paths through other regions of high electron density, at frequencies of 1000 to 10,000 Mc.

The objectives of the attenuation measurements program were to measure: (1) one-way attenuation of CW RF signals at 1000, 5000, and 10,000 Mc through the fireball and its near vicinity as a function of time, (2) one-way attenuation of a C-band (5775 Mc) signal through the burst region and through other regions of high electron density as a function of time, (3) attenuation of RF signals passing through the D-, E-, and F-layers of the ionosphere at selected frequencies between 37 and 1800 Mc as a function of time and space, (4) electron line density as a function of time and space, and (5) electron density as a function of time and space.

6.2.3 Instrumentation. Burst-induced radar noise was measured during all five Fish Bowl events by the instrumentation listed in Table N.1. The location of the DAMP ship for each event is shown in Appendix D.

Radar clutter was observed during all five Fish Bowl events by the instruments listed in Table N.2. The ships and aircraft carrying clutter instrumentation are also listed in Table N.2. Figure 6.1 is a photograph of the 86-foot-diameter antenna at Johnston Island, used by SRI in Project 6.9.

Radar refraction and refractive jitter were measured on all five Fish Bowl events by the instrumentation listed in Table N.3. Figure 6.2 is a photograph of the DAMP ship. Rocket-firing schedules for Projects 6.1 and 6.13 are given in Appendix F.

Attenuation at radar frequencies was measured directly on all five Fish Bowl events by instrumentation listed in Table N.4. The location of ships used as receiving stations is shown in Appendix D. The general experimental plan for obtaining data on attenuation is shown in Figure 6.3.

Measurements of electron line density and electron density were accomplished by instrumentation listed in Table N.5. Figure 6.4 is a photograph showing four Project 6.13 Nike-Apache rockets equipped with C-band beacons on Johnston Island. Figure 6.5 is a photograph of the Project 6.1 shipboard antenna system.

6.2.4 Results, Noise. The data obtained on the Fish Bowl events is adequate to determine directly the amount of noise injected into radar and communications antennas by such bursts. The function of altitude and yield in determining the amount of radar interference may also be deduced from the data. A typical radar receiver with a noise figure of 3 db corresponding to internal noise of 290° K would be subjected to a 30-fold increase in the noise background level for a short time by the Check Mate burst. On the other hand, Star Fish produced only a small amount of noise jamming. Further analysis of the radiometer data will permit calculations of: added noise arising from the burst region, attenuation through the fireball, temperature of the fireball, and electron density in the disturbed region.

The highest antenna temperatures were observed for Check Mate, with a maximum of 9,000° K at S-band. Smaller antenna temperatures nearly proportional to the burst altitudes were measured for King Fish, Blue Gill, and Tight Rope. As expected, the duration of the signals was shortest at $K_a$-band (35,000 Mc) where the average duration was 30 seconds. The excess antenna temperatures at S- and L-bands lasted approximately 10 times as long as those at $K_a$-band. The peak temperatures did not appear to be a strong function of the weapon yield as had been previously expected.

Selected raw data on maximum excess temperature is tabulated in Table 6.2. This data has not been corrected for the burst size relative to the antenna beam size. The approximate duration of the excess temperature is shown in Table 6.3.

Such increases in noise can degrade radar performance. The actual reduction in signal-to-noise ratio for any particular radar system requires a detailed analysis of the individual system characteristics.

6.2.5 Results, Clutter. A very good correlation was found to exist between the spatial extent of radar clutter from the burst region and the visual effects. Table 6.4 shows the duration of this clutter as measured by SRI on Johnston Island. Star Fish produced no significant burst region clutter and is not included in the table.

The DAMP ship also obtained data on burst region clutter at C-, L-, and UHF-bands.

The SRI radar on Johnston Island observed echo signal-to-noise ratios considerably in excess of 30 db (echoes were saturated). These echoes were observed on radars with sensitivities of about 40 db less than the sensitivity of radars planned for use in ballistic missile defense applications. Thus, the echoes observed would be seen with signal-to-noise ratios in excess of 70 db on future ballistic missile defense systems radars and

would make it difficult to track a reentry vehicle in the burst region. In addition, these echoes are sufficiently intense to be seen in the side lobes of such radars when tracking targets outside the burst region.

A preliminary investigation of the echo amplitude characteristics showed that the burst area echoes at all three frequencies saturated to some degree within the first 60 seconds. The onset of echoes usually occurred a few seconds after burst; absorption at very early time was sufficient to black out any echoes. For Blue Gill, the 1210-Mc echoes first appeared at H+3 seconds, the 850-Mc echoes appeared at H+5 seconds, and the 398-Mc echoes appeared at H+8 seconds.

The existence of radar clutter from the vicinity of high-altitude nuclear detonations has now been established. Previous effects tests and predictions have suggested that such burst-region clutter might be seen, but the fact that it was seen so early and for so long a time is of great importance to ballistic missile defense radar design.

Energetic beta particles and ionized debris, confined by the geomagnetic field, travel to the conjugate points producing radar clutter, auroras, and absorption in those areas as they reenter the atmosphere. Extensive field-alined radar clutter from Teak and Orange was observed during Hardtack. Much of this bomb-produced clutter is believed to be due to ionization that becomes alined with the earth's magnetic field into long columns, which scatter anisotropically. Field-alined ionization is by no means the entire story; absorption, localized debris cloud, shock waves, and other traveling disturbances complicate the picture so that no single radar location, or single frequency, is adequate to separate the effects observed and to resolve the uncertainties. During Fish Bowl, long-lasting, field-alined auroral clutter was observed in both the Northern and Southern Conjugate Areas after Star Fish, Check Mate, and King Fish.

The ionospheric clutter formed in the Southern Conjugate Area was found to be quite restricted in spatial extent at early times. To observe this clutter, the radar must be directed to a point approximately 75 km in altitude and down range sufficiently to look perpendicular to the field lines. The clutter area appears to expand after tens of seconds, and at late times can become quite widespread. Observations in the Southern Conjugate Area indicate that a systematic error exists between the conjugate point calculated using Finch and Leaton coefficients (Monthly Notices, R. Astron. Soc., Geophys. Sup., Vol. 7, pp 314-317, 1957) for 48-term expansion of the magnetic field and the observed conjugate point. This error is about $\frac{3}{4}°$ latitude from the true conjugate point located south of the calculated point. No error in longitude was noted.

The field-alined clutter in the Northern Conjugate Area was observed for several hours after Star Fish, Check Mate, and King Fish. Echoes at 400 Mc persisted considerably longer than at the higher frequencies. The overall significance of this clutter in relation to ballistic missile radar systems must await further data analysis.

The Canton Island 27-Mc radar received echoes from the tube of ionization and/or debris connecting the burst region and the magnetic conjugate region on all tests except Tight Rope.

6.2.6 Results, Refraction. A very considerable body of data on refraction of radar signals was obtained by Projects 6.1 and 6.13. Much more data reduction and analysis is required to assess the significance of refraction and refractive jitter measured during Fish Bowl. Figure 6.6 shows the periods of time around H-hour during which rocketborne beacons and transmitters were aloft and operating. No gross refraction of radar signals was readily apparent from a preliminary analysis of the data. However, it appears that refractive jitter may be a severe problem under some conditions. On Blue Gill, Project 6.13 encountered severe angular jitter between H+318 seconds and H+348 seconds and

actually lost track due to jitter at H+546 seconds. On King Fish, track loss at H+321 seconds has been tentatively attributed to angular jitter.

Initial radiations from high-altitude detonations caused widespread ionization for 1 to 2 seconds, which induced tracking scintillations at a frequency as high as 20 cps. This prompt effect adversely affects radar tracking capability and makes target discrimination more difficult. Effects at later times depend upon the location of debris and other regions of intense ionization.

6.2.7 Results, Attenuation. Radar signals from rocketborne transmitters also provided one-way path attenuation information during the periods of time around H-hour shown in Figure 6.6. Test results indicate that the fireball is opaque to radar frequencies for 40 to 60 seconds after burst. Figure 6.7 is an example of the type of data obtained. The figure shows the AGC (automatic gain control) record obtained on Ship S-3 during Blue Gill for X-, C-, and L-band frequencies. The rocketborne CW transmitter from which the data was obtained was launched from Johnston Island at H−112 seconds. As viewed from Ship S-3, the transmitter was behind the fireball at burst time and remained behind the fireball for at least 150 seconds.

Star Fish was not effective in degrading radar system performance. No intensive absorption of the type that would affect radar propagation persisted for more than a few seconds. No debris pancake was formed. There were no intense clutter effects at radar frequencies.

No fireball attenuation measurements were made on Check Mate. The burst-produced ionization did not prevent track of a C-band beacon by Project 6.13, but careful data analysis will be required before extrapolation can be made to other frequencies and other types of tracking systems. Radio noise and long-lasting UHF auroral clutter tentatively appear to be more effective in degrading radar than attenuation at the Check Mate yield and altitude.

The King Fish burst would have caused considerable reduction in sensitivity of any radar attempting to track a target through the fireball region. At L-band, the attenuation would have been in excess of 114 db for 16 seconds decreasing to 30 db between H+16 and H+39 seconds. The actual reduction in overall defensive effectiveness would depend critically upon the actual radar. The King Fish burst also produced a beta patch that may have remained stationary for as long as 30 seconds before moving northward. Severe attenuation through this beta patch at both C- and L-bands was observed for 40 seconds after burst. It is concluded that the occurrence of a King Fish burst in the locale of a ballistic missile defense radar would seriously degrade its performance for appreciable lengths of time.

The most serious effect of Blue Gill was the fireball blackout. X-band attenuation exceeded 30 db for 40 seconds with recovery at H+80 seconds; C-band attenuation was greater than 52 db for 40 seconds with recovery at H+90 seconds; L-band attenuation exceeded 47 db until H+65 seconds with recovery at H+10? seconds. In addition, gamma-, X-ray-, and beta-induced ionization produced blackout outside of the fireball, which caused very large L-band attenuation until H+60 seconds to distances of 15 to 20 km from the fireball center. A more extensive ionized region out to at least 50 km caused severe attenuation at 37 Mc for more than 30 minutes. It is difficult to imagine a ballistic missile defense system in which such performance degradation could be tolerated. The Blue Gill burst, in addition to causing fireball blackout, also degraded radar performance by producing extensive long-lasting radar clutter (to H+25 minutes at UHF), by causing angular tracking errors, and by producing an increase in background noise.

The Tight Rope detonation produced a well-confined fireball that was opaque to radar frequencies. Strong reflections from the fireball were observed for 4 minutes after burst.

Fireball attenuation is most difficult to determine without extensive data analysis because of the tight geometry associated with the small (0.7-km radius at 10 seconds) fireball, but it is known that X- and C-band frequencies were blacked out or highly attenuated on paths through the fireball for 7 to 17 seconds after burst. Severe L-band attenuation through the fireball is believed to exist for times up to 1 minute after burst. There is not enough information yet available to translate these times into a solid angle of the absorbing region, but the absorption is certainly sufficient in both time and space to be of some concern to ballistic missile defense radars.

## 6.3 DEBRIS HISTORY

6.3.1 Background. The dispersion of nuclear debris deposited in the upper atmosphere as a result of a high-altitude detonation depends markedly upon the height of burst. Debris distribution will be affected by the magnetic field, high-altitude winds, and diffusion processes. It is useful to determine the location of this debris as a function of time in order to arrive at a better understanding of the phenomena of high-altitude detonations and their effects. In addition to direct measurements, the location of debris may be inferred from effects measurements obtained by such instruments as vertical and oblique sounders, riometers, and clutter radars. Photography and spectroscopy also yielded data bearing on debris history; the data is presented in Section 6.6.

Project 6.7 rocketborne magnetometers, beta detectors, mass spectrometers, gamma detectors, faraday cups, and photometers gathered information on early debris history in the immediate burst region. Project 6.5b balloonborne gamma and neutron detectors made measurements in the Southern Conjugate Area. Gamma detectors in aircraft mapped debris in the burst and conjugate regions. Optical resonance scattering techniques were used by Project 6.6 for detection and tracking of debris at selected Pacific sites, and Project 6.12 satellite observations attempted to perform a worldwide survey for evidence of fission debris.

Following the radiative phase of a nuclear detonation, about 25 percent of the bomb yield remains in the form of hydrodynamic energy of the debris. The debris then expands until brought to rest by the surrounding medium. For lower altitude shots, the fireball and debris rise and expand. The hydrodynamic streaming of the air around the fireball causes an upwelling of air at the bottom of the fireball that eventually converts it into a toroid. This interaction imparts a lateral velocity to the fireball, and the debris is spread out horizontally. For higher altitude shots, radioactive decay of the fission debris provides relativistic electrons, which may be guided to the opposite hemisphere by the geomagnetic field. Those beta rays that mirror at altitudes above about 200 km will drift eastward. However, because of the scattering at the mirror points, betas may drift only a short distance to the east before they are removed.

The low atmospheric density at the altitude of Star Fish permitted the debris to expand to great distances. At early times, the primary interaction was with the geomagnetic field. If the debris is highly ionized, it excludes the magnetic field from its interior as it expands, forming a bubble in the magnetic field. The larger the fraction of debris that is ionized, the greater the energy available to interact with the magnetic field and the larger the bubble. As the magnetic pressure outside the bubble increases, the ionized portion of the debris is slowed and finally stopped when the magnetic pressure equals the material pressure. The neutral portion of the debris is not affected by the magnetic field and continues to expand.

The high-altitude Fish Bowl shots provided an opportunity to verify experimentally (or refute) various theoretical models of detonation phenomenology as related to the ultimate fate of the debris.

6.3.2 Objectives. The objectives of the debris measurements program were to determine: (1) interaction of the debris with the geomagnetic field, (2) state of ionization of the debris as a function of time, (3) flux of gamma and beta radiation from the debris as a function of time, (4) extent of electron trapping by the geomagnetic field, (5) location of the debris as a function of time, (6) density of selected nuclear debris constituents over a wide geographical area as a function of time, (7) processes (i.e., diffusion, magnetic guiding, wind transport, turbulence) that act to distribute the debris and the relative importance of each, (8) amount of ionized debris guided to the conjugate area by the geomagnetic field and the debris arrival time, (9) ion density by species in the burst region, and (10) intensity and spectral distribution of aurora.

6.3.3 Instrumentation. The instrumentation employed to determine debris history is listed in Table 6.5.

The Project 6.5b balloonborne gamma detectors and neutron counters were released from Samoa and from a ship in time to drift to the approximate conjugate point and be at 100,000-foot altitude at burst time. Preburst flights were made to obtain background data; postburst flights were also made to determine long-term effects.

Project 6.5b photometric and photographic instrumentation consisted of six tricolor photometers, five all-sky cameras, two time-of-arrival photometers, two camera spectrographs, and two 35-mm cameras.

Project 6.6 used both birefringent and four-barrel interference photometers. In both types of instruments, photomultipliers with high cathode efficiency and filters were used. Four-barrel photometers were used at Johnston Island and on Ships S-2 and S-4; birefringent photometers were located on Ship S-1, French Frigate Shoals, Tutuila, and Tongatabu.

The Project 6.10 gamma-ray spectrometer was installed in the project KC-135, which operated in the Southern Conjugate Area at an altitude of about 40,000 feet. At this altitude, the atmosphere above the aircraft causes 5 to 10 scatterings of gamma rays in the 0.5- to 1.0-Mev energy range. Gamma rays in the 4- to 5-Mev range undergo only two or three scatterings with much less degradation of energy. Suitable calculations are required to properly interpret the measured energy spectrum.

Project 6.8 used riometers to measure ionospheric absorption and synchrotron radiation. The riometer, or relative ionospheric opacity meter, was originally developed for the International Geophysical Year (IGY) by Little and Leinbach at the Geophysical Institute, College, Alaska. Riometer stations operating at frequencies of 20, 30, 60, and 120 Mc were established at various distances and directions from ground zero. Other stations were located about the conjugate points. Twenty-two sites (Table 6.5) were chosen for riometer locations. Following installation, in May 1962, the equipment was kept in continuous operation so that typical quiet-day curves for each area could be obtained. By measuring the intensity of cosmic noise received at the earth's surface with riometers, the variations in ionospheric absorption at various frequencies with respect to time after detonation and distance from burst point could be determined.

Project 6.7 launched five rockets for Star Fish and two for Check Mate to study magnetic containment of debris. Trajectories for the Star Fish rockets are shown in Figure 6.8 and listed in Table 6.6. All project rocket payloads were identical. The complete payload weighed 433 pounds and was 26 inches in diameter and 52 inches long. Instrumentation in the payload is listed in Table 6.7. Data was telemetered to receiving stations on Johnston Island, Canton, French Frigate Shoals, Oahu, and Hawaii.

Projects 6.2 and 6.3 launched rockets from Johnston Island during Star Fish, King Fish, and Blue Gill. Project 6.4 had instrumentation in some of the rockets for Star

Fish and King Fish. The rocket-firing schedules and types of measurements are given in Appendix F.

Project 6.12 attempted to investigate the spread of fission debris around the earth with specially designed research packages on Discoverer satellites. Because of the schedule slippages encountered in attempting the nuclear detonations, the project was not able to obtain data during the time of primary interest.

6.3.4 Results, Shot Star Fish. The Star Fish debris was not confined locally, and there are indications that more than half of the debris was ultimately deposited in the Southern Conjugate Area. The initial expansion of the debris had a velocity asymmetry of about 3 to 1 with the initial velocity being about 2,000 km/sec horizontally and about 700 km/sec vertically. The initial excursion of the debris in the downward direction was less than 200 km. The Project 6.2 gamma ray scanner was not able to map the burst region debris contours, because the detectors were saturated by bremsstrahlung radiation. Project 6.6 photometers observed lithium at all stations. Stations in the Johnston Island area noted a maximum concentration of lithium during the first twilight. At Tutuila, the maximum concentration of lithium was observed during the third twilight. Barium, ionized barium, and zirconium were detected only from Johnston Island and the close-in stations. Reduced concentrations of debris were measured during the 2 weeks following the event. The data obtained will permit a calculation of specie density contours.

Gamma ray mapping by U-2 aircraft several hours after burst indicated that the debris concentration in the Northern Conjugate Area was 10 times greater than in the burst region. A gamma ray counter in the Project 6.10 aircraft in the southern area indicated that the debris was centered about 200 miles west of the true conjugate point and that about 50 percent of the Star Fish fission debris was deposited in the southern hemisphere. The debris appeared to have a very sharp northern boundary and a diffused southern boundary. The Project 6.5b balloonborne gamma ray detectors obtained data that, on preliminary analysis, indicates that substantially more than half of the Star Fish debris was deposited in the Southern Conjugate Area.

Riometer records following Star Fish are difficult to interpret because of synchrotron radiation. In general, noise exceeded the attenuation at riometer stations within 20° of the magnetic equator; varying amounts of attenuation were observed elsewhere. Some debris did remain below the burst, with a maximum density at about 300-km altitude at about H+25 minutes. Very little debris was below 150-km altitude at this time. This shows that, at least in the downward direction, very little debris became neutral at early times. A nonuniform pattern of debris below the burst point is indicated by a second maximum in attenuation measured at several riometer stations. This debris could be toroidal in shape with a radius of about 150 km.

The geographical distribution of delayed attenuation is consistent with containment of charged debris by the geomagnetic field, yielding areas of strong attenuation at each end of those field lines passing through the burst point. These areas were about six times longer along the magnetic field than across it. The attenuation observed in Alaska indicated that an appreciable fraction of the debris must have risen to several thousand kilometers above Johnston Island. However, there is no indication that a significant quantity of debris escaped from the earth.

Synchrotron radiation showed that an artificial belt of electrons, trapped in the magnetic field, was produced by Star Fish. There was an intense burst of synchrotron noise, peaking within 5 minutes after detonation, detected at sites along the magnetic field line within 23° from the magnetic equator. About 25 percent of the electrons producing noise in this burst made at least one drift around the world. There was a second maximum in

noise that followed the first maximum by 22 to 23 minutes. A third maximum was detectable on several riometers. At Huancayo, Peru, the fourth maximum was also observed. This indicates that the electrons remained partially bunched for several passes around the world.

6.3.5 Results, Shot Check Mate. The initial size of the Check Mate fireball remained nearly constant for several minutes after the detonation. After the initial fireball formation, the fireball rose as a whole and elongated along the magnetic field. The debris rose to approximately 250-km altitude and spread into long streamers along the magnetic field, slowly forming an arc that stretched all the way between the conjugate points. The main part of the northward-moving debris stopped within a few minutes. The debris also drifted eastward as a unit with a velocity of 100 to 150 km/hr for the first few hours. An estimated 5 percent of the debris was deposited in the Southern Conjugate Area.

Photometers on Johnston Island detected ionized barium from 180-km altitude down to about 100 km. Below 100 km, the barium had probably recombined. Neutral barium, lithium, and zirconium were also detected at Johnston Island. No debris was detected by photometers in the Southern Conjugate Area. At the second twilight (H + 21 hours), ionized and neutral barium were still present at Johnston Island; however, there had been a marked decrease since morning, and at succeeding twilights all species were below threshold.

Immediate attenuation was observed by the riometer stations within 900 km of Johnston Island and by the M/V Acania at the southern conjugate point. Delayed attenuation was experienced at stations in the burst area and along the magnetic meridian north of the burst point. The delayed attenuation at Ships S-4 and S-7 and the DAMP ship is consistent with what would be expected from fission debris rising to an altitude of 200 to 300 km. The DAMP ship riometer noted the beta patch sweeping across the antenna as the debris rose. Except for the immediate attenuation noted by the Acania, no southern hemisphere riometers observed effects from Check Mate.

Trapped beta electrons from the Check Mate burst were very quickly lost by collision. Riometer stations along the magnetic meridian through the detonation point recorded excess noise for a short time. However, no synchrotron radiation was noted at Christmas Island, Palmyra, or any station to the east of the detonation.

6.3.6 Results, Shot King Fish.

By 90 seconds, the fireball was primarily growing along the magnetic field lines. Early instabilities in the expansion were not apparent, and no jetting of debris occurred.

Riometers observed immediate attenuation in the northern region between Johnston Island and French Frigate Shoals. Delayed attenuation measured at riometer stations north of the burst point is consistent with a rising debris cloud that deposited debris along geomagnetic field lines above an altitude of 350 km. The decrease of attenuation is very closely proportional to $t^{-1.2}$, indicating that the debris did not continue to expand. The bulk of the fission debris was deposited at the base of those magnetic field lines lying between 400- and 700-km altitude above ground zero. Riometer records also indicate a low-lying debris region (100- to 150-km altitude) containing perhaps 10 percent of the debris that expanded to a radius of about 200 km within 15 minutes.

The gamma ray counting rate as measured by the U-2 aircraft at H + 6 hours was greater by a factor of 40 at French Frigate Shoals than at ground zero. Measurements

of gamma ray intensity in the southern hemisphere indicate that only a very small fraction of the fission debris was deposited in the Southern Conjugate Area.

No significant quantity of long-lived betas were trapped in the geomagnetic field. The artificial electron belt loss rate was exceedingly high. Peru recorded an increase in noise of 10 percent above background at H+11 minutes, but there is no indication of further eastward movement of the belt.

6.3.7 Results, Shot Blue Gill. The behavior of the Blue Gill fireball was reasonably consistent with preshot predictions. Initially, a well-defined fireball was formed, which grew to a radius of several kilometers in a few seconds.

A luminous cloud, presumably the bomb debris, was observed within the fireball. This cloud rose relative to the fireball as a whole, eventually pushing through the top of the fireball and spilling down the sides. Still later the cloud evolved into a torus which continued to rise to an altitude of about 80 km, at which time vertical motion ceased.

The debris from Blue Gill was contained by the atmosphere, with late-time motion being determined primarily by wind patterns, and with no significant influence by the magnetic field. The debris moved at a velocity of about 100 km/hr, on a heading of approximately 70°. No neutrons, delayed gamma rays, or resonant scattering from debris were detected in the southern hemisphere, indicating that all the debris remained in the burst area as was anticipated. The balloonborne gamma detectors in the Southern Conjugate Area did observe a sharp increase in background count, but the energy distribution indicates that this count is due to bremsstrahlung from betas. Birefringent photometer data from Ship S-1 (located in the Johnston Island area) shows that there was a very small trace of ionized barium and a small amount of neutral lithium from 130 km down to 90 km at the first morning twilight. At the second twilight, a reduced amount of lithium was observed. No other photometer stations detected any debris.

At Johnston Island, riometer measurements were made on 30, 60, and 120 Mc. The maximum attenuation observed was 15 db. The attenuation decreased to 7.8 db at about H+7 minutes. A further slight decrease in attenuation to about 7.6 db occurred between H+7 and H+13 minutes, after which it increased to 7.8 db by about H+20 minutes. After H+50 minutes, the attenuation decreased monotonically to 3 db at about H+85 minutes. Recovery was complete by H+4.5 hours.

Similar results were observed on 60 Mc, where the maximum attenuation observed was 18 db. The initial fast recovery rate lasted until H+3 minutes, when the attenuation had fallen to 6.5 db. A minimum of 3.2 db was observed at H+7 minutes. An increase to 4.8 db followed, and the attenuation remained at this value until H+32 minutes, when recovery began. By H+45 minutes, the attenuation had fallen to 3 db, and the return to normal was completed by H+3.5 hours. The maximum attenuation observed on 120 Mc was about 2 db. This had decreased to 1 db by H+5 minutes, and then slowly decreased to an unmeasurable value by H+65 minutes.

The initial blackout and relatively fast recovery appear to be caused by prompt gamma-ray ionization, together with a contribution from prompt neutrons and beta rays. The decrease in rate of recovery probably corresponds to the onset of a significant beta-ionization contribution. As the debris cloud spreads and covers a greater fraction of the riometer antenna pattern, the observed attenuation tends to increase. At the same time, the overall beta activity is decreasing as $t^{-1.2}$, tending to decrease the attenuation. For a while, the opposing tendencies nearly balance, and the attenuation remains essentially constant. Finally, the beta-ionization region has completely covered the antenna pattern, and the attenuation decreases with the decaying beta activity.

Riometers aboard Ships S-1 through S-4, located near ground zero, observed effects very similar to those on Johnston Island. In the Southern Conjugate Area, no attenuation was observed at any site except at Samoa, and on the ships Acania and Hifofua. The Acania reported prompt 100-percent absorption on 30 Mc with recovery to 3 db by H + 2 minutes. The prompt blackout was probably caused by Compton electrons following the field lines to the conjugate point. Ships S-6, S-7, and S-8, located 420 to 485 km north of the burst point, observed prompt attenuation of 8 to 3 db at 30 Mc but no delayed attenuation. French Frigate Shoals, at 875 km from the burst point, was the most distant station to report any prompt attenuation. The fact that no delayed attenuation was observed on the DAMP ship (135 km north of ground zero) until H + 60 minutes supports the conclusion that the debris did not go much above 100 km.

Blue Gill produced no trapped betas and so no synchrotron noise.

6.3.8 Results, Shot Tight Rope. The Tight Rope debris was contained locally. The fireball formed a torus between 10 and 20 seconds

The fireball rose to a maximum altitude of 30 to 40 km. Soon after this, the debris location was governed by the atmospheric mass motions. By H + 3 to H + 4 hours, the debris was still over Johnston Island with a windblown tail at 270° true. By H + 18 hours, the debris had been blown 500 km at about 290°. By D + 1 day, the debris had settled well into the atmosphere, probably at an altitude lower than that of the burst point.

Photometric observation of resonant scattering was made from Ships S-1, S-2, and S-4, and at Johnston Island, Tutuila, Tonga, and French Frigate Shoals. No debris, not attributable to the previous King Fish event, was detected. A balloonborne gamma ray detector in the Southern Conjugate Area detected no effects.

Riometer stations within 10 km of ground zero observed immediate attenuation of 3 to 6 db at 30 Mc. Immediate attenuation was observed out to 100 km but not to 200 km from ground zero. The Acania riometer, in the conjugate area, noted an immediate 1-db attenuation at 30 Mc, presumably caused by neutron decay electrons and Compton electrons guided to the area by the magnetic field. No other riometer stations in the southern hemisphere detected any effects. Delayed attenuation due to debris-induced ionization was recorded by stations near the burst point. Recovery to normal background occurred within 10 minutes.

## 6.4 WEAPON OUTPUT AND KILL MECHANISMS

6.4.1 Prompt Neutron Measurements. Measurement of neutron fluxes from high-altitude detonations was first attempted during Operation Hardtack; however, equipment problems limited the data obtained. The Fish Bowl Series presented an opportunity to measure prompt neutron flux and spectrum close to high-altitude bursts using a proven detector system.

The objective of Project 2.1 was to measure neutron flux as a function of distance from high-altitude nuclear detonations.

The instrumentation consisted exclusively of the Nuclear Defense Laboratory (NDL) threshold detector system. This system consists of a series of materials activated through capture of, or fission by, neutrons with energies above a threshold energy, as listed in Table 6.6.

It should be noted that $U^{236}$ and $Pu^{239}$ do not possess natural thresholds; however, by the use of a $B^{10}$ shield, an artificial cross section can be produced. Four complete

detector systems were located on the backplate of each of the three pods flown on Thor Fish Bowl events. After recovery, the neutron packages were removed from the pods as soon as possible and taken to a project mobile laboratory for analysis. Scintillation counting techniques were used to measure activities induced in the various detector materials from which the exposure fluxes were calculated.

Table 6.9 presents the data on the average neutron flux measured. The Star Fish pod at 8.4 km had an orientation nearly nose-on to the burst with the mass of the pod interposed between the detectors and the burst. On King Fish, only the detectors from the close-in pod were recovered.

Neutron flux measurements for Star Fish, Blue Gill, and King Fish must be considered successful, although shielding factors caused by pod misorientation complicated final data corrections.

6.4.2 Prompt Gamma Measurements. Early predictions of the effects of nuclear weapons detonated at high altitude led to gamma measurements during Operations Teapot and Hardtack. Since these operations, considerable interest has been generated in the effects of prompt radiation from high-altitude bursts on the guidance systems and electronic components of missile weapons systems.

The objective of Project 2.2 was to measure total gamma radiation dose as a function of distance from high-altitude nuclear detonations.

Gamma dose measurements used the following techniques: (1) darkening of photographic film, (2) photoluminescence phenomenon of silver phosphate glass, (3) production of hydrogen and carbon dioxide in an oxygen-saturated aqueous formic acid solution, (4) optical density change in cobalt-activated borosilicate glass, and (5) thermoluminescence of manganese-activated calcium fluoride.

Three different film emulsions, covering the general range from 0.1 rad to about $5 \times 10^4$ rads, were exposed in National Bureau of Standards (NBS) film holders. The use of the NBS film holder essentially eliminated energy dependence from the film measurements. Film calibrations and data readout were accomplished by the U. S. Army Signal Corps.

The range of the glass microdosimeters (glass rods) was extended, by appropriate heating and readout techniques, to approximately $1 \times 10^6$ rads.

Radiolysis of formic acid exposed in transparent quartz ampoules produced hydrogen, hydrogen peroxide, and carbon dioxide. Determination of the molecular product yield provided the information necessary to calculate the gamma dose.

The cobalt-activated borosilicate glass, on exposure to radiation, was pronouncedly darkened. The amount of change in absorption at 360 microns gave direct readings of gamma dose when compared to plates previously calibrated.

After exposure to radiation, the thermoluminescent calcium fluoride detector, upon heating, emitted light which was measured by a photomultiplier tube. A plot of the luminescence versus temperature at a constant heating rate, compared to calibration plates, provided the gamma dose.

All detectors required neutron dose corrections.

Three detector packages were placed in each pod for each event. The detector package was mounted to the pod substructure approximately 18 inches below the backplate.

Table 6.10 presents the available data. The Star Fish Prime data is difficult to interpret and correct, because pod misorientation presented many unknown shielding factors. The center-position pod on King Fish was not recovered. The formic acid dosimeters provided no reliable gamma dose data because of dose rate dependence. The calcium

fluoride thermoluminescent dosimeters, exposed in Star Fish, provided measured doses generally high compared to other systems. This difference is not fully explained but is believed to be due to dose-rate dependence.

The project must be considered to have accomplished its objective. The gamma flux on Star Fish Prime was lower than predicted. This low flux cannot be explained at present. On future tests, placement of the gamma dosimeters near the exterior of the vehicle would minimize the dose correction problems imposed by pod or instrument mass shielding. It appears that further development is required to obtain dose-rate dependence information and neutron interaction information on present dosimeters and to develop new measurement systems.

6.4.3 Alpha Contamination Monitoring. Following the destruction, on the launch pad, of the Blue Gill Prime missile and warhead, a project was instituted to provide an accurate monitoring of the alpha contamination occurring downwind from any future similar incidents.

The objective of Project 2.3 was to determine the alpha hazard following the destruction of a missile-mounted warhead in the vicinity of the missile launch pad.

The instrumentation consisted of two systems, one for gross plutonium contamination and the second for plutonium particle size analysis. The gross detection system utilized four collection methods: (1) 12- by 6-inch concrete blocks, (2) staplex high-volume air samplers, (3) cyclone air samplers, and (4) cellulose acetate sticky paper. The particle size determination system used four-stage cascade impactors to separate particles into four size ranges and passive collectors consisting of silicone-resin-coated microscope slides.

Both Thor missile pads, both Nike-Hercules launchers, and the XM-33 launch pad were instrumented with both land and downwind waterborne arrays. Around the Thor pads, the land arrays consisted of three arcs, each containing 88 concrete monitoring blocks, 44 microscope slides, 8 sticky paper samples, and 4 staplex air samplers. The small rocket land arrays each had two arcs containing 39 concrete monitoring blocks and 39 microscope slides. The water arcs, for all events, consisted of an arc of six rafts anchored approximately $\frac{1}{2}$ mile downwind from the launch pad. Each raft was equipped with an electric generator, one cyclone air sampler, two concrete blocks, two microscope slides, one staplex air sampler, one cascade impactor, and one sticky paper sampler. All electrically operated equipment (cascade impactors, staplex and cyclone air samplers) were activated by tone barrel relays 60 seconds prior to lift-off. The cascade impactors operated for a period of 5 minutes after lift-off and the air samplers for a period of 30 minutes after lift-off.

During the period this project was operational, only the Blue Gill Double Prime missile was destroyed. This destruction occurred approximately 90 seconds after lift-off and at an altitude of approximately 100,000 feet. As a result, no data was obtained by the project.

6.4.4 Reentry Vehicle Kill Mechanisms. There have been postulated five possible kill mechanisms for use against ICBM warheads: (1) crushing or breaking up of the reentry vehicle (R/V) because of blast, (2) neutron heating and consequent melting of the fissionable materials, (3) ablation of surface materials of the R/V by vaporization and/or melting to the point where the R/V cannot survive reentry, (4) thermomechanical loading generated by the pressure of the vapor generated when the R/V surface is exposed to short-time thermal radiation from an intermediate altitude detonation, and (5) X-ray-

induced impulsive loading of the R/V structure by the pressure of the vapor generated at the R/V surface by absorption of X-rays from a weapon detonated in near-vacuum conditions.

The primary objective of the pod program in Fish Bowl was the investigation of the ablation, thermomechanical, and X-ray kill mechanisms. Previous attempts to evaluate kill mechanisms, on Shot Logan at the Nevada Test Site (NTS) and during Operation Hardtack in the Pacific, had produced little data. Shot Marshmallow, at NTS, was successful in investigating X-ray effects. No previous tests have been performed to investigate the thermal kill mechanism. Blue Gill, provided the opportunity to evaluate the thermomechanical kill estimates. King Fish and Star Fish allowed X-ray effects experiments.

Thermal Effects. The objectives of Project 8A.3 were to investigate, for an intermediate-altitude burst, (1) the existence of the postulated thermomechanical effect and its properties, (2) the characteristics of the thermal source as viewed at the test vehicle surface, (3) the nonthermomechanical effects (such as material ablation), and (4) the proportion of observed effects attributable to X-rays.

The instrumentation (Figure 6.9) used in Blue Gill generally falls into four categories based on the objectives.

The existence and magnitude of the thermomechanical effect was investigated by means of indent recorders and spall gages. An indent recorder is basically a piston and anvil arrangement with different materials of interest exposed on the head of the piston. The impulse imparted to the piston was delivered to the anvil in the form of an indent. Pistons with various ratios of mass to exposed area were used in an attempt to develop a time history of the effect through analysis of piston response times compared to measured impulse. Forty-eight indent recorders were exposed on each of the three Blue Gill pods.

The spall gage was a lucite cylinder, supported by styrofoam, with a lead disk glued to the lucite on the surface exposed to the burst. It was anticipated that the stresses set up in the gage by the thermal reactions would cause fractures in the lucite, thus proving the existence of a pressure pulse generated at the surface of the lead. To provide for a range of pressure pulses, the enclosing heat shields were pierced by different sizes of apertures for different gages. One instrument, with four aperture sizes, was used on each pod.

Ablation effects were investigated by 18 ablation condensation gages on each pod. The gages exposed various materials of interest with each sample material having a hole drilled down the center of the sample which terminated in the gage body. It was believed that, as the materials vaporized, some vapor would be forced inside the gage and there plate-out on the sidewalls. Analysis of the plated-out materials was expected to help in development of the mechanics and pressures involved in ablation and to aid in determination of amounts of materials lost. Thirteen different materials were investigated on each pod.

Source information was investigated by use of thermal pinhole cameras, cutoff filter spectral gages, reflective coating spectral gages, and long-time thermal gages. The thermal pinhole cameras had two major functions; to measure the time history of the absorbed thermal radiation, and to measure the spatial characteristics of the thermal source. Apertures were drilled in the micarta heat shields that covered the pinhole camera gage body. Each gage provided four apertures, one on top and three spaced equidistantly about the side. The thermal radiation incident through each pinhole caused irreversible structural changes in the heat-sensitive detector slab. Seven cameras were used on each pod.

The cutoff filter spectral gage utilized a variety of cutoff filters to allow only a portion of the energy spectrum to impinge on a detector material. By observing the relative intensity transmitted through different filters, it would be possible to derive information concerning the spectral distribution of radiation from the source. Filter materials used were fused quartz, titanium dioxide, magnesium fluoride, and aluminum oxide. Three aperture sizes and two detecting materials provided the dynamic range desired. Four gages, providing 16 data channels, were used on each pod. The spectral gages with reflective coatings had the same objective, the investigation of source spectral distribution, but achieved discrimination between wavelengths by use of reflective coatings of known properties, with wavelengths selectively passed or reflected. Six such gages on each pod, with six combinations of detector materials and reflective coatings, provided, with redundancy, 24 data channels per pod.

The long-time thermal gage was designed to derive the total thermal pulse experienced by the pod over a relatively long period. The gage is basically a heat sink containing strips of materials having a range of melting temperatures. Two heat sink materials, steel and copper, and five strip materials provide the great range of temperatures covered. The heat sink, exposed to the thermal radiation, increases in temperature, causing the strip materials to melt to a depth proportional to their melting points and, thus, to the thermal radiation absorbed.

At the intermediate altitude of Blue Gill, the X-ray flux from the nuclear burst is mostly absorbed by the atmosphere; however, some X-rays were expected to reach the close-in (2,500-foot nominal distance) pod. In order to determine this X-ray flux, and thus differentiate its effects from the thermal effects, an X-ray pinhole camera was mounted in the close-in pod, and X-ray photocell detectors were mounted in all three pods. The pinhole camera had a focal length of 12 inches and diameter of 3.75 inches. Three pinhole sizes were used. The detector materials, steel, lead, and magnetic mylar tape were used in the film plate. The photocell detector used as a sensitive element a Sylvania 131 long-persistence phosphor. X-ray impingement on the phosphor caused a light flash, the intensity of which was detected by the photocell and was stored by stepping a series of magnetic latching relays.

All three Blue Gill pods were recovered, but the middle-distance pod was damaged, and some instruments were lost. The indent recorders apparently functioned as intended; however, many of the samples, glued to the piston heads, were missing. Lead samples appeared to have melted off, and other metals showed various degrees of melting. In some cases, the bonding had failed. Nearly all anvils showed indents, and most appear to be valid data. Although the calibration and readout of data are not complete, preliminary data indicates impulse to refrasil on the order of $10^4$ dyne-sec/cm$^2$. The spall gages showed loss of the lead foil but no observable fracture of the lucite. Ablation condensation gages appear to have worked as expected. The ablation data presented in Table 6.11 is preliminary. Most metal samples showed varying degrees of melting and resolidification. Pyrolytic graphite samples appeared to be unaffected except for one sample that had laminations parallel to the surface. This sample appeared to have lost material through delamination. All other instruments appear to have functioned as intended, but results must await the completion of the data readout.

The thermal experiment appears to have been a success; however, ambiguity in reduced data casts some doubt on the validity of impulse data recorded for different materials. All materials appear to give approximately the same impulse readings. This has led to speculation that the vapor cloud created by ablation of the refrasil backplate cover effectively shielded the instruments from the burst after the first few milliseconds

and that the impulse recorded is essentially that of refrasil vapor pressure. Resolution of this problem must await final reduction of data. Pending receipt of final data, no recommendations can be made.

X-Ray Effects. X-ray effects were investigated on two events, Star Fish Prime and King Fish. Project 8B participated in both events. Project 8A.3 participated in King Fish only.

The objectives of Project 8B were to measure (1) the total X-ray-induced momentum on materials of interest and (2) the X-ray flux characteristics. The objectives of Project 8A.3 were to measure: (1) total impulse due to interaction of the weapon energy with selected materials, (2) impulse due to X-rays alone, (3) impulse due to energy forms other than X-rays, (4) time history of the total loading, (5) ablation from materials of interest, (6) characteristics of the X-ray source, (7) characteristics of any non-X-ray source, and (8) to separate, by controlled measurement, the effects due to X-rays from those due to other energy sources.

Project 8B instrumentation was essentially the same for both events (Figure 6.10). The instruments were of two types, effects and diagnostics. Effects instruments included three variations of a basic indentor gage, a metallurgy gage, samples of reentry vehicle materials, and a fracture gage.

The indent recorders utilized a piston-anvil arrangement in which the pistons, made of various materials exposed to the burst, delivered momentum to the anvils where the momentum was recorded as an indent. Aluminum and magnesium pistons were used with lead anvils. The three variations were achieved by the manner in which the materials of interest were contacted by the pistons. The Mark I design was used to record the impulse due to metal blowoff, with the metal samples of interest glued to the top of the piston surface. The Mark II design tested primarily R/V and plastic materials samples. In this design, the center of the piston face was relieved to a predetermined depth, and the material sample was inserted into this space and glued in place. The instrument case design assured that only the material of interest was exposed to the burst. The Mark III design utilized a striker slab of material covering the entire surface of the gage body with the piston held in contact with the striker plate by a retaining spring. This design was necessary because of the relative X-ray transparency of some materials of interest. By using the material of interest as the striker plate, the thickness could be increased, over that possible with the Mark II, to provide X-ray opacity. In all designs, the anvil was free-floated by a spring, and the pistons were held in place by retaining springs. Approximately 20 materials of interest were exposed in each pod.

The metallurgy gages utilized known characteristics of selected metals as indicators of pressure and temperature histories. Stable or metastable structural alterations occurred when the samples were subjected to the X-ray-induced thermal and peak pressure gradients. The samples were mounted in the case below an aperture that exposed part of the sample, and were supported by a styrofoam shock absorber, designed to prevent damage to the sample when the X-ray impulse drove the sample toward the rear of the case. Ten different metallurgical samples were exposed in each pod.

The R/V materials gages mounted samples of selected R/V structures for exposure to burst effects. The samples included not only heat shield material but also bonding and intermediate layers, and R/V substructure. The cross-sectioned structure samples were mounted in a gage body and held in place by springs to isolate the effects on the samples from the effects on the gage body. Seven different structural samples were exposed on each pod.

The fracture gage was designed to give information as to the shape of the X-ray-induced blowoff pulse. The gage was designed to blow off on exposure to the X-ray flux, transferring a compressive pulse to the lucite cylinder. By studying the fracture pattern produced in the lucite, an estimate of the duration and peak amplitude of the pulse could be made.

Diagnostic instruments consisted of carbon calorimeters, K-edge filters, and a plated hole instrument. The calorimeter was a carbon disk utilizing temperature-sensitive paints as the element to record the peak temperature at equilibrium. Two calorimeters were flown in each of the outer pods.

The K-edge instruments were designed to provide spectral information. Filter elements pass certain wavelengths preferentially, and these were detected on a stack of alternate layers of metal foils and mylar plastic. Seven different filter elements were used and, in the detector stacks, three different metal foils provided additional ranges for the flux levels. Fourteen detector channels were provided in each pod.

The plated hole gage was basically a cone-shaped hole drilled in a block of carbon, with the inside of this hole plated with one of three metals: chromium, lead, or gold. The X-rays, impinging on the carbon block at the end near the apex of the cone, penetrated the carbon and were attenuated selectively with wavelength. The energy density recorded by the plated metal should decrease monotonically as distance from the apex of the cone increases. Analysis of vaporization, melting, heating, and in chromium, crystalline changes, provides information on spectral energy distribution within the incident flux. For King Fish, the design of this instrument was modified to provide a cone of carbon resting within a cone-shaped hole in the instrument body. A gap was provided between the carbon cone and the gage body which provided the plated surface.

Project 8A.3 instrumentation for King Fish was basically the same as that used for Blue Gill. Indent recorders were identical, but additional recorders were provided with beryllium windows, which were intended to be relatively transparent to X-rays but to prevent the piston seeing any type of nonpenetrating energy. An additional control was provided on these pistons by having one with a blowaway hatch to be blown away by the X-rays, thus proving the penetration of the beryllium window. The piston should record no indent, thus proving the opacity of the window to late-time radiations.

Spall gages and ablation condensation gages, identical to those for Blue Gill, were used, but materials of interest were, in some cases, changed. The thermal pinhole cameras were modified by the addition of an X-ray-opaque hatch, to be blown away by the X-ray impulse, and thus expose the detector element to the thermal or debris energy fluxes. In addition, reflective coatings were used on some of the detector elements. Two X-ray intensity gages were added to the instrument array on the project pod. These were stacks of plastic sheets with metal plating or with metals imbedded in the plastic. The incident flux and spectrum were derived from the depths, within the stack, at which phase changes occurred in the metals. Several aperture sizes were used, and in one gage the problem of aperture closure was tested by making the aperture a slot tapered from zero width to 3-mm width.

Long-time thermal gages, as used in Blue Gill, were used on the close-in pod on King Fish. X-ray pinhole cameras with focal lengths of 4 and 12 inches and a new type of structural gage were used. This structural gage, a disk of material supported by a hollow cylinder, was to test the effects of X-rays on bare structural materials.

Large errors in pod orientation were experienced on Star Fish. The close-in pod was almost nose-on to the burst, and none of its instruments were exposed directly to the burst. Instruments on the middle pod viewed the burst with an angle of 43°, and the outer pod viewed the burst with an angle of 41°. In addition, the outer pod was almost

twice as far away from the burst as desired. Because of these excessive look angles, none of the source parameter instruments operated. Many of the indent recorders and R/V materials gages on both the middle and outer pods did operate, and it is estimated that approximately 50 percent of the desired data was obtained. Impulse and material effects data was obtained but has not yet been reported in final form. Some of the R/V structure samples did experience failures of varying degrees under the X-ray flux. It is hoped that metallurgical techniques used on some gage bodies and on the metallurgy gages will provide some source parameter data.

Of the three pods flown on King Fish, only two were recovered, and on one of these the entire backplate and all but one of the X-ray instruments were missing. The close-in pod, which carried the Project 8A.3 instruments, was recovered intact, and all instruments appear to have functioned as designed. The one instrument recovered in the other recovered pod also belonged to Project 8A.3.

Project 8B obtained no data from King Fish. On the instruments recovered, X-ray impingement areas were prominent. On the indent pistons, approximately half the exposed samples were lost, primarily through bonding failures. Almost all of the indent recorders provided indents. The impulses vary with the material exposed but generally appear to be of the order of $10^3$ dynes/cm$^2$ for this distance of approximately 8,200 feet from the burst. Fracture gages showed no observable results other than the loss of the lead foil covering. The samples in the ablation condensation gages showed effects ranging from almost complete disintegration, for Avcoat 19 and Rad 58B, to essentially no change in pyrolytic graphite.

None of the thermal cameras showed discernible images. The X-ray intensity gages showed stippling of the beryllium windows, but X-ray source images were not visible. The long-time thermal gages were unaffected except for cracking of quartz filters. The X-ray pinhole cameras did show images of the X-ray source, and structural gages showed varying degrees of deformation depending on material and disk thickness.

All of these observations are preliminary and definitive data awaits publication of the Project Officers Report. It appears that considerable X-ray effects data was obtained, but the validity and interpretation of the data depend on many calibration and correction factors.

## 6.5 GEOPHYSICAL EFFECTS

6.5.1 Background. Early speculations had led to the conclusion that high-altitude nuclear explosions should produce global hydromagnetic effects in the upper atmosphere, which could be detected by highly sensitive, ground-based magnetometers and earth current instruments. Shots Teak and Orange of Operation Hardtack produced widespread magnetic effects in the Pacific area. In addition to instrumentation by US Army Electronics Research and Development Laboratory (USAERDL), AFCRL, and others in the Pacific area, magnetometers recorded data in Iceland, Sweden, the Russian Arctic, French Antarctic, Algeria, Ghana, Arizona, and New Jersey during Argus II and Argus III, in 1958. The physical mechanisms which generate these phenomena and the mode(s) of propagation continue to be puzzling.

6.5.2 Objectives. The objectives of the magnetometer and earth current measurements were: (1) to obtain data on geomagnetic field effects from high-altitude nuclear detonations and (2) to help evaluate the feasibility of using these devices for the effective detection of high-altitude nuclear detonations of unknown origin.

6.5.3 Instrumentation. Many different types of variometers (fast-response magnetometers) and magnetometers were employed in the Pacific area and worldwide. Appendix O lists the location and types of these instruments.

In a considerable number of cases various earth current systems were also emplaced. Due to the difficulty of calibrating such systems, their primary purpose was for waveform and arrival time data. In addition to the funded projects, magnetometer and earth current data were obtained from scientific sources throughout the world. A partial list of these is included for information and reference as Table 6.12.

A large amount of various geophysical data was collected by the Armour Research Foundation (now Illinois Institute of Technology, Research Institute) under Project 6.5b from all over the world. This data has been forwarded to the DASA Data Center.

6.5.4 Results. A very large amount of magnetometer and earth current data was collected during the operation, but for the most part, only onset times, magnitudes, waveforms, and durations have been reported. There is much more data analysis work to be done. One overall result of importance is that it appears feasible to detect high-altitude nuclear detonations with magnetic sensing devices, because the signature of such detonations is completely different from natural earth magnetic disturbances.

Star Fish data was obtained from all project stations except Okinawa, which was in a typhoon alert status. Unofficially, data was also received from Paris, Ghana, Pennsylvania, Australia, Tasmania, Alaska, Massachusetts, Texas, Maine, Florida, and New Jersey. Signals were generally much greater than anticipated, with many equipments being saturated at early times. Launch area signals of 150 gammas were reported. A helium magnetometer on Hawaii reported a signal of 300 gammas. There were two distinct signals in the early period. The first, at H = 0, was of relatively high frequency, short duration (less than 1 second). A large-loop magnetometer on Hawaii measured a rise time of 5 μsec for this pulse. The rise time appeared somewhat slower in the conjugate areas. The second signal generally arrived 1.5 to 2.0 seconds after detonation. Maximum signal arrived in the conjugate area at H + 3.5 seconds with a predominant frequency of 0.3 cps. The late-time signal was very complex. Identical equipment measured the arrival time to be 0.4 second later at Tongatabu than at Samoa.

Star Fish earth current signals lasted on the order of 40 seconds with E-W systems showing amplitudes of twice N-S systems. Arrival times and waveforms generally agreed very well with magnetometer data.

Results from Phase II of Dominic were generally more complicated than from Star Fish. At first look, the Project 6.5b magnetometers and earth current instruments appeared to show no data for this phase. The signals again arrived in two parts, the first an almost instantaneous EM pulse followed by a later magnetic pulse with generally increasing period. Table 6.13 shows the onset time for each event at the Project 6.5e locations.

Apparently, the propagating medium interacts in some manner with the primary signal. The primary signal appears to be a structureless broadband pulse containing an equal distribution of frequencies from nearly dc to the 100-kc or low-Mc region. Results of Project 6.5e initially indicate that, for burst heights above 400 km, signal propagation is apparently isotropic, whereas for lower burst heights, propagation is increasingly anisotropic.

Very few measurements were obtained on Tight Rope.

Check Mate results were negative at Okinawa, Wake, Trinidad (variometer), and Tongatabu (low-sensitivity N-S variometer). An earth current record was obtained in Trinidad. Records indicate prompt arrival (within milliseconds) of a 2-cps signal, an

arrival at about H+1 second (½ cps), and distinctive arrivals up to H+27 seconds. The large-loop magnetometer on Hawaii received a signal in the direction of a decrease in the earth's magnetic field reaching a minimum of −0.117 gamma/sec at H+15 msec.

Also at Hawaii, a helium magnetometer recorded a minimum of −2.5 gammas at H+2 seconds. A N-S variometer record at Samoa showed a slow oscillation with a period of 15 to 20 seconds, which did not appear on the E-W record. A helium magnetometer on Samoa recorded a signal decrease to −0.07 gamma at H+0.030 second. The first maximum was 0.2 gamma at H+5.6 seconds.

At Blue Gill event time, all equipment was operational, although negative results were reported from Trinidad, Okinawa, and Wake. The recorded signals were relatively simple and of low amplitude. Variometer records lasted about 40 seconds in the Southern Conjugate Area, 20 seconds on Canton, and 7 seconds on Kauai. Magnetometers on Samoa and Canton showed sizable slow changes: 1.3 to 4.3 gammas at Samoa, 100 milligammas to 1.1 gammas at Canton. The large-loop magnetometer signal on Hawaii decreased to a minimum of −0.055 gamma/sec at H+15 msec. Later signals were overridden by a 1-cps modulation and a very weak oscillation with a period of 10 to 12 seconds. A helium magnetometer at Samoa recorded a −0.95 gamma signal at H+3 seconds. Small-amplitude (0.15 gamma) 40-second-period oscillations were observed for several hours postshot. Good earth current signals were observed at many stations.

All equipment was operational during King Fish, although negative results were reported from Trinidad, Okinawa, and Wake. King Fish results were the most complicated of all the events. A Samoa variometer showed a prompt arrival (30 to 40 msec) followed at H+0.5 second by a rectangular-appearing pulse, which may represent a succession of arrivals, probably as a result of dispersion. This type of signal lasted for 1.25 seconds at Samoa, 2.5 seconds at Tongatabu, and 2 seconds at Canton. A N-S variometer on Kauai presented a complex record, whereas the E-W instrument showed only a short period prompt pulse. The Southern Conjugate Area variometer records show effects up to 4 minutes; Kauai up to 30 seconds. Variometer signals in the Southern Conjugate Area reached a strength of about 2 gammas.

The large-loop magnetometer on Hawaii had a first minimum of −0.156 gamma/sec at H+0.015 second, crossing the zero line at H+0.030 second, and a maximum of 0.234 gamma/sec at H+0.060 second. For the first 2 seconds, a low-amplitude 2.0-cps signal was visible. Between 3.0 and 10 seconds, a 0.3-cps signal predominated. The only activity after 15 seconds was a 60-second-period train of oscillations that lasted for several minutes.

The helium magnetometer on Hawaii recorded a first minimum of −1.3 gammas at H+4 seconds. The signal crossed the zero line at H+19 seconds and oscillated about this line with an amplitude of approximately 0.3 gamma with a progressively increasing period.

The helium magnetometer on Samoa recorded a minimum of −1.0 gamma at H+3 seconds and a maximum of 1.1 gamma at H+11 seconds. Later signals show an oscillatory character with gradually changing periods.

The earth current recorded at Hawaii was saturated for more than 1 hour after an initial negative signal at H+0.1 second. An earth current signal on Samoa initially went positive to 0.1 mv/1,000 feet at H+0.1 second, crossed the zero line at H+0.2 second, went to a minimum of −0.5 mv/1,000 feet at H+0.7 second, followed by a sequence of six complete 0.6-cps oscillations.

Only minor effects were noted from Tight Rope. At Kauai, a high-sensitivity N-S loop showed an 8-milligamma pulse at H+0.2 second lasting 0.1 second. The E-W record showed a small pulse at H+0 lasting 10 msec. At Canton, the N-S earth current showed

a small effect with a maximum of 20 μv lasting for a minute. The E-W earth current on Canton showed a slight effect for about 20 seconds.

A Russian high-altitude detonation took place on 22 October 0340:45Z,

An earth current was recorded at Trinidad with a strength of 2,000 μv/km N-S and 3,300 μv/km E-W, peak to peak. Variometers in Trinidad recorded peak intensity of 100+ milligammas on the N-S loop, and 100 milligammas on the E-W loop. A prompt signal arrival was noted on the Kauai N-S variometer, lasting less than a minute.

Another Russian shot took place on 28 October 0441:19Z,

. A variometer at Kauai recorded a signal of short duration, virtually over at H+2 seconds. Several arrivals were noted, the strongest at about H+6 seconds with a period of about 5 seconds and a strength of about 100 milligammas.

## 6.6 OPTICAL AND BIOPHYSICAL EFFECTS

6.6.1 Background. Shots Yucca, Teak, and Orange, high-altitude shots of Operation Hardtack,

In particular, Teak and Orange produced optical effects in the form of large fireballs and extensive auroral displays. Although many optical records were made of the phenomena in the burst region, instrumentation was generally inadequate to record fully the extensiveness of the display. In addition, reports indicated similar displays in a southern conjugate region near the Samoa-Fiji area. Although no instrumentation covered this region, the reports tended to verify the Christofilos theory, i.e., the trapping of electrons in the earth's magnetic field.

Accordingly, CHDASA planned and rapidly executed a series of three high-altitude detonations (Argus Series) in the South Atlantic to verify this effect. Because of the impending test moratorium, time did not permit the recording of the visible effects of these three detonations.

The resumption of atmospheric testing in 1962 presented the first opportunity to fully instrument and record these effects since their disclosure during the 1958 test series.

6.6.2 Objectives. The objectives of the optical program for Fish Bowl were alined within three main areas: visible effects, infrared effects, and biomedical effects. One project was assigned to each of these areas.

The project assigned to the visible portion had the overall goal of accomplishing optical recordings. These would provide a unifying spatial and temporal framework that would permit the recording, isolation, and identification of all the visible phenomena associated with the events. Specific objectives were to provide: (1) high-speed photographic recordings of the fireball region from both surface and airborne stations to determine the energy disposition at early times; (2) medium- and high-speed photographic recordings of the fireball region from both surface and airborne stations to determine vertical asymmetries, overall hydrodynamic motion, debris shock, and late-time debris motion; (3) high-dispersion time-resolved and static spectroscopy of the burst region to identify and follow: atomic and molecular processes, continuum emission processes, and afterglow and residual debris-cloud emissions; (4) low-speed photographic recordings from surface stations to record the spatial and temporal development of artificial auroras; (5) high-dispersion time-resolved spectroscopy in the Southern Conjugate Area to identify and follow spectral emission processes at that location; and (6) extensive qualitative (sensitometrically controlled) still- and motion-picture coverage of all events in both the burst and auroral zones.

The second main area of investigation concerned itself with the infrared effects of the high-altitude nuclear detonations on weapon systems that employ infrared techniques for

detection, tracking, homing, and surveillance. Emphasis was placed on those infrared effects that may degrade defense systems relating to early warning, terminal intercept, and penetration. Specifically, the project sought to investigate the detailed spatial and temporal characteristics of the fireball thermal output and airglows in the region from 0.2 to 7.0 microns, with special emphasis at 2.7 and 4.3 microns. Secondly, the project sought to determine the processes in the perturbed upper atmosphere that lead to these radiations, in order to confirm theories and to develop scaling and prediction techniques relating to the effects.

The third or biomedical area was concerned with the chorioretinal burn hazard that may result from the detonation of nuclear weapons at high altitudes. There were two specific objectives: (1) to test and improve methods for predicting the threshold distances at which chorioretinal burns will be produced, particularly from high-altitude detonations, and (2) to test the responses of protective devices and various phototropic materials to the thermal and visible radiations produced by nuclear detonations.

6.6.3 Instrumentation. A relatively large number of both ground and airborne stations were used on all shots. Ground stations were located on Johnston, Maui, Hawaii, Fiji, Samoa, and Tongatabu (Table 6.14). Seven instrumented aircraft were used on most shots at optimum distances and positions relative to each of the bursts. Two KC-135 aircraft (Figure 6.11) were jointly used to collect optical and infrared data. Five C-118 aircraft were used exclusively for biomedical data collection. Other than for minor instrument repointing, stations remained unchanged for all events. The interior of the Johnston Island DOD photo station is shown in Figure 6.12.

The optical aircraft, however, were repositioned for each shot to allow optimum pointing of the instrumentation that was set at fixed-look angles within the aircraft. The shot time positions of the optical-infrared aircraft are given in Appendix P. Burst position data in Appendix P is early data. Corrected burst positions are given in Table 1.2.

The slant range to the biomedical aircraft for each of the high-altitude shots on which they participated is given in Table 6.15.

A consolidated list of infrared instrument characteristics is given in Appendix Q. A consolidated list of optical instrument characteristics is given in Appendix R. The instrument lists are not complete; only representative instruments are listed. A complete listing of instrumentation is contained in the Project Officers Report (POR) for each of the project areas.

6.6.4 Results. In general, it appears that the well-known characteristics of atmospheric fireball formation and growth change drastically as the altitude of detonation increases. From preliminary study, it appears that altitude of detonation has a far greater effect than yield in this respect (Figure 6.13). Although Blue Gill had 20 times the yield of Tight Rope, the fireball size, growth, and rate of rise were not greatly different. If a comparison is made between Tight Rope and Check Mate, or between Blue Gill and King Fish, where only the altitude is different, tremendous differences appear. Another interesting comparison is that of the Star Fish 1.4-Mt detonation and the Check Mate In neither case was an X-ray-heated fireball formed, rather weapon debris was thrown out and expanded in what appeared to be a hydrodynamic manner. The maximum diameter of visible debris was measured in both cases

Tight Rope. This shot, behaved in a manner very similar to a near-surface detonation (Figure 6.14). First, a spherical radiative fireball, created by X-ray-heated air, was formed and then grew. The optical opacity of the fireball was somewhat less than would be found in a near-surface detonation. It was possible to detect a debris shock formed at about $\frac{1}{10}$ second which moved out rapidly and caught up with the radiative fireball.

No visible stream of electrons, beta patch, or aurora were formed.

Relative radiance curves for three spectral bands are given in Figures 6.15 through 6.17. Time has not permitted calculation and plotting of all curves in absolute values. The data reduction phase will take into account instrument calibration, pointing corrections, window, and atmospheric corrections as well as readout of additional channels of data. The Tight Rope thermal pulse was similar in character to that from Shot Yucca of Operation Hardtack.

A well-defined maximum, minimum, and interval of constant intensity were resolved on the rise to the first maximum. Evidence of similar irregularities were encountered on the leading edge of the Yucca pulse. The reported time to minimum could be in error due to the inaccuracies inherent in the field data reduction technique. The ratio of the intensities of second to first maximum was observed to decrease with decreasing wavelengths.

Tight Rope produced chorioretinal burns in animal specimens at slant ranges from 11.5 to 56 naut mi. No significant burns were produced beyond this range. The lesions produced varied from 1.2 mm in diameter at the 11.5-naut mi station to 0 19 mm in diameter at the 56-naut mi station.

Blue Gill. This shot, proved to be one of the most interesting of the series. For the first time, a series of shock and rebounding waves were clearly recorded within the radiative fireball of X-ray-heated air (Figure 6.18). The fireball rose at a relatively constant rate throughout the first 2 minutes at which time preliminary measurement ceased (Figure 6.19).

The fireball was initially a nearly perfect sphere with blue streams of electrons extending north and south for a distance of approximately two fireball diameters at early times. These appeared to be closely alined with the earth's magnetic field lines at shot altitude. Other than this rather localized effect, no auroral phenomena were observed. After about 3 minutes, the fireball developed into a conventional vortex toroid, which grew slowly and persisted visibly nearly 30 minutes.

The visible, near-infrared, and 1.58-micron detectors all gave signals of an order of magnitude above natural sky background for about 2,000 seconds (Figures 6.20 through 6.22). As the early curves cannot be made to fit a power law function, it is doubtful that the effect is due to fission product decay. Rather the emission phenomenon appears to be due to a one-body aerochemical reaction. Later data analysis may confirm or deny this early assumption.

Chorioretinal burns were produced in all animals at all exposure stations from 32.7 naut mi out to 103 naut mi as a result of Blue Gill. In many instances, the burns were so severe that they were obscured by hemorrhages within the eye. There is some reason to believe the aircraft were positioned incorrectly due to erroneous predicted brightness values. This matter will receive considerable study.

Two humans accidentally received chorioretinal burns on Johnston Island during this event. Both were military personnel who have since been assigned to the School of Aerospace Medicine for continued observation and treatment. This unfortunate occurrence will, however, present the first opportunity to correlate chorioretinal burn comparisons in both human and animal subjects on a single well-instrumented detonation.

Some visible aurora was observed in the Southern Conjugate Area in the form of a brief white flash. No other phenomenon was recorded at that location.

King Fish. This shot, produced several interesting visual phenomena, probably associated with the beginning of a transition zone between the denser atmosphere below this altitude and the thinner atmosphere above. The detonation produced a relatively large, transparent, nonsymmetrical fireball, which grew quite rapidly in size —well out of proportion to the device yield (Figure 6.23). In addition to its rapid growth, the fireball rose at a faster rate than any of the other shots of the series,

During its growth, the upper limb was preceded by a reddish glow that moved upward ahead of the fireball and appeared to have the characteristics of a shock wave.

The time history of King Fish in the first 5 μsec as recorded by a camera located on Johnston Island is shown in Figure 6.24. The first frame recorded approximately the first 0.1 μsec after the beginning of the release of the X-ray energy. The outward expanding shells shown in subsequent frames represent X-ray pulses made visible by the air fluorescence process. The existence of three distinct rings, which implies the presence of three X-ray pulses, is a most interesting phenomenon and the following explanation has been suggested.

Late-time fireball photographs show that the King Fish fireball had developed definite asymmetries. A strong group of beta-ray auroral streamers were seen following the geomagnetic lines down to the north. A shock wave was seen penetrating the auroral streamers. three shocks emanated from the fireball. The group of streamers developed a slight bend a short distance below the fireball, and a definite bend developed beneath the fireball. The region between the fireball and the bend was probably partially ionized air left in the wake of the fireball. This plasma temporarily froze the magnetic field lines that were stretched between the initial and present positions of the fireball.

The fireball photographs taken after detonation time of King Fish showed a filamentary structure in the upper region of the fireball. This structure appeared to be associated with the geomagnetic field lines originally excluded from the expanding fireball and their return into the excluded volume. The debris was seen to be widely dispersed throughout the fireball. From Maui, the original fireball was seen to be rising, preceded by a bright red, expanding air-shock region such as was seen during Shot Teak. The evidence that the major component of the light from the red air shock lies in the 6,240- to 6,390-Å region, and that a major portion of the red flux reaching the Haleakala station lies in that wavelength band, is borne out by comparison of the signals

received through the narrow 6,300-Å (half power 6,240 to 6,390Å) channel and the wideband red (5,640 to 6,400 Å) channel filters. By 300 seconds, virtually no red light outside of this band was received. The emission within the band decayed, approaching a half-life of 125 seconds. This red glow was most probably the atomic oxygen 1D-3P doublet at 6,300 to 6,363 Å, excited by the high temperature behind the shock front. Assuming no further excitation after 300 seconds, and assuming further that collisional quenching at low (less than 200 km) altitudes is no longer important at 300 seconds, the 125-second half-life appears to be indicative of the OI forbidden red transition. It must be emphasized that this is a preliminary result, which will be subject to further readout of data from these channels and from that in the other photomultiplier systems, microdensitometry of the films, and to a more careful analysis of the response of the phototube-filter combinations.

Radiance versus time curves for the 0.4- to 0.5-micron and 4.8- to 5.5-micron bands are given in Figures 6.25 and 6.26, respectively.

Animals exposed to the fireball at distances ranging from 65 to 405 naut mi experienced no chorioretinal burns. It would appear that the large area of the fireball did not produce a sufficiently bright surface to inflict visible damage to the eye.

Check Mate. This shot, appeared to define the upper limit of the transition zone,

No fireball, or sphere of X-ray-heated air was produced. Rather, weapon debris was thrown outward at a rapid rate (Figure 6.27).

Early recordings show sharp spikes protruding from the rapidly expanding spherical debris mass. Also shown is a faint halo at great distances from the burst, probably caused by light emission from metastable excitations in the X-ray deposition region. Recordings made show clearly that the debris from Check Mate is not distributed isotropically at early times, but is confined mainly to an expanding toroidal ring. This conclusion is supported by other pictures which show that the plane of the ring is normal to the axis of the weapon at detonation time. Photographs show that the instabilities in the debris motion had developed into massive jets.

the Check Mate fireball was characterized by both the instabilities noticed earlier and by a beta-ray aurora. These features were taken by a cloud camera in an aircraft located north of the burst. At + 35 seconds, the fireball was rising fast, and the auroral streamers appear to be disconnected from it. This latter effect probably was caused by a local distortion of the magnetic field lines when they were frozen in the ionized gases of the fireball. This behavior was similar to that observed during King Fish. Photographs which portray the development of the debris aurora from the late fireball stage show the debris ring beginning to lose its circular shape.

Thereafter, the debris gradually slowed down and stabilized at an altitude of 250 km by 75 seconds.

Relative radiance curves for the 0.75- to 1.0-micron and 1.88- to 2.55-micron bands are given in Figures 6.29 and 6.30, respectively. Time has not permitted reducing these curves to absolute values. Absolute values for the 4.8- to 5.5-micron band are given in Figure 6.31.

Because of the low predicted visible output, no animal specimens were exposed on this event. Many phototropic filters and electromechanical goggles and components were exposed. Details of the materials and components exposed and the results of the exposure can be found in the appropriate POR's.

Star Fish. This shot, 1.4 Mt at 400 km, produced no conventional fireball. The weapon debris moved outward at a very rapid rate, reaching a

diameter of about 65 km in 20 msec (Figure 6.32).

The early stages of the debris expansion of Star Fish were recorded by several high-speed cameras. The films distinctly show a rapidly expanding shell, which leaves behind a slower moving core. Measurements on this film showed that this shell is expanding radially with a velocity of 1.6 m/μsec. The station on Mauna Loa, Hawaii, proved to be an ideal location from which to view large-scale auroral effects; photographs taken by a camera operating at 100 frames/sec clearly show the early-time history of the debris as it expanded with the earth's atmosphere. An upward-moving component of the debris was observed to rise from the inner core; the downward-moving debris is seen to collide with the earth's atmosphere and produce a marked increase in the brightness of the sky over a considerable region beneath the burst point.

A number of time exposures using 35-mm still cameras located directly below the burst recorded the late-time phenomena when light output was weaker. Two such photographs show auroral streamers extending upward and generally following the geomagnetic lines heading toward the Southern Conjugate Area. This auroral display continued at later time. The general red glow that extended over a large volume of space surrounding the burst area is attributed to emission in the red lines of atomic oxygen.

Photographs taken from Tongatabu show the southern hemisphere aurora as a concentration of streamers almost due north of the station. The same display was observed visually almost due south from Tutuila and Samoa. This auroral display was not associated with the main auroral concentration, which was southeast of Tutuila. Further details and examples of the photography are contained in the POR's.

Strong radiation was observed at 5.3 microns from the production of nitric oxide. Upper and lower limit calculations on radiation intensities to be expected from nitric oxide indicate that levels are considerably above what might be expected from an IRBM/ICBM target. The radiation at 5.3 microns was about three orders of magnitude greater than predicted as observed by three of the four 5.3-micron photometers for approximately 70 seconds (Figure 6.33).

As predicted for this event, no signals were observed in the 2.7-micron region. Intense optical-IR background radiation in the 0.8- to 1.1-micron region was four orders of magnitude above normal, 90 seconds after detonation. At 700 seconds, the intensity was still one order of magnitude above the natural background. Many auroral/airglow lines and bands were observed to be extremely bright and persistent. Typical of the narrow band spectral data was strong radiation in the neighborhood of 3,460 Å for about 150 seconds; this persistent radiation has been tentatively attributed to either the (1-10) Vegard-Kaplan band at 3,425 Å or the (NI)31 transauroral multiplet at 3,466 Å.

Although animal specimens were exposed to the detonation at distances ranging from 297 to 834 naut mi, no retinal burns were produced. Thus, no retinal burns resulted from any of the shots of the series above 90 km for the yields and altitudes tested.

6.6.5 Participation in AEC Developmental Tests. Retinal burn and flashblindness studies were conducted on the AEC airdropped diagnostic shots. (See POR-2014.)

The flashblindness project participated on eight of these events. It was found that no loss in visual acuity occurs for a night-adapted observer exposed for intervals approaching 10 msec to the detonation of megaton weapons in the lower atmosphere at ranges greater than 10 miles. Photographic records of time-intensity characteristics of weapon flashes were obtained from oscilloscope traces of the output of photo receivers. It is hoped that final data analysis and extrapolation to lower yields and closer ranges will provide information necessary for the final design of flashblindness protective equipment responsive over a wide range of yields.

## 6.7 BLAST AND PRESSURE EFFECTS

6.7.1 Background. Although no successful close-in blast measurements were made on high-altitude detonations in previous operations, the surface level measurements of overpressure-time taken during Operation Hardtack indicated that, for nuclear detonations up to altitudes of 250,000 feet, the effects of blast at altitude could be substantial and that overpressures at the earth's surface could be predicted. Some theories were developed, and machine calculations were made in an attempt to find a means of determining blast effectiveness under the conditions of interest. However, as burst altitude is increased, the partition of released energy changes, and consequently, the apparent blast yield, at altitude, cannot be predicted with any accuracy. The Fish Bowl Series offered an opportunity to make measurements close to high-altitude nuclear bursts as well as the usual surface overpressure measurements.

6.7.2 Objectives. The objectives of the blast and shock measurement program were: (1) to obtain close-in measurements of peak overpressure and overpressure-time from high-altitude nuclear bursts, (2) to obtain peak acceleration and acceleration-time measurements for specific vehicles close to high-altitude nuclear detonations, (3) to obtain surface level measurements of peak overpressure and overpressure-time from high-altitude nuclear detonations, and (4) to determine the blast effectiveness, early blast-thermal interaction, and missile response to high-altitude nuclear detonations.

6.7.3 Instrumentation. To obtain the close-in measurements desired, the Ballistic Research Laboratories (BRL), Aberdeen Proving Ground, Maryland, (Project 1.1) provided pressure and acceleration gages for mounting in the instrument pods carried aloft by the Thor missile (Figures 6.34 and 6.35). Two types of pressure gages, two types of accelerometers, and one type of shock spectra sensing device were utilized.

Since all time-dependent gages had a limited recording time, it was necessary to provide a sequence timer to turn on the gages in each pod just before burst time. The programer selected was crystal-controlled with a variable R-C network for manual adjustment of total time. The missile lift-off signal activated this programer which, after the lapse of the preset time, activated the gages. Once activated, one gage controlled the recording time of the other gages in each pod.

At the Star Fish altitude, no actual overpressure was expected close-in to the burst; therefore, only two pressure gages were flown on this event. These gages were mounted in the middle-distance (S2) pod. Two accelerometers, two shock spectra gages, and one programer were mounted in each of the pods.

On Shots Blue Gill and King Fish, four pressure gages, two accelerometers, and two shock spectra gages were mounted in each pod. Programers were used in all pods except the middle and far (K2 and K3) pods for King Fish. These pods depended on activation by a gamma switch, used previously as backup in all other pods, to start the recording gages.

Further details on the above instrumentation are contained in POR-2010.

Surface level measurements were made by two project agencies, BRL and AFCRL. BRL utilized Wiancko microbarographs and Statham low-pressure strain gages, changing sensing device ranges as necessary to cover the ranges of overpressures predicted for each event. For Star Fish, stations were established at Johnston Island and on scientific ships S-1 (USS Oak Hill) and S-4 (USNS Point Barrow). For Shots Blue Gill, King Fish, Tight Rope, and Check Mate, the Johnston Island and Ship S-4 stations were continued, but the station on Ship S-1 was moved to Wheeler AFB, Oahu.

For all shots, stations were activated shortly before burst and operated postshot for sufficient time to insure reception of all pressure waves. AFCRL, for Star Fish, established stations at Midway, Samoa, Wake, and Shemya (Alaska), each station using NBS microbarographs N-3 and N-6. On subsequent shots, the Wake and Shemya stations were eliminated. All stations were operated continuously for the duration of their establishment.

Further details on this instrumentation are contained in POR's 2010 and 2020.

6.7.4 Results. Pod Data. On Star Fish, all instruments in Pods S1 (near) and S2 (middle) operated satisfactorily. In Pod S3 (far), only the gages not requiring electrical power operated. The malfunction of other gages was attributed to battery failure. Pressure and acceleration gages did not reveal any discernible data. The shock spectra gages did show fluctuations, but plots of the data presented no clear trend of accelerations for any pod.

On Blue Gill, only those gages not requiring electrical power operated in B1 (near) and B2 (middle) pods. The cause of the malfunction of the remaining gages is undetermined. All gages in B3 (far) operated, but on some of the gages the time base markings were not present. On all gages that functioned, there were discernible fluctuations in the recording throughout the recording time. However, the fluctuations were somewhat sinusoidal in appearance, and there were no apparent differences from one pod to another, therefore no shock parameters could be implied. All of the shock spectra gages showed evidence of inputs; however, the data gave no obvious pattern of vibration.

On King Fish, all gages in K1 (near) operated, but some recordings were lacking the time base. In K2 (middle), only the spring-motored gages operated. Since this pod was badly damaged by water impact, it is believed that these gages were activated at water impact. Apparently, the gamma switch failed to activate the gages at burst time. All gages in this pod were damaged to some degree. Pod K3 (far) was never recovered. On all recordings obtained, there were sinusoidal fluctuations similar to those seen in Blue Gill, and nothing that could be pinpointed as data was discernible. The shock spectra gages again showed inputs, but no obvious pattern of vibration and no shock parameters could be deduced. Investigation and examination of all these gages is continuing in an attempt to interpret the recordings obtained.

On Star Fish and King Fish, no overpressure data was expected, but shock spectra and acceleration data were anticipated. On Blue Gill, no overpressure data were expected from the two outer pods. The procurement of overpressure data on the close-in pod was considered marginal, because the pod velocity at burst time was in excess of 10,000 ft/sec. Calculations indicated that the pod had to be within 3,000 feet of the burst to be overtaken by the shock wave. Beyond 3,000-foot separation, the pod would outrun the shock wave.

Surface Measurements. On Star Fish, the recorder aboard Ship S-4 malfunctioned, and no data was obtained. On Ship S-1, the prevailing ambient conditions, wind up to 20 knots and ship roll of up to 20°, completely obscured any signal from the overpressure wave. The Johnston Island station operated successfully, reporting a maximum overpressure of 170 microbars at the surface, with a positive phase duration of 10 seconds and an arrival time of 455 seconds after burst.

On all other high-altitude events, all stations were operated except the Oahu station during King Fish and the Ship S-4 station during Tight Rope. Table 6.16 presents data obtained. No discernible data was obtained on any of the high-altitude events by the Midway, Samoa, Wake, or Shemya stations.

BRL also operated the Johnston Island and Oahu stations during all airdrops conducted in the vicinity of Johnston Island, and the Ship S-4 station for two of these events. Table 6.17 shows data available.

For these events, instruments were also placed on the target barges and on the USS Forster. However, the data from these instruments has not yet been reduced.

6.7.5 Summary. Close-in blast data from high-altitude events was not obtained. It had been predicted that any data obtained would be marginal at best. Although some records were obtained, their interpretation is not possible at present, and instrument functioning must be considered marginal. Surface level measurements, using long proven techniques, were successful. However, the loss of data on Star Fish indicates the need for stable platforms for instruments to measure the very low overpressures generated by high-altitude events.

Further development should be pursued to produce a system of instruments capable of measuring blast parameters close to high-altitude events. Means of positioning these instruments must also be further investigated. To insure success, it appears necessary to place instruments above, and moving toward, the burst.

## 6.8 ATMOSPHERIC PARAMETERS

6.8.1 Background. Accurate information on certain atmospheric properties was required during Fish Bowl, in order to: (1) relate test data to theories of blast and shock phenomena in the upper atmosphere, (2) relate observed radiation fluxes to ionization produced, (3) determine the mass transport of nuclear debris by high-altitude winds, and (4) measure diffusion coefficients.

Since the atmospheric physical properties are somewhat variable, the climatological data based on previous measurements was not adequate to properly interpret other data or to determine debris motion.

6.8.2 Objectives. The objectives of the atmospheric parameters measurements program were: (1) to determine profiles of air density in the 30- to 105-km altitude region, (2) to deduce atmospheric pressure and temperature from the density measurements, (3) to measure wind velocities, diffusion coefficients, regions of turbulence, and eddy spectra in the altitude region between 60 and 150 km, and (4) to determine whether the nuclear detonations had any effect, on atmospheric circulations at high altitudes, that would persist for hours.

6.8.3 Instrumentation. In the falling sphere experiment, air density was calculated from the equation for aerodynamic drag applied to a free-falling 7-inch rigid sphere that contained a transit-time accelerometer with omnidirectional characteristics. The sphere was ejected from a Nike-Cajun rocket vehicle (Figure 6.36) at an altitude of about 60 km during the upleg portion of the trajectory. The sphere velocity at ejection was sufficient for it to attain an apogee altitude of nearly 158 km.

Because of inherent design features, the transit-time accelerometer provided incremental data rather than continuous information. Thus, the value of air density obtained represents an average value for the altitude region traversed by the sphere during the measurement. Density values were averaged over a greater altitude range at the higher altitudes. This resulted from a reduction in sphere drag acceleration due to decreases in both air density and sphere velocity. On the upleg portion of a typical sphere trajectory, accelerometer transit-times increased until the instrument no longer responded to the very small accelerations. This threshold sensitivity limited measurements of drag acceleration to approximately $10^{-4}$ g, corresponding to an altitude of about 105 km, with

the Nike-Cajun trajectory. On the downleg portion of the sphere trajectory, good data was again obtained at an altitude of about 105 km, corresponding to the accelerometer threshold sensitivity.

The drag acceleration data was telemetered from the sphere and used to calculate atmospheric density. However, to make this data meaningful, the sphere trajectory had to be accurately known. By successive integration of the acceleration data, the sphere velocity and trajectory were determined. This property made it possible to successfully use the falling sphere technique without tracking facilities, but the accuracy is limited because the acceleration is measured only during part of the flight. In the Fish Bowl Series, radar tracking was used to obtain a more accurate trajectory for the falling sphere.

The technique used to measure high-altitude winds involved the ejection of a sodium vapor trail from the second stage of a Nike-Cajun rocket at dusk or dawn twilight. The rockets were tracked by radar.

The sodium was sunlit and, as a result of emission of resonance radiation, was visible against a darkened background for about 20 minutes. The trail was photographed simultaneously from Johnston Island, and Ships S-1, S-2, and S-4, permitting subsequent triangulation to determine the altitude of various parts of the cloud.

During the period when the trail is visible, its shape undergoes continuous changes due to the wind velocity at various altitudes. If the trail expansion is radial in a coordinate system moving with the wind, the magnitude and direction of motion of the trail center gives a direct measure of the winds in that region.

6.8.4 Results. Good data was obtained by both the falling sphere and the sodium vapor trail experiments. Tables 6.18 and 6.19 show time of rocket firings and the success or failure of each flight.

Rockets 1 through 4, for the falling sphere experiment, were launched during June and July. On these flights no measurements of detonation-produced changes in the atmosphere were made or planned. The data obtained on ambient air density is in general agreement with that expected at Johnston Island.

During October and November, Rockets 5 through 9 were launched; one for background data and the other four a few minutes after Check Mate, Blue Gill, King Fish, and Tight Rope. All, except the post-Tight Rope rocket, provided excellent data. Measurable heating effects and reduction in density were observed after the detonations.

The data obtained from the sodium vapor experiment showed that the winds in the D- and E-regions before Star Fish were typical for this location and time of year. The measurements at dawn following Star Fish showed that the atmosphere was considerably disturbed. The wind directions, in particular, were completely different from those normally observed. Above 97 km, the wind was from almost due north, probably due to induced currents parallel to the magnetic field.

During October and November, data was obtained after Blue Gill, at three different times after King Fish, and at dusk before Tight Rope. King Fish caused a considerable disturbance of winds in the ionosphere, whereas only a relatively small perturbation was produced by Blue Gill. Following King Fish, the winds had returned almost to normal by dusk on D+3 days. The perturbation caused by King Fish was not as pronounced as that produced by Star Fish.

**TABLE 6.1 FREQUENCY BANDS OF MILITARY INTEREST**

| Band | Frequency Range | Wavelength meters |
|---|---|---|
| VLF | 3 to 30 kc | $10^5$ to $10^4$ |
| LF | 30 to 300 kc | $10^4$ to $10^3$ |
| MF | 300 to 3,000 kc | $10^3$ to $10^2$ |
| HF | 3 to 30 Mc | 100 to 10 |
| VHF | 30 to 300 Mc | 10 to 1 |
| UHF | 300 to 3,000 Mc | 1 to 0.1 |

TABLE 6.2 MAXIMUM EXCESS TEMPERATURES

All temperatures in °K.

| Shot | 925 Mc | 3000 Mc | 35,000 Mc |
|---|---|---|---|
| Star Fish | 250 | 22 | Negligible |
| Check Mate | 4000 | 9000 | 8700 |
| King Fish | 670 | 4700 | 4700 |
| Blue Gill | 350 | 2200 | 3300 |
| Tight Rope | 55 | 730 | 2000 |

TABLE 6.3 DURATION OF EXCESS TEMPERATURE

Duration is approximate time required for a 10-fold decrease from maximum observed.

All times in seconds.

| Shot | 925 Mc | 3000 Mc | 35,000 Mc |
|---|---|---|---|
| Star Fish | >120 | >120 | — |
| Check Mate | 220 | 150 | 9 |
| King Fish | 60 | 30 | 14 |
| Blue Gill | 160 | 110 | 46 |
| Tight Rope | 60 | 120 | 18 |

TABLE 6.4 DURATION OF BURST REGION CLUTTER

All times in minutes.

| Frequency | Check Mate | King Fish | Blue Gill | Tight Rope |
|---|---|---|---|---|
| Mc | | | | |
| 1210 | 3 | 9 | 10 | 6 |
| 850 | 3 | 12 | 12 | 6 |
| 398 | 7 | 18 | 25 | 8 |

TABLE 6.5 DEBRIS HISTORY INSTRUMENTATION

| Instrumentation | Project | Location | Shot | Remarks |
|---|---|---|---|---|
| Gamma-ray detector | 6.5b | Conjugate Area | All | Telemetry from balloonborne detector |
| Neutron detector | 6.5b | Conjugate Area | All | Telemetry from balloonborne detector |
| Photoelectric detector | 6.5b | Conjugate Area | All | Time of onset of auroral emission |
| Photometer | 6.5b | Conjugate Area | All | Emission at 6300 Å, 5577 Å, and 4278 Å |
| Photometer | AFTAC* | Wake, Midway | All | Emission from LI, BA, BA', and ZR |
| Photometer | 6.6 | Johnston, S-1, S-2, S-4, S-5, Tongatabu, F. F. Shoals, Tutuila | All | Emission at 6708 Å, 6130 Å, 5535 Å, 4554 Å of neutral LI, BA, and ZR, and ionized BA |
| Riometer | 6.8 | Boston, Midway, Wake, Tutuila, Tongatabu, Oahu, Johnston, S-1 thru S-6, F.F. Shoals, Palmyra, Canton, DAMP Ship, Viti Levu, Acania, Christmas, Peru, Rarotonga, Trinidad | All | Measured synchrotron radiation and ionospheric absorption |
| Riometer | 6.5b | Tongatabu, Tutuila | All | Measured synchrotron radiation and ionospheric absorption |
| Gamma-ray detector | AFTAC* | Hickam | All | Gamma-rays counted by a U-2 aircraft in burst and northern conjugate area |
| Gamma-ray spectrometer | 6.10 | Fiji | All | Gamma-rays counted by a KC-135 aircraft in the southern conjugate area |
| Rockets | 6.7 | Johnston Island | SF/CM | Magnetic field strength, neutron, beta, and gamma fluxes from rocketborne sensors |
| Gamma-ray scanner | 6.2 | Johnston Island | SF/KF/BG | Mapped debris region using rocketborne sensors |
| Rockets | 6.3/6.4 | Johnston Island | SF/KF/BG | Electron and ion densities, X-ray and gamma-rays (prompt and delayed), electron temperature and ion species from rocketborne sensors |
| Gamma-ray detectors | 6.12 | Satellite | SF | No data obtained |

* Air Force Technical Applications Center.

TABLE 6.6 PROJECT 6.7 ROCKET TRAJECTORIES FOR STAR FISH

| Rocket Number | Launch Time | Distance from Burst at H−0 | Nominal Splash Coordinates |
|---|---|---|---|
| | sec | feet | |
| 1 | H−462 | 800* | 24.6 N 170.06 W |
| 2 | H−266 | 400* | 24.6 N 170.06 W |
| 3 | H−160 | 100† | 6.14 N 171.83 W |
| 4 | H−140 | 200† | 0.29 S 172.49 W |
| 5 | H−510 | 1,000‡ | 0.29 S 172.49 W |

* Measured perpendicular to field line through burst away from surface.
† Measured perpendicular to field line through burst toward surface.
‡ Measured along the field line through burst toward the south.

TABLE 6.7 PROJECT 6.7 ROCKET PAYLOAD INSTRUMENTATION

| Instrument | Data |
|---|---|
| Rubidium vapor magnetometer | Total instantaneous magnetic field intensity |
| Hall effect magnetometer | Component of instantaneous magnetic field intensity parallel to spin axis of payload |
| Beta counters (6 per payload) | Instantaneous flux of fission beta particles |
| Gamma counters (3 per payload) | Instantaneous flux of fission gamma and of bremsstrahlung |
| Faraday cups (3 per payload) | Debris ion current and fission beta current |

TABLE 6.8 MATERIALS USED IN NDL THRESHOLD DETECTOR SYSTEM

| Detector | Threshold Energy | Reaction |
|---|---|---|
| Gold | Thermal energy up to 0.3 ev | $Au^{197}$ (N, $\gamma$) $Au^{198}$ |
| $U^{235}$ | 1.5 kev (x/$B^{10}$ shield) | Fission |
| $Pu^{239}$ | 10 kev (x/$B^{10}$ shield) | Fission |
| Np | 0.63 Mev | Fission |
| $U^{238}$ | 1.5 Mev | Fission |
| Sulfur | 3.0 Mev | $S^{32}$ (N, P) $P^{32}$ |
| Magnesium | 6.3 Mev | $Mg^{24}$ (N, P)$Na^{24}$ |
| Aluminum | 8.1 Mev | $Al^{27}$ (N, $\gamma$) $Na^{24}$ |
| Zirconium | 12.1 Mev | $Zr^{90}$ (n, 2n)$Zr^{89}$ |



Page 162 deleted.

TABLE 6.12 UNFUNDED GEOPHYSICAL EFFECTS INSTRUMENTATION

| Instrument | Location | Sponsor |
|---|---|---|
| Earth current | Newton, Massachusetts | Space Science, Inc. |
| Variometer | State College, Penna. | HRB-Singer, Inc. |
| Earth current | Ghana, West Africa | University of Chana |
| Variometers (N-S) (E-W) (vertical) | Brisbane, Australia | University of Queensland |
| Flux-gate magnetometer | Brisbane, Australia | University of Queensland |
| Variometer | Hobart, Tasmania | University of Tasmania |
| Magnetic and earth currents | Cold Bay, Alaska and Oamaru, New Zealand | Mather and Wescott |
| Metastable-helium magnetometer | Near Dallas, Texas | Texas Instruments |
| Large-loop magnetometer | Lebanon, New Jersey | USAERDL |
| Earth current | Lebanon, New Jersey | USAERDL |
| Rubidium vapor magnetometer | Lebanon, New Jersey | Columbia University |
| Earth current | Flamingo, Florida | USAERDL |
| Large-loop magnetometer | Baxter State Park, Maine | University of Maine |
| Large-loop magnetometer | Columbia, South Carolina | University of South Carolina |

TABLE 6.14 GROUND STATION POSITIONING DATA

| Station | Information | Actual Position (Preliminary) |
|---|---|---|
| Photo Station J820 Johnston Island | Latitude | 16°44'6"N |
| | Longitude | 169°31'43"W |
| | Absolute altitude | 7 feet |
| Mauna Loa Site Hawaii | Latitude | 19°32'21"N |
| | Longitude | 155°34'42"W |
| | Absolute altitude | 11,150 feet |
| Tutuila Site Samoa | Latitude | 14°19'18"S |
| | Longitude | 170°50'10"W |
| | Absolute altitude | 600 feet |
| Ovalau Site Fiji | Latitude | 17°41'36"S |
| | Longitude | 178°49'54"E |
| | Absolute altitude | 200 feet |
| Tongatabu Site Tonga | Latitude | 21°03'56"S |
| | Longitude | 175°04'33"W |
| | Absolute altitude | 20 feet |
| Haleakala Site, Maui Island, Hawaii | Latitude | 20°42'30"N |
| | Longitude | 156°15'25"W |
| | Absolute altitude | 10,000 feet |
| Camera Station J-811 Johnston Island | Latitude | 16°44'06.4"N |
| | Longitude | 169°31'43.4"W |
| | Absolute altitude | 10 feet |

TABLE 6.15 SLANT RANGES OF BIOMEDICAL AIRCRAFT

All distances are given in nautical miles slant range to burst.

| Shot | Aircraft | | | | |
|---|---|---|---|---|---|
| | P-1 | P-2 | P-3 | P-4 | P-5 |
| Star Fish Prime | 297 | 371 | 487 | 694 | 734 |
| Check Mate | No participation | | | | |
| King Fish | 506 | 113 | 205 | 306 | 405 |
| Blue Gill Triple Prime | 44 | 56 | 79 | 103 | Abort |
| Tight Rope | 25.8 | 56 | 99 | 150 | — |

TABLE 6.18 FALLING SPHERE MEASUREMENTS

| Rocket Number | Date | Time | Shot | Remarks |
|---|---|---|---|---|
| | 1962 | | | |
| 1 | 1 Jun | 1800W | — | Good data obtained. Shot postponed. |
| 2 | 19 Jun | 2230W | — | Good data obtained. Shot aborted. |
| 3 | 8 Jul | H−30 min | Star Fish | Good data obtained. |
| 4 | 23 Jul | 1940W | — | Good data obtained. Shot postponed. |
| 5 | 19 Oct | H + 10 min | Check Mate | Good data obtained. |
| 6 | 26 Oct | H + 15 min | Blue Gill | Good data obtained. |
| 7 | 29 Oct | 2300W | — | Background data. Good data obtained. |
| 8 | 1 Nov | H + 10 min | King Fish | Good data obtained. |
| 9 | 3 Nov | H + 4 min | Tight Rope | Failure of second stage to ignite produced much less than normal altitude, with consequent loss of most of the data. |

TABLE 6.19 SODIUM VAPOR TRAIL MEASUREMENTS

| Date | Time | Shot | Remarks |
|---|---|---|---|
| 1962 | | | |
| 1 Jun | Dusk | – | Rocket or payload failed. No data obtained. |
| 3 Jun | Dusk | – | Rocket or payload failed. No data obtained. |
| 19 Jun | Dusk | – | Rocket or payload failed. No data obtained. |
| 8 Jul | Dusk | Star Fish | Good data obtained. |
| 9 Jul | Dawn | Star Fish | Good data obtained. |
| 23 Jul | Dusk | – | Rocket second stage failed to ignite. No data obtained. |
| 23 Jul | Dusk | – | Good data obtained. |
| 15 Oct | Dusk | – | Rocket failed to reach programed altitude. No data obtained. |
| 19 Oct | Dusk | Check Mate | Flight canceled because of cloud cover. |
| 20 Oct | Dawn | Check Mate | Rocket misfired. No data obtained. |
| 25 Oct | Dusk | Blue Gill | Flight canceled because of cloud cover. |
| 26 Oct | Dawn | Blue Gill | Good data obtained. |
| 31 Oct | Dusk | King Fish | Rocket second stage failed to ignite. No data obtained. |
| 1 Nov | Dawn | King Fish | Good data obtained. |
| 2 Nov | Dawn | – | Good data obtained. |
| 2 Nov | Dusk | – | Good data obtained. |
| 3 Nov | Dusk | Tight Rope | Good data obtained. |
| 4 Nov | Dawn | Tight Rope | Rocket failed. No data obtained. |

Figure 6.1 86-foot-diameter antenna, Johnston Island
(DASA-26-6191-62 photo)

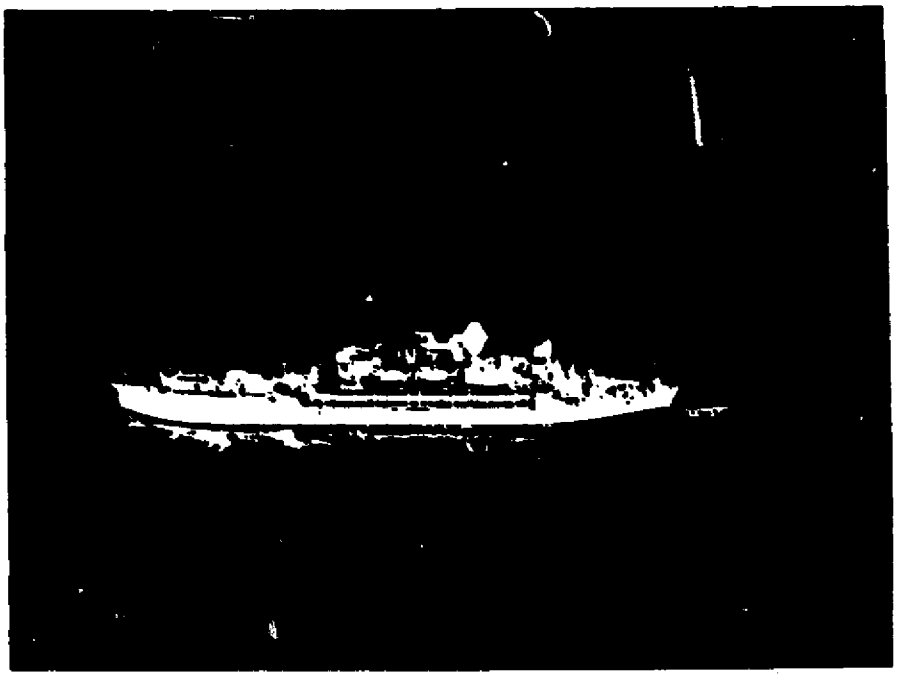

Figure 6.2 DAMP ship, USAS American Mariner.
(DASA-26-6744-62 photo)

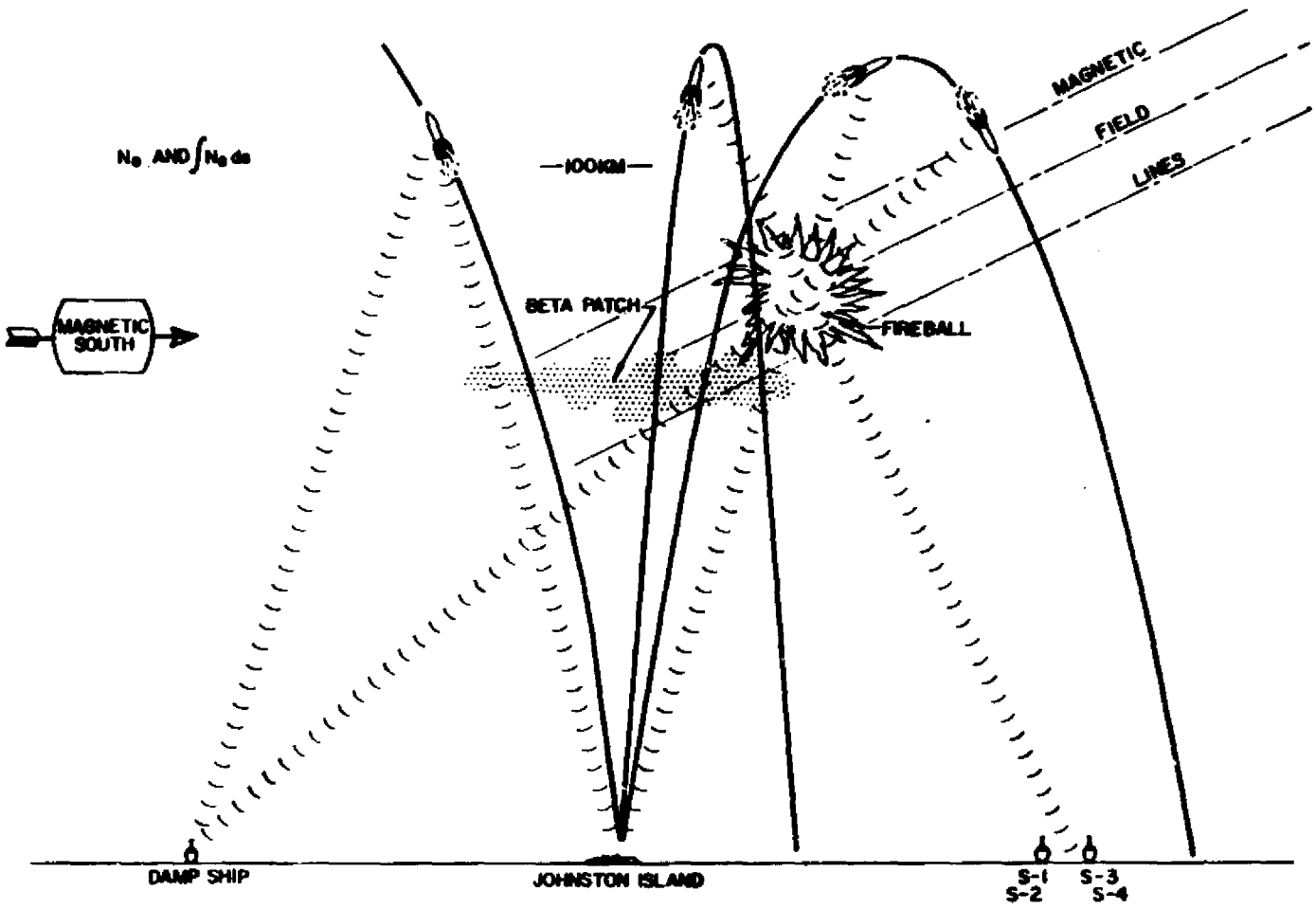


Figure 6.3 General experimental plan, radar attenuation.

Figure 6.4 Nike-Apache rockets with C-band beacon payloads. (DASA-26-6079-62 photo)

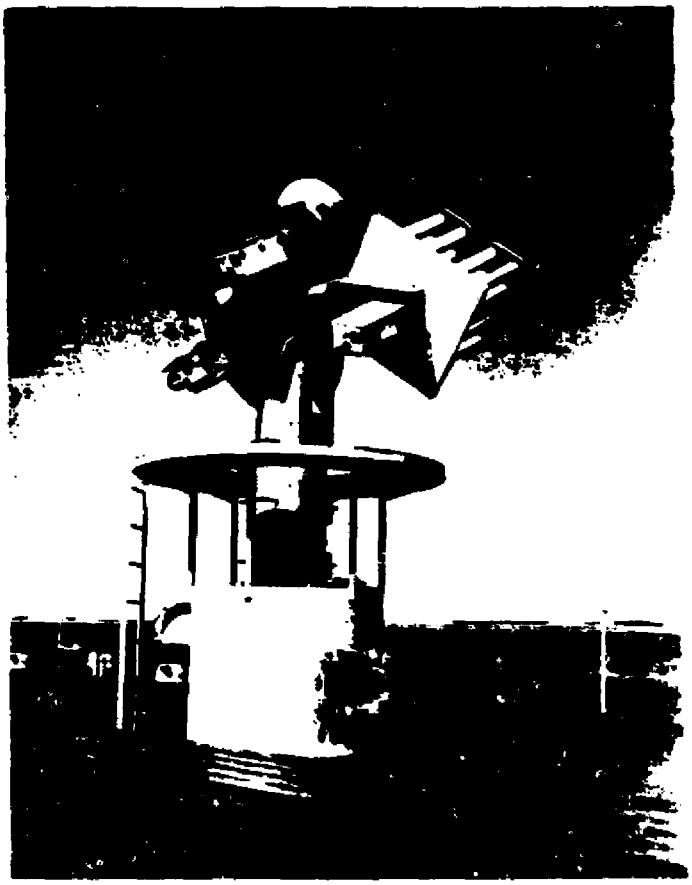

Figure 6.5 Shipboard antenna pedestal with L-, C-, and X-band antennas. (DASA-26-6835-62 photo)

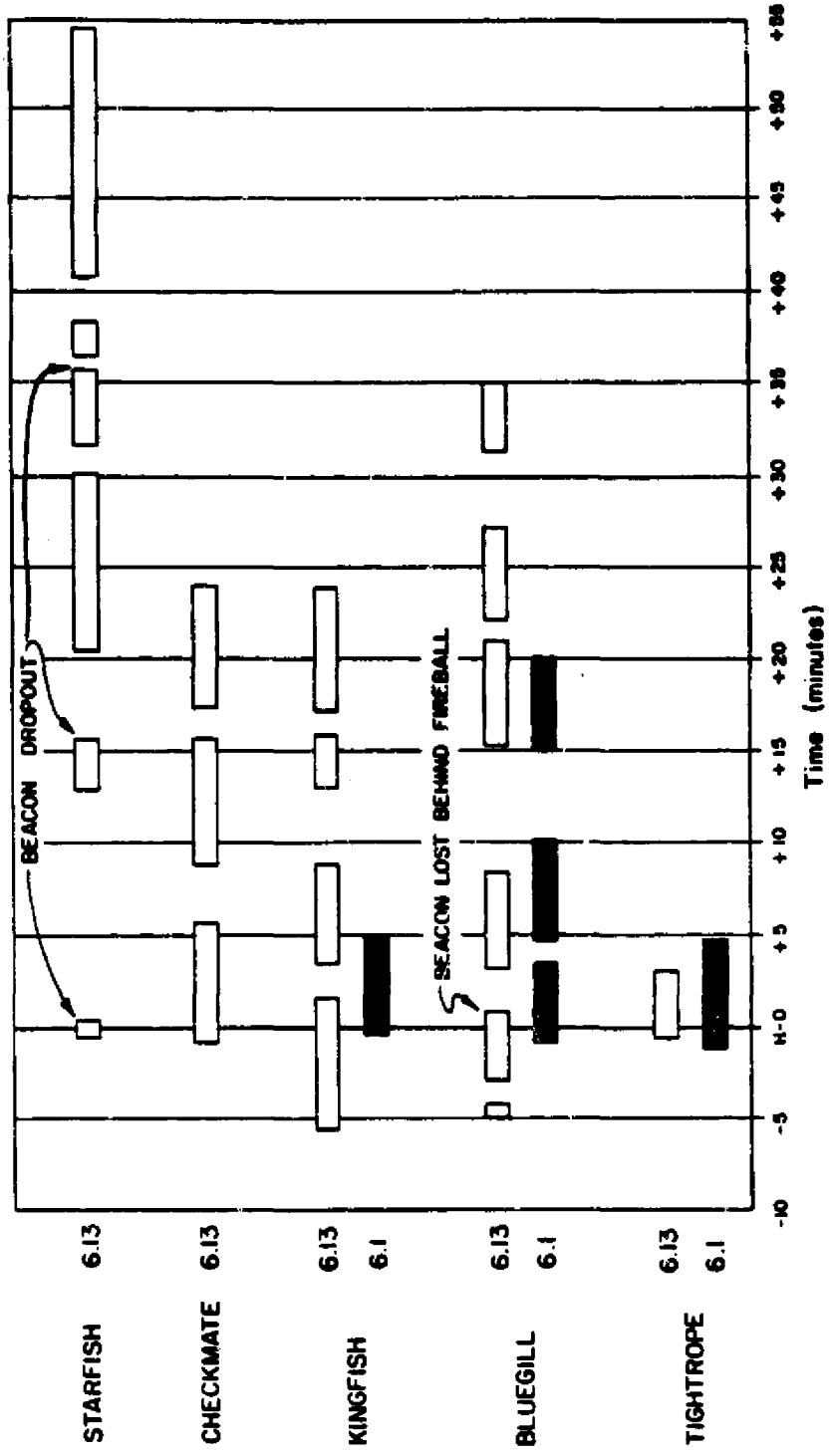


Figure 6.6 Data gathering times for Project 6.1 and 6.13.

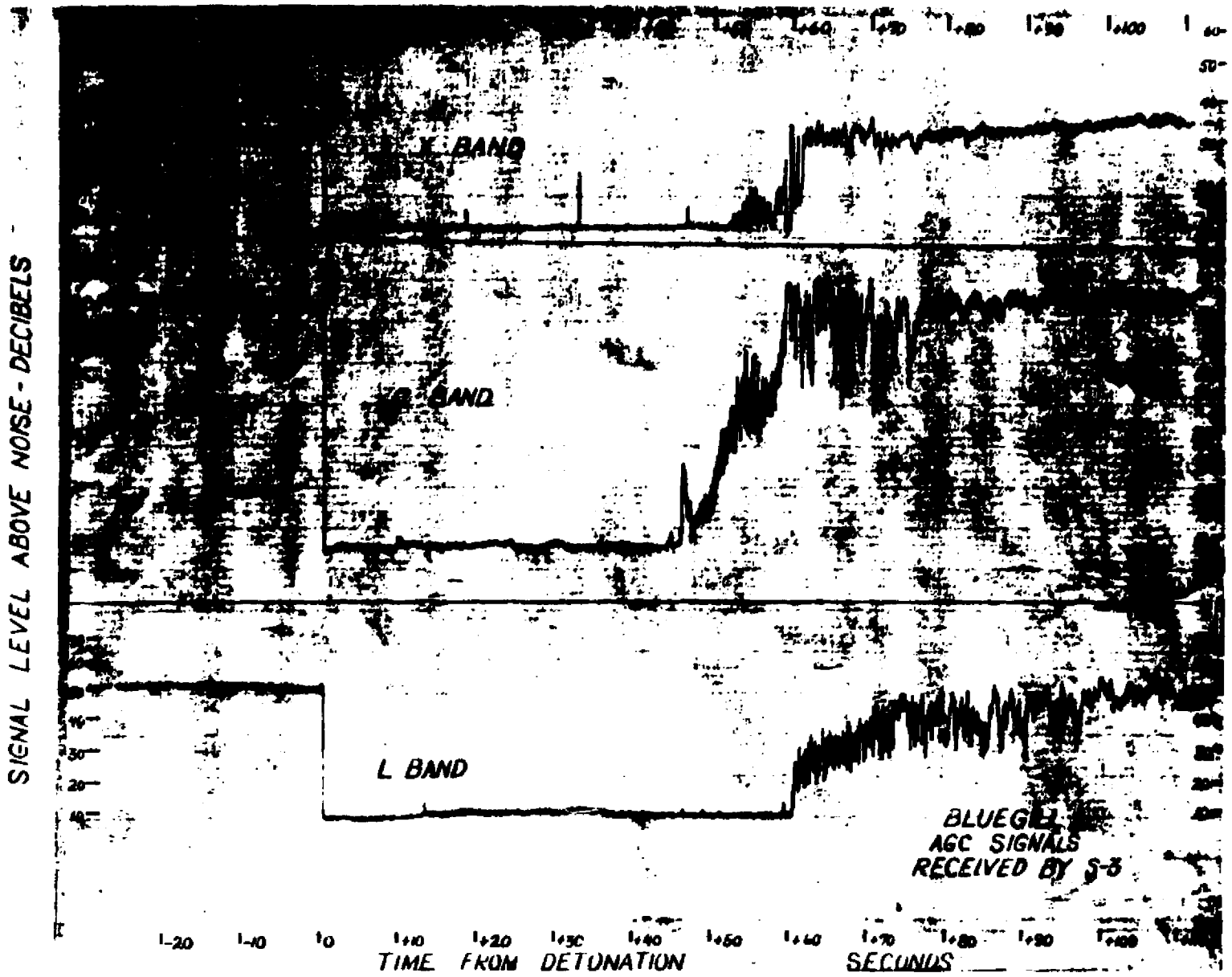


Figure 6.7 AGC record.

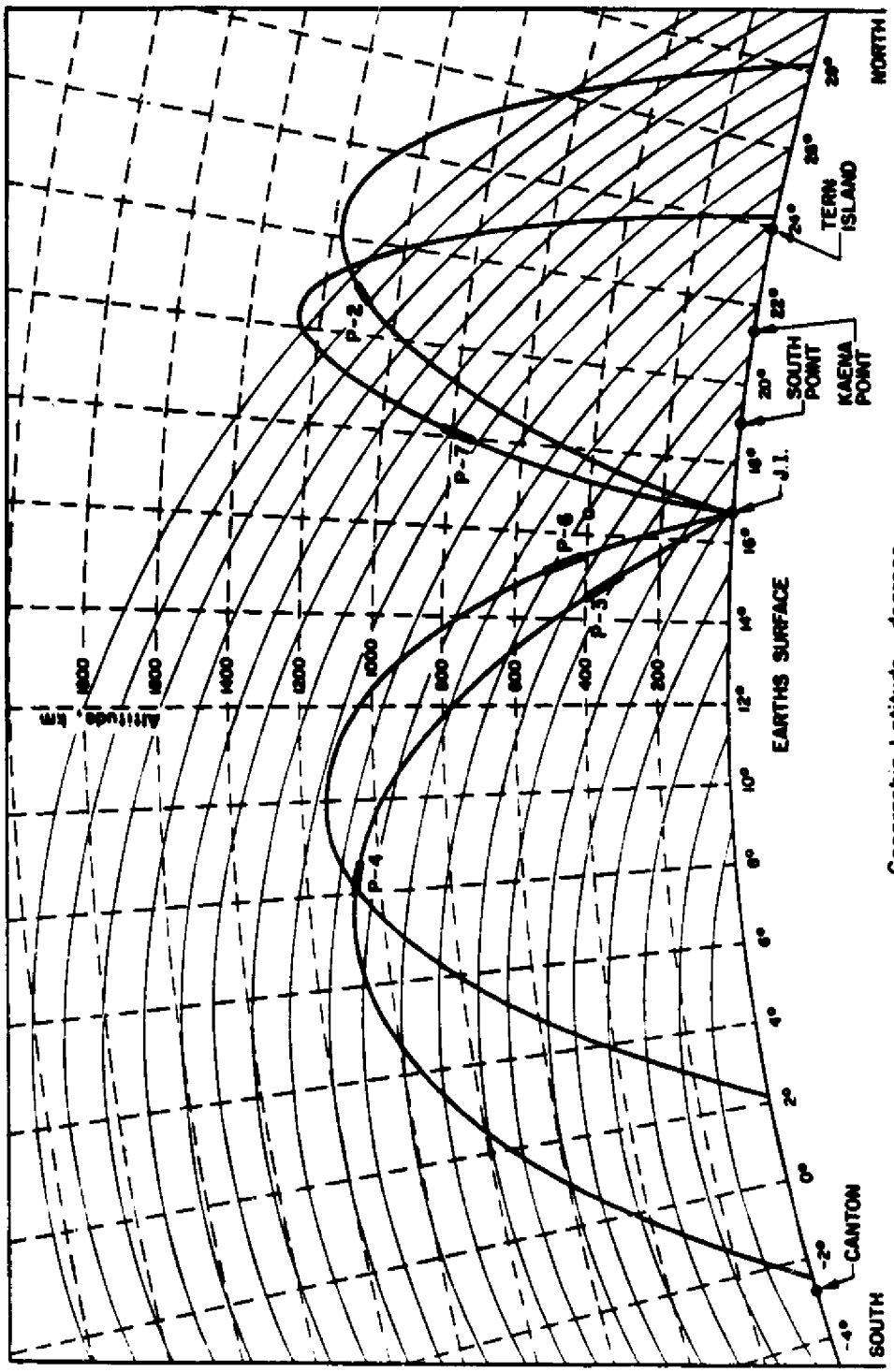


Figure 8.8 Rocket trajectories, Project 6.7, Shot Star Fish.

**Figure 6.9 Instrument array, Project 8A.3. (DASA-26-5986-62 photo)**

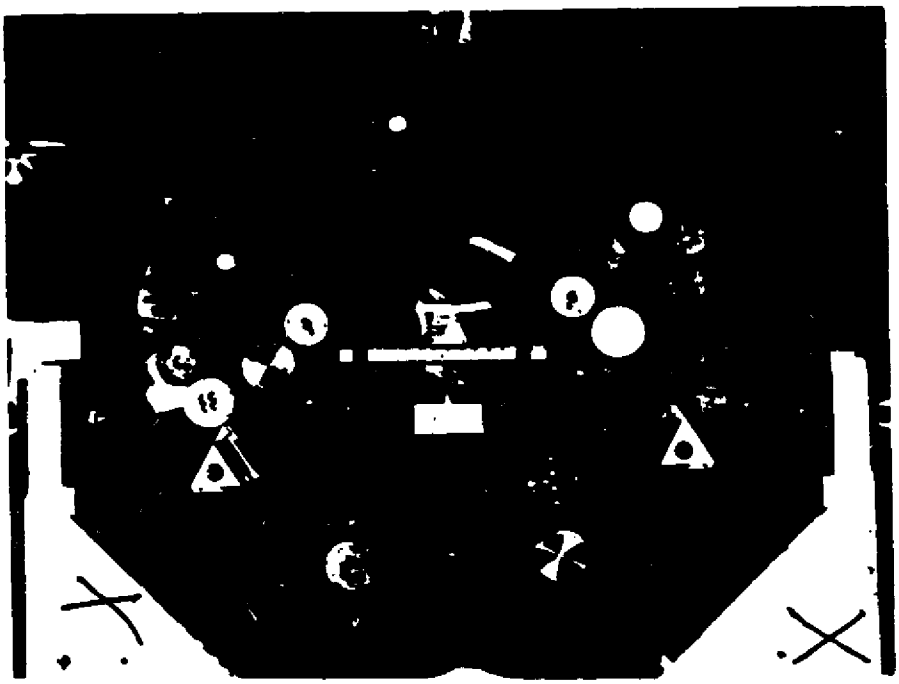

Figure 6.10 Instrument array on base of pod, Project 8B. (DASA-26-6246-62 photo)

Figure 6.11 Optical infrared aircraft, KC-135.
(DASA-26-14526-62 photo)

Figure 6.12 Interior of DOD photo station, Johnston Island. (DASA-26-6656-62 photo)



Pages 178 through 196
deleted.

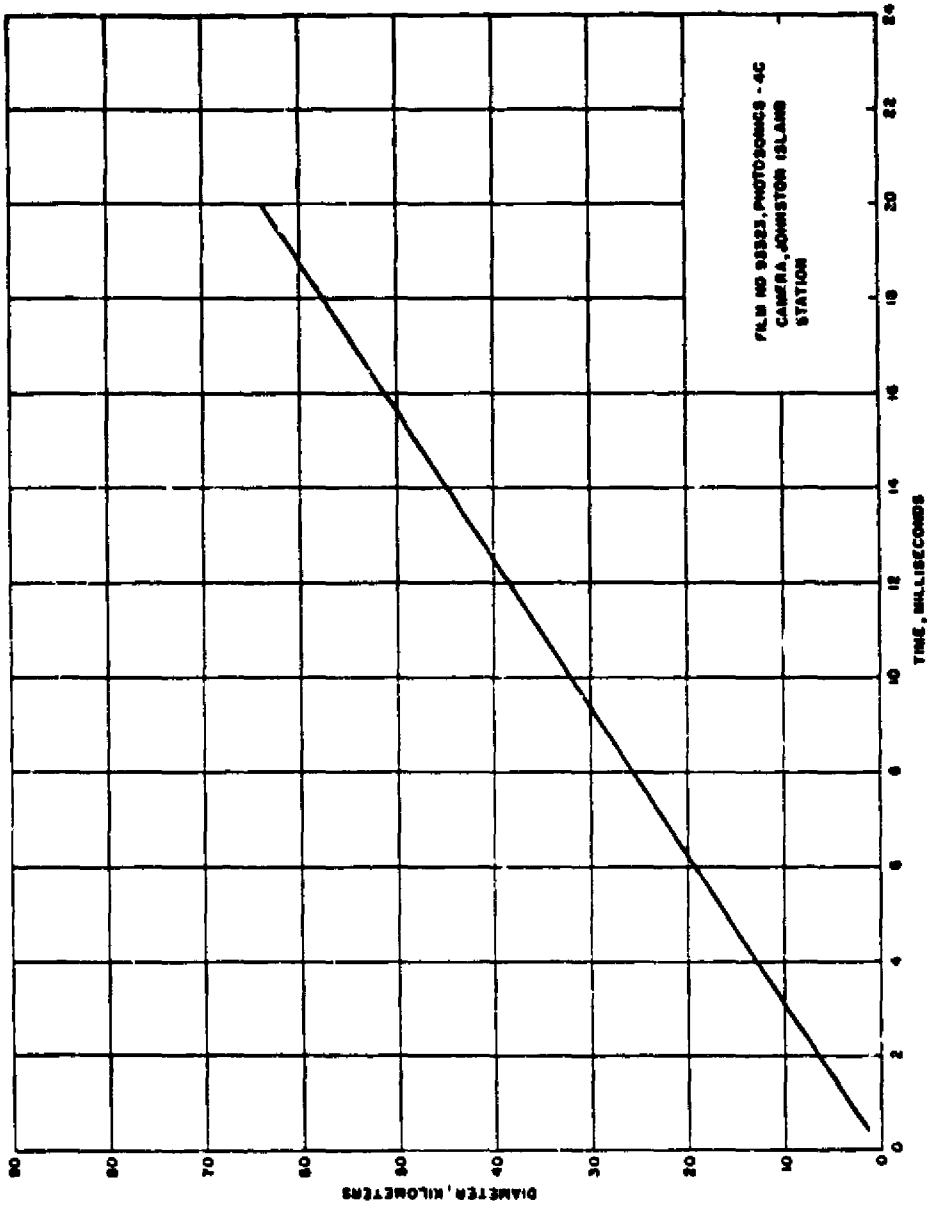


Figure 6.32 Debris diameter versus time, Shot Star Fish.

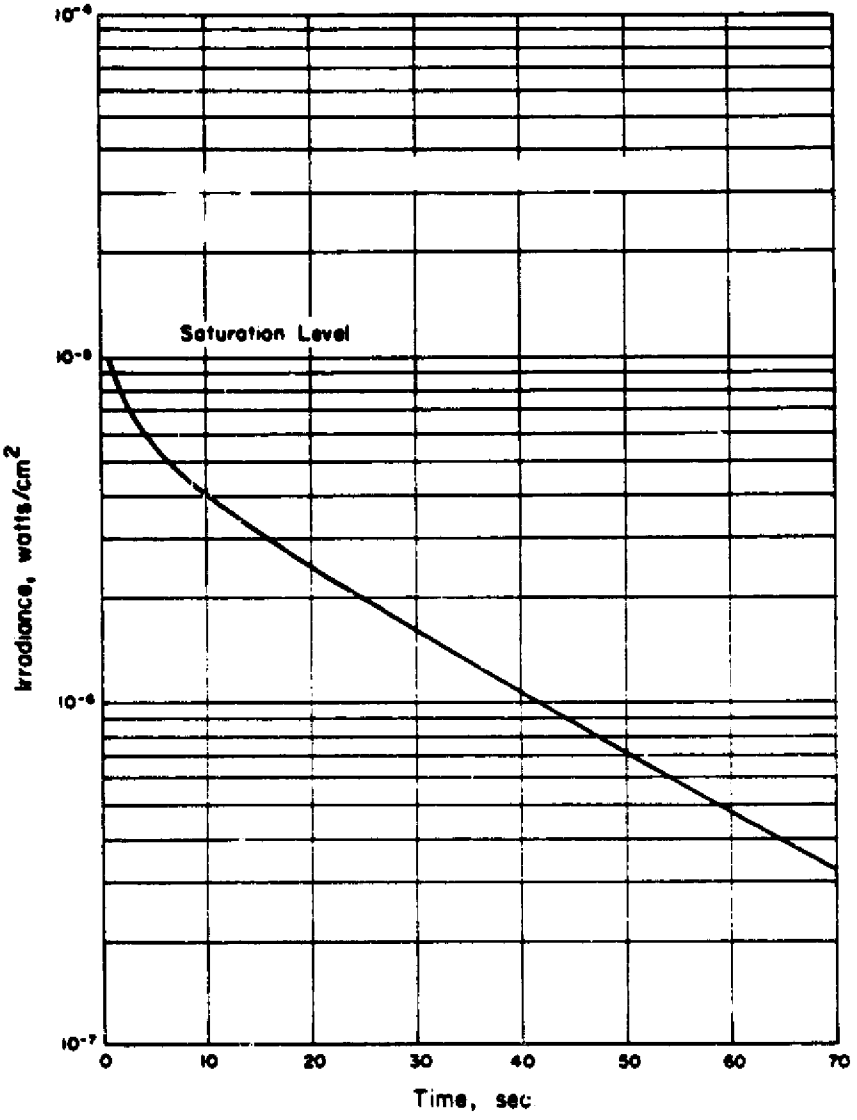


Figure 6.33 Irradiance versus time, 4.8 to 5.5 microns, Shot Star Fish.

**Figure 6.34 Blast instrument installation, Project 1.1. Also shows flywheel motor, tracking transponders and battery power supply. (DASA-26-5916-62 photo)**

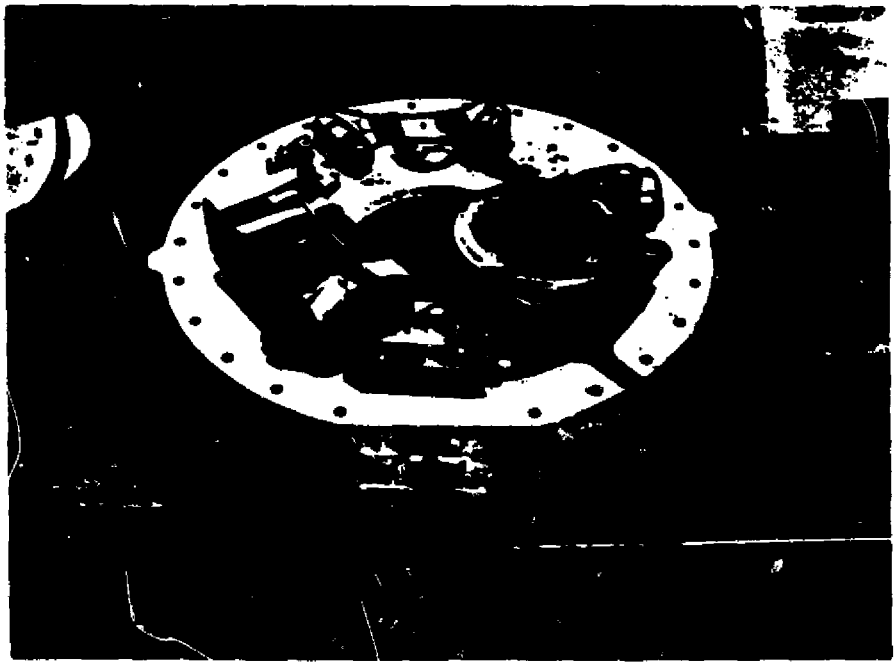

Figure 6.35 Accelerometer installation, Project 1.1. (DASA-26-5963-62 photo)

Figure 6.36 Nike-Cajun rocket with falling sphere payload. (DASA-26-5981-62 photo)

Chapter 7

## SUMMARY

Overall, Operation Dominic was very successful in that the great majority of the scientific objectives were achieved. In reviewing the operational, logistic, and fiscal aspects of the operation, it is obvious, however, that considerable improvement can be made in any similar future operation. Many of the problem areas were recognized at the time, but action for improvements could not be taken because of imposed time limitations. It is interesting to note that a previous plan to execute a similar operation stated that a minimum of 18 months would be required for the preparation phase.

A major deficiency noted was the lack of early coordination between Headquarters DASA, Washington, D. C., and the Weapons Effects and Tests Group (WET) at Sandia Base, New Mexico. This was basically due to the extremely compressed time schedule, not due to any lack of channels or to personalities. Early coordination is essential if the group fielding the DOD experiments is to understand thoroughly the basic objectives of each program. This understanding is necessary for the basis of decisions made in the field concerning each project.

The Fish Bowl program (events) and schedules were changed throughout the operation because of changing technical requirements and operational interactions and difficulties. Such changes must be expected in any future operation and allowances made during the planning phases to allow flexibility.

## 7.1 ADMINISTRATION AND SUPPORT

It is of primary importance that properly trained personnel are available in a large operation such as Dominic. Augmentation of WET by inadequately skilled personnel is extremely detrimental to the DOD in general. High standards for personnel are essential if the DOD scientific group is to maintain the respect of the national scientific community and successfully achieve the assigned missions.

Because of the late arrival of key personnel on augmentation, the administrative effort suffered in that organization, job training and orientation had to be accomplished rapidly before deployment. Insufficient time was available to smooth out standing operating procedures (as indicated in the discussion in Chapter 2) for classified document control, postal services, orders, and pay and allowances services.

Security problems were complicated by personnel arriving in the Pacific without proper clearances. Some personnel were not properly oriented on security, resulting in security violations that could have been avoided. Classification of photography remained a problem throughout the operation, because all photographs were classified Secret Restricted Data until reviewed by an authorized classification officer. Too few classification officers were assigned, resulting in voluminous documentation to control Secret Restricted Data photography.

Public releases were centrally controlled during Operation Dominic, resulting in ill feeling on the part of governments in the Southern Conjugate Area. Planning in the future

must provide for the timely furnishing of releases to the various governments. Although this was not their responsibility, personnel of TU 8.1.3 were expected to provide releases and to placate the governments when releases arrived late or from other than official sources.

## 7.2 OPERATIONS

The technical operations centers (TOC's) established at Johnston Island and Hickam AFB were essential to the success of the operation. Future plans should contain detailed plans for TOC's and should provide for adequate communications. The Dominic TOC's were originally conceived to be modest installations, but by necessity soon grew into complex centers.

Great care should be exercised in the future to obtain shot-time locations, speeds, courses, headings, and altitudes (aircraft) of aircraft and ships participating in the scientific collection effort. The procurement of this data was difficult in Dominic, in spite of preevent requests. Positioning criteria for both ships and aircraft must be realistic and must be thoroughly coordinated between the technical and operational personnel.

Greater care should be exercised in the small rocket program to insure closer conformity with established safety criteria. This will require better storage facilities, safe separation distances between launchers and other facilities, and better management. This last item ideally could be provided by utilizing a single agency to operate a small rocket control center, supervise rocket assembly, etc.

Readiness reporting became more satisfactory as communications improved. If the status of remote stations is to be considered when event time nears, rapid communications must be available. Simple voice codes were used during the Fish Bowl Series, greatly simplifying operations. Greater use of these codes should be considered in the future.

The tracking system used by TU 8.1.3 was extremely slow in producing usable data. Redundancy should be provided in the system to insure obtaining positioning data. Computer programs should be written prior to deployment. In Dominic, the original concept of data reduction long after completion of the operation was quickly discarded. Data reduction, especially in the tracking project, must be rapid to permit early evaluation of results. The equipment used in Dominic appeared satisfactory, but should be improved.

Clear lines of authority are needed in remote areas such as the Southern Conjugate Area. Control in that area was almost nonexistent due to lack of firm policies. Duties delegated to local project personnel must be clearly understood. Consideration should be given to more formal relationships with other governments in order to prevent ill feelings over relatively small matters. This is important where great interest exists in test programs. Where possible, early notification of pending tests to local government officials is desirable, along with description of the expected visible effects of the tests.

Equipment sent to remote locations must be thoroughly inspected and repaired prior to shipment. It is costly to airlift replacement equipment when simple precautions can prevent operating under pressure resulting from equipment malfunctions.

Participation on the AEC developmental events on Christmas Island again demonstrated the problems of fielding experiments with unproven equipment. This was shown by the extreme problems that developed with the Project 7.3 aircraft, due to the rush to deploy to the test area without proper preparation.

Although communications were ultimately satisfactory during Dominic, they should be improved in any future operation and should be phased in earlier in the preparation period. The use of makeshift systems is to be discouraged because of low reliability.

## 7.3 SPECIAL INTEREST AREAS

The pods as used for instrument carriers in Dominic were marginal in performance. Stabilization was unsatisfactory, resulting in much lost data. No pod system should be considered for use in a future operation without complete testing, to include satisfactory instrumented test flights. It is apparent from Dominic experience that instrumented pods are practicable and that they can be used to collect data not otherwise obtainable.

High-performance aircraft can be modified to serve as excellent instrument platforms, if exacting positioning is not required. The ability to fly over existing high cloud layers was of great benefit to the optical programs. Modification of modern stressed-skin aircraft is a complex engineering job, and adequate time must be programed for such modification if premium time rates are to be avoided by contractors.

## 7.4 SCIENTIFIC ACTIVITY

The experiments fielded in the Fish Bowl Series, in particular, and Operation Dominic, in general, were very successful. In spite of the great distances involved and the sometimes marginal communications, the various projects were able to measure the effects as programed. The greatest loss of data was in those projects depending on pod performance. These projects were able to fulfill some objectives, but did not in all cases obtain acceptable results.

For detailed scientific results, the reader is referred to the quick-look reports published by Joint Task Force EIGHT and by the DASA Data Center, Santa Barbara, California; and the POR's published by DASA (Appendix A).

Appendix A

## LIST OF PROJECT OFFICERS REPORTS

| Project Number | Title | POR (WT)' Number |
|---|---|---|
| OPERATION DOMINIC, SHOT SWORD FISH | | |
| 1.1 | Underwater Pressures (NOL) | 2000 |
| 1.2 | Surface Phenomena (NOL) | 2001 |
| 1.3a | Effects of Underwater Nuclear Explosions on Sonar Systems at Close Range (NEL) | 2002 |
| 1.3b | Effects of an Underwater Nuclear Explosion on Hydroacoustic Systems (NEL) | 2003 |
| 2.1 | Radiological Effects from an Underwater Nuclear Explosion (NRDL) | 2004 |
| 3.1 | Studies of Shock Motions of Hull and Equipment (DTMB) | 2005 |
| 9.1 | Ship Damage Assessment and Technical Support of Test Elements (BuShips) | 2006 |
| | Scientific Director's Summary Report (DTMB) | 2007 |
| OPERATION DOMINIC, FISH BOWL SERIES | | |
| 1.1 | Blast Measurements at Various Distances from High-Altitude Nuclear Detonations (BRL) | 2010 |
| 1.2 | Shock Photography (NOL) | 2011 |
| 2.1 | External Neutron Flux Measurements (NDL) | 2012 |
| 2.2 | Gamma Radiation Measurements (NDL) | 2013 |
| 2.3 | Alpha Contamination Monitoring (NDL) | 2052 |
| 6.1 | Fireball Attenuation (ELRDA/AFSWC) | 2015 |
| 6.2 | Gamma-Ray Scanning of Debris Cloud (BRL) | 2017 |
| 6.3 | D-Region Physical Chemistry (BRL) | 2018 |
| 6.4 | E- and F-Region Physical Chemistry (AFCRL) | 2019 |
| 6.5a | Ionospheric Soundings and Magnetic Measurements (AFCRL) | 2020 |
| 6.5b | Ionospheric Measurements in Southern Conjugate Area (IIT) | 2021 |
| 6.5c | Vertical Ionospheric Sounding Measurements (NBSCRPL) | 2022 |
| 6.5d | Effects of Thermonuclear Radiation on the Ionosphere (RPA) | 2023 |
| 6.5e | Magnetic Measurements (SRDL) | 2024 |
| 6.6 | Long-Term Debris History (GCA) | 2025 |
| 6.7 | Debris Expansion Experiment (AFSWC) | 2026 |

| Project Number | Title | POR (WT) Number |
|---|---|---|
| 6.8 | Riometer Measurements (AFCRL) | 2027 |
| 6.9 | Radar Clutter Measurements (SRI) | 2028 |
| 6.10 | High-Altitude Nuclear Detonation Effects on Ionospheric Properties (AFCRL) | 2029 |
| 6.11 | HF Communication Experiment (SRDL) | 2030 |
| 6.12 | Piggyback Satellite Packages (AFCRL) | 2031 |
| 6.13 | RF Measurements and Optical Measurements (AMCD) | 2032 |
| 7.2 | Radiofrequency Radiometry (MITLL) | 2034 |
| 7.4 | Communication Propagation Investigation Equipment (ASD) | 2044 |
| 8A.1 | High-Altitude Nuclear Detonation Optical-Infrared Effects (AFCRL) | 2035 |
| 8A.2 | Optical Phenomenology of High-Altitude Nuclear Detonations (EG&G) | 2036 |
| 8A.3 | Structural Response to Thermal Radiation from High-Altitude Fireball (ASD) | 2037 |
| 8B | Nuclear Weapon X-Ray Effects as Measured by Passive Instruments (AFSWC) | 2038 |
| 8C | Reentry Vehicle Tests (AFSWC). POIR is considered final. | 2039 |
| 9.1a | Atmospheric Properties (AFCRL) | 2040 |
| 9.1b | Ionospheric Wind Measurements (AFCRL) | 2051 |
| 9.4b | Pod and Recovery Unit Fabrication (AFSWC) | 2041 |
| 9.6 | Tracking and Positioning (Cubic) | 2042 |
| OPERATION DOMINIC, CHRISTMAS AND FISH BOWL SERIES | | |
| 4.1 | Production of Chorioretinal Burns by Nuclear Detonations and Tests of Protective Devices and Phototropic Materials (AFSAM) | 2014 |
| 7.1 | Electromagnetic Signal, Underwater Measurements (KN) | 2033 |
| OPERATION DOMINIC, CHRISTMAS SERIES | | |
| 4.2 | Photoelectric and Psychophysical Measures of Nuclear Weapons Flashes (NADC) | 2016 |
| 7.3 | Microwave Attenuation Due to Nuclear Burst (ELRDA) | 2043 |
| 7.5 | Thermal Radiation from Air Burst Nuclear Weapons Incident on Low-Altitude Aircraft (ASD). Published as ASD-TDR-62-823; available from Defense Documentation Center (formerly ASTIA), Arlington Hall, Arlington 12, Virginia | |
| Operation Dominic: Organizational, Operational, Funding, and Logistic Summary | | 2053 |

Appendix B

## MAPS OF PACIFIC ISLANDS

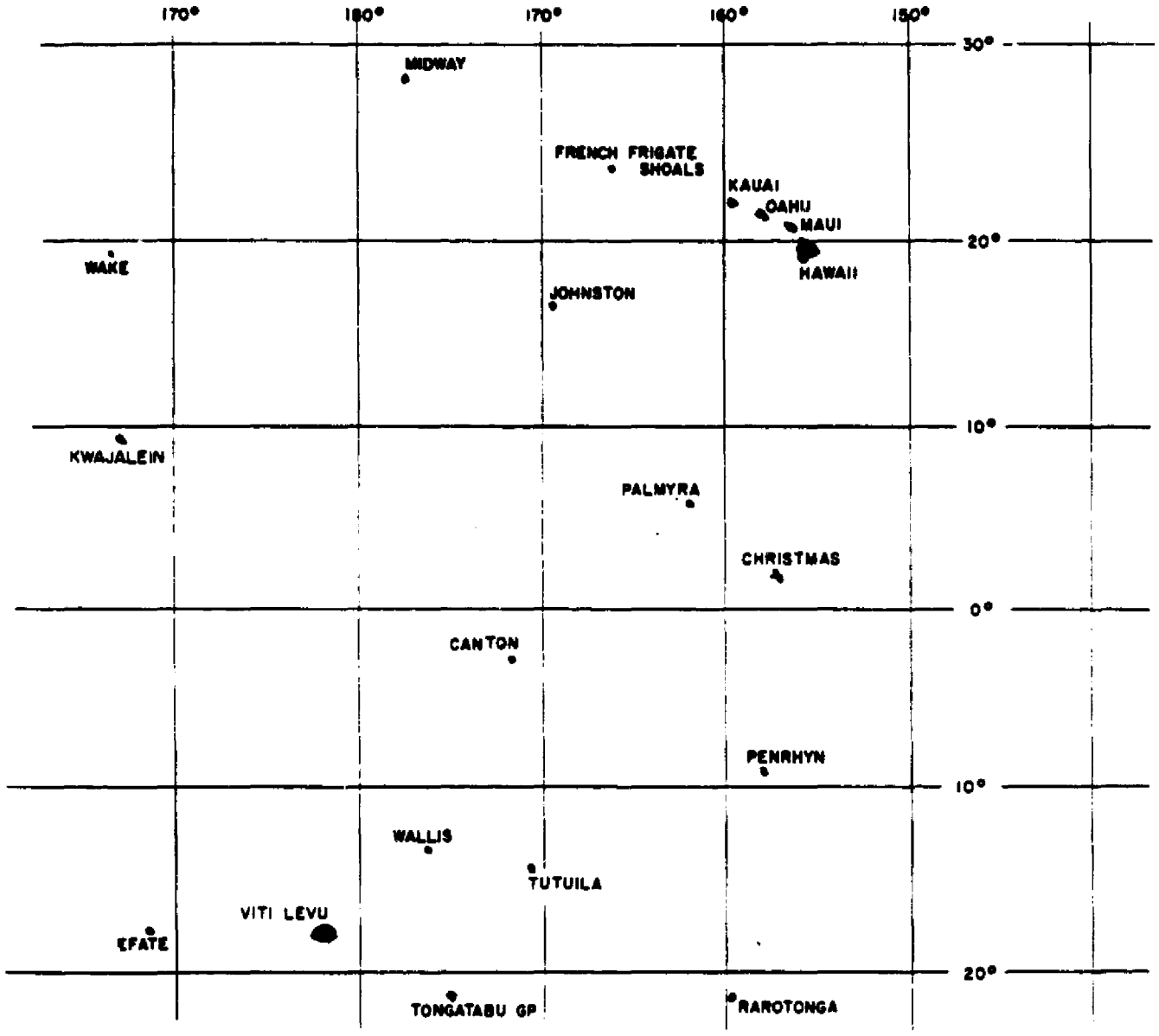


Figure B.1 Pacific Ocean area.

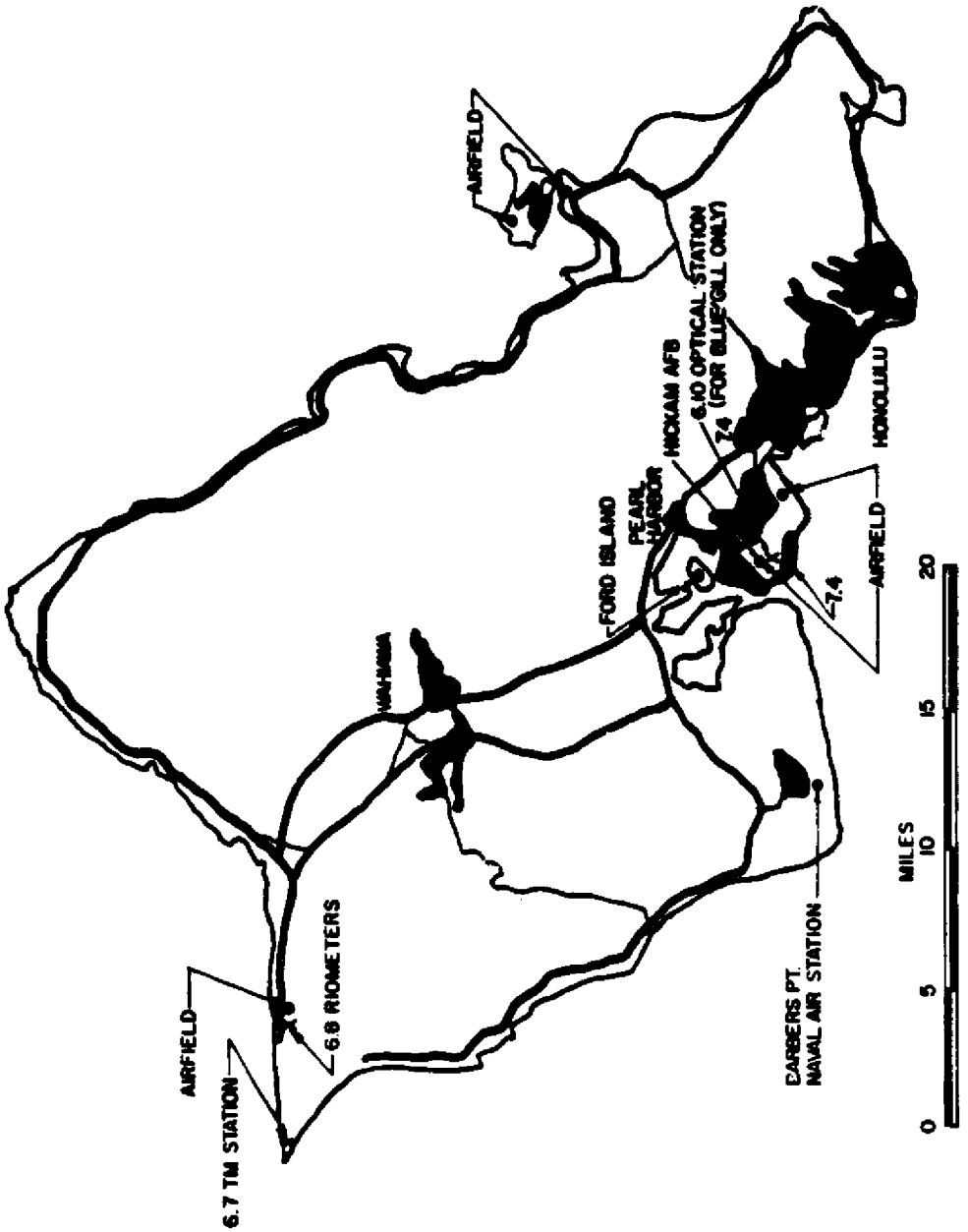


Figure B.2 Oahu.

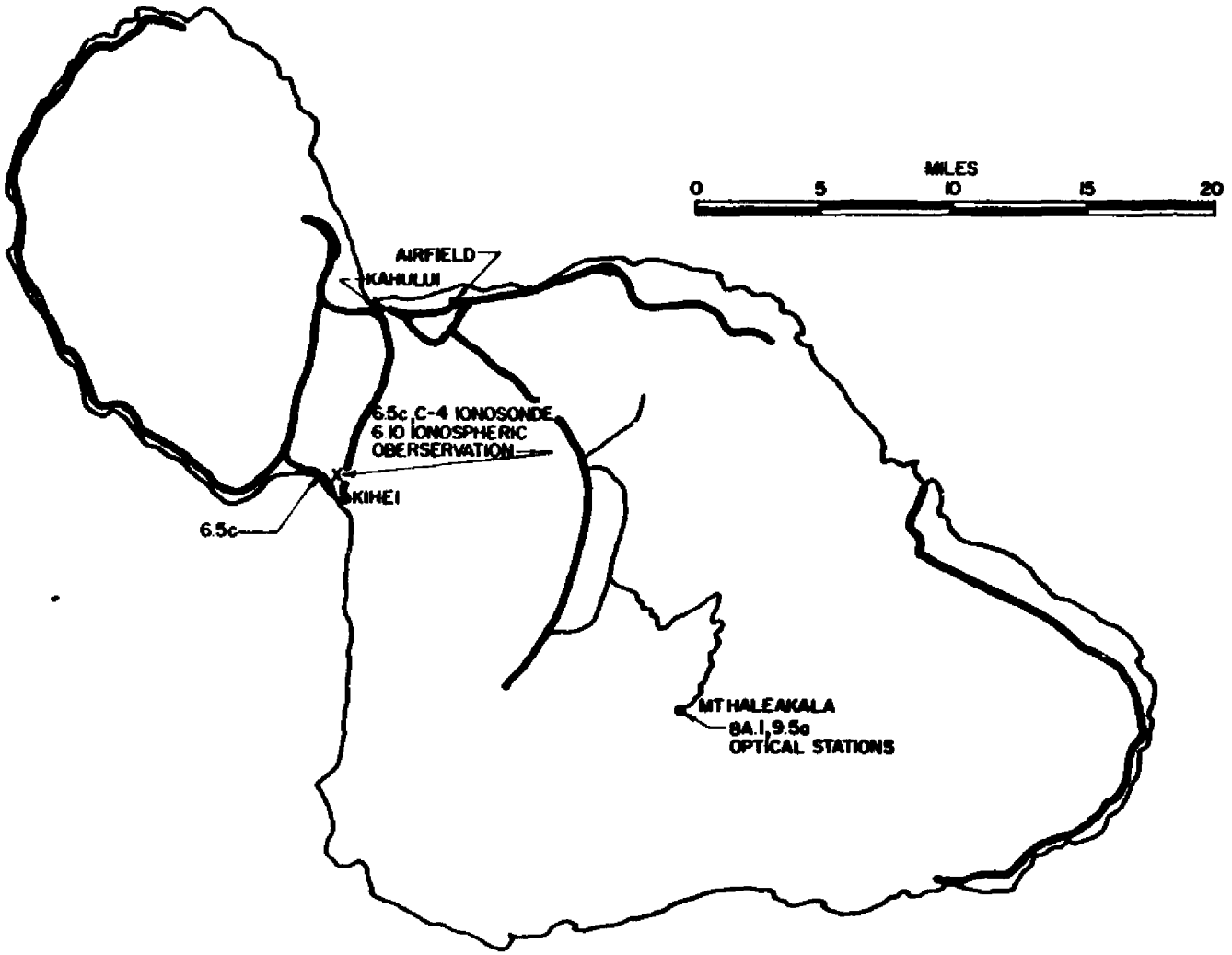


Figure B.3 Maui.

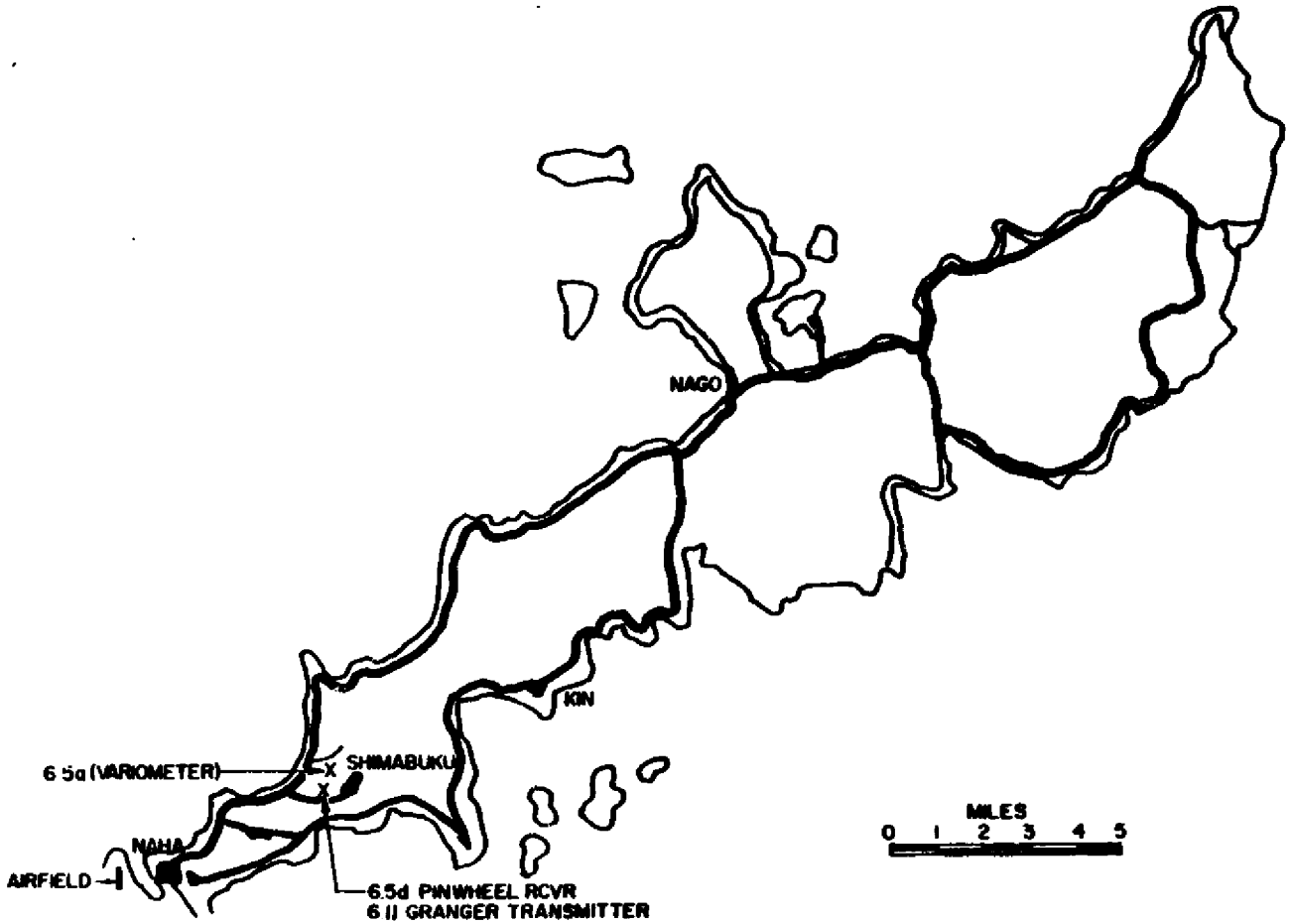


Figure B.4 Okinawa.

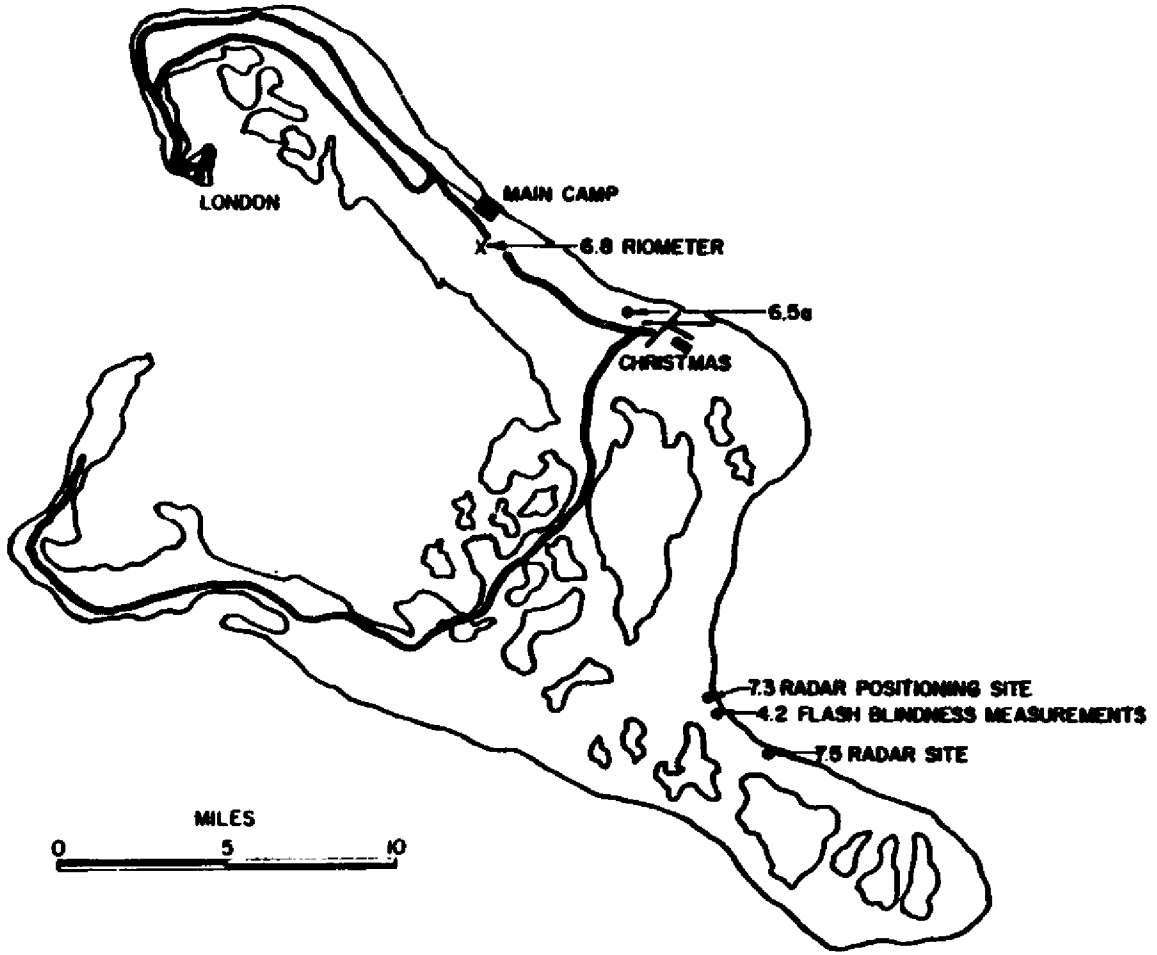


Figure B.5 Christmas Island.

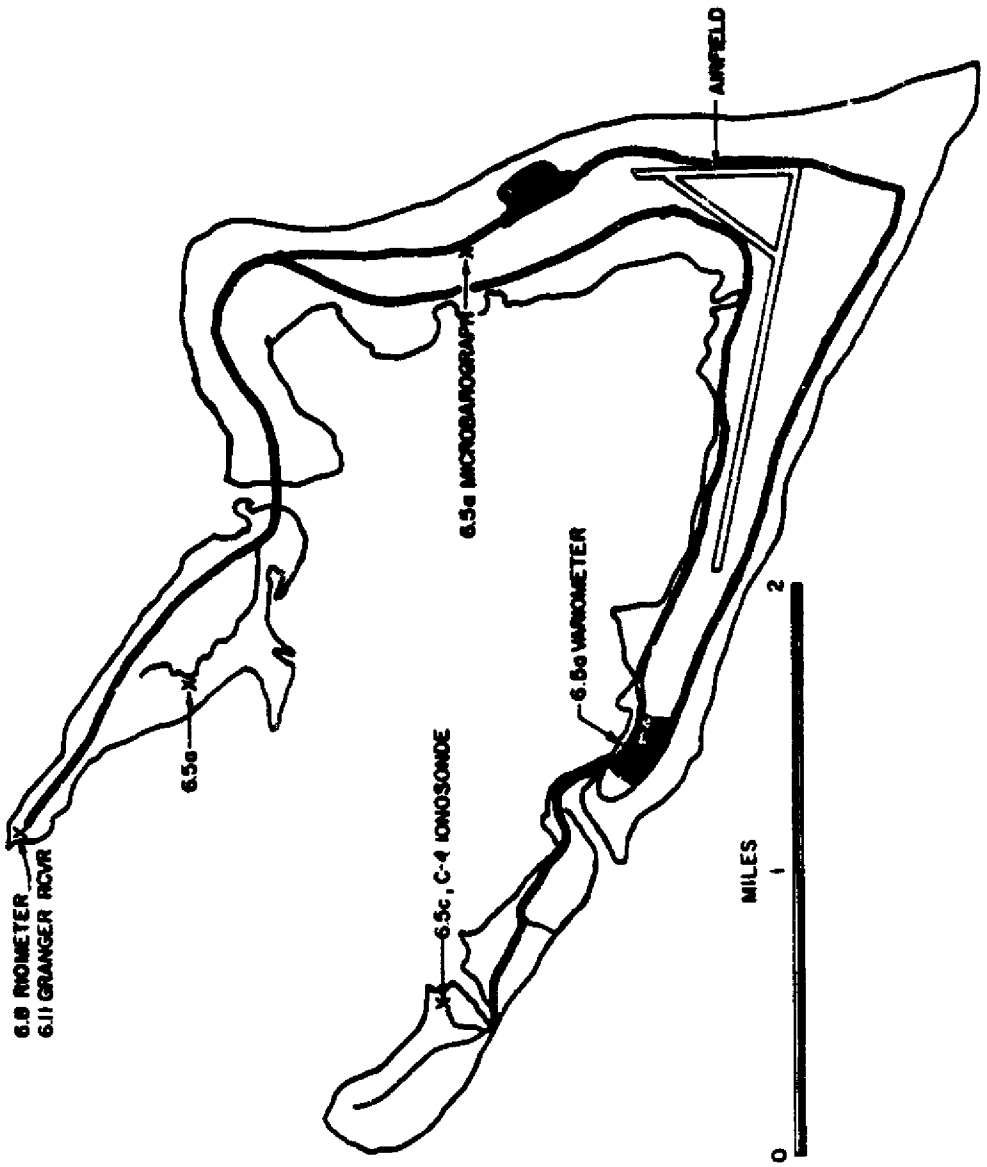


Figure B.6 Wake.

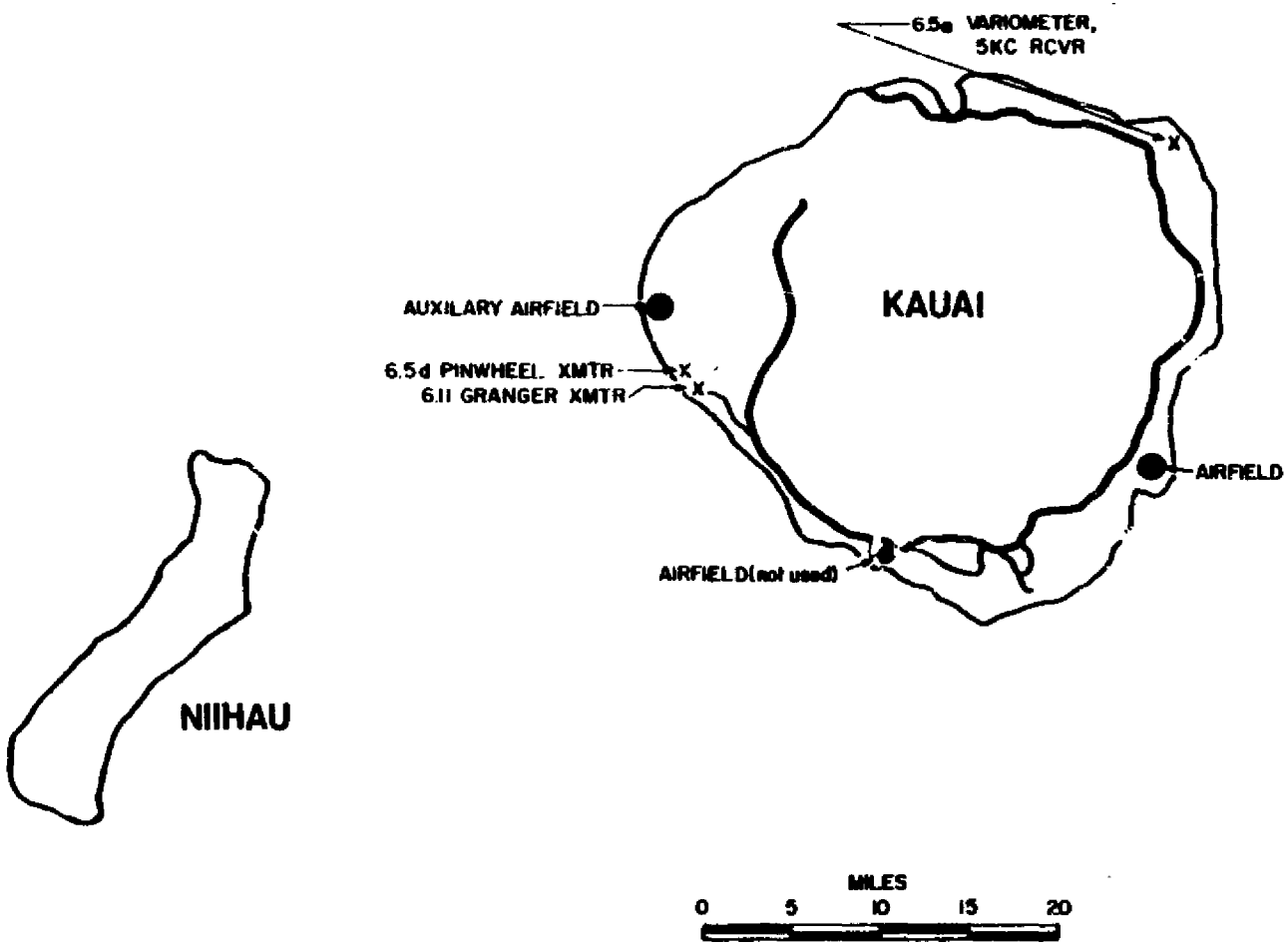


Figure B.7 Kauai.

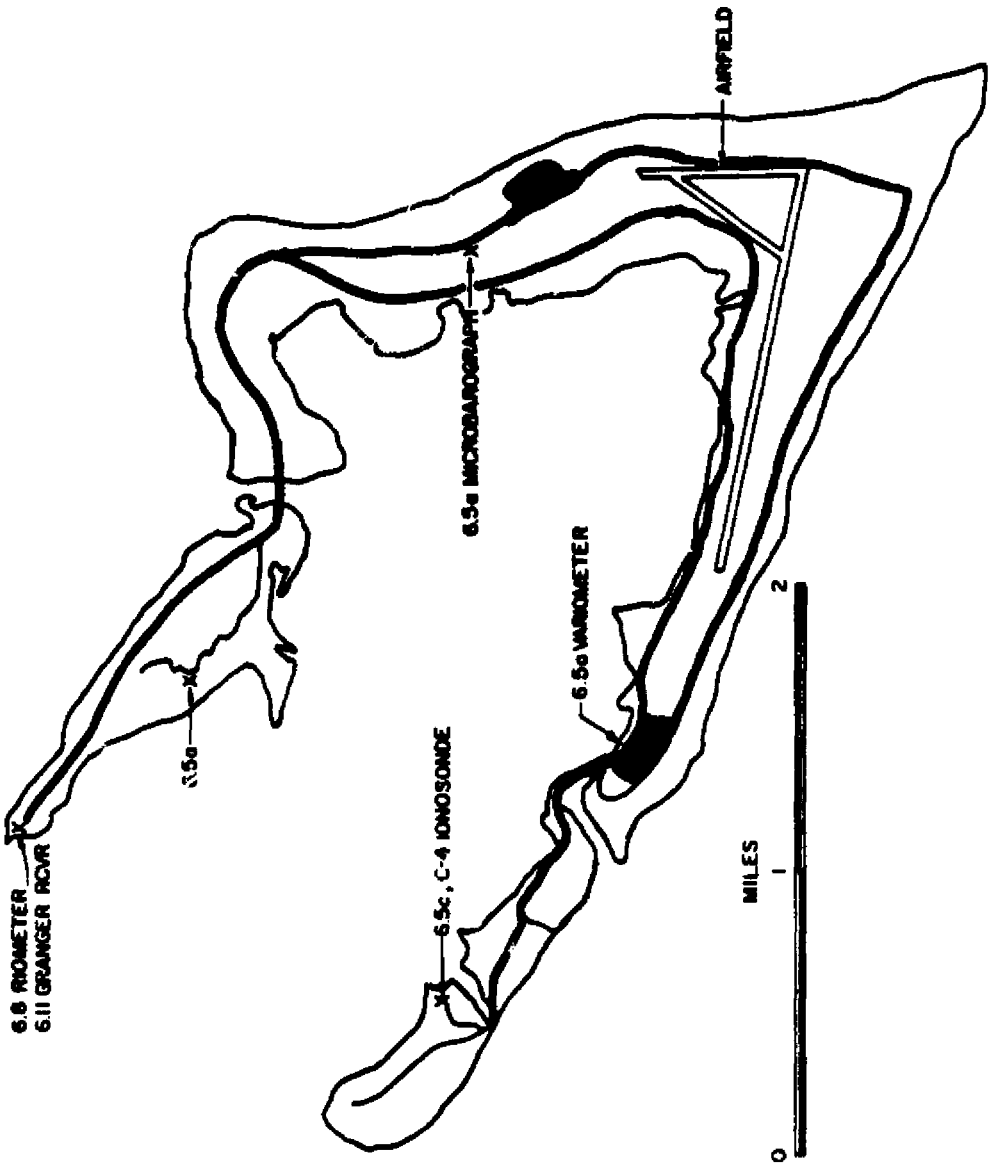


Figure B.6 Wake.

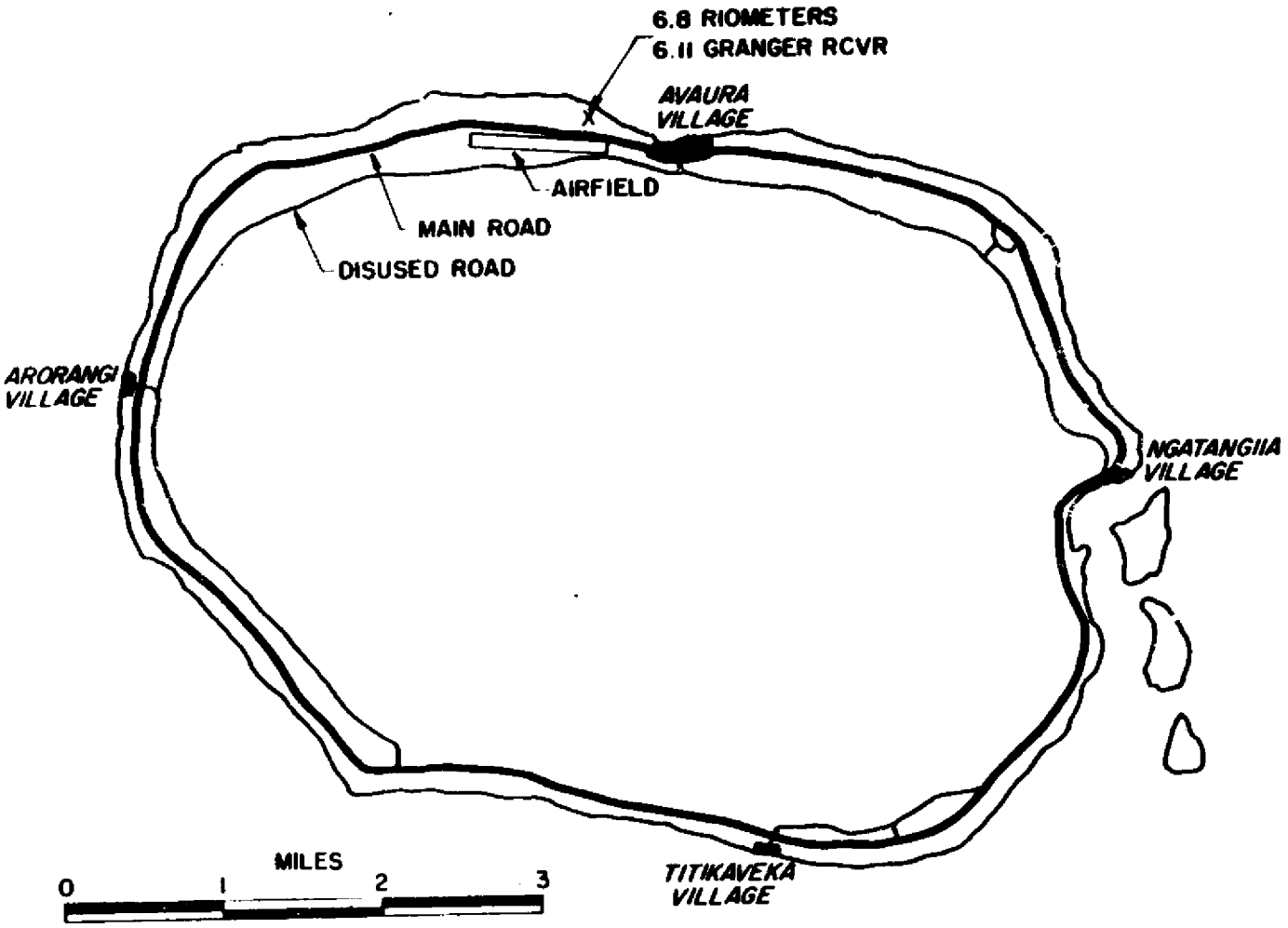


Figure B.8 Rarotonga.

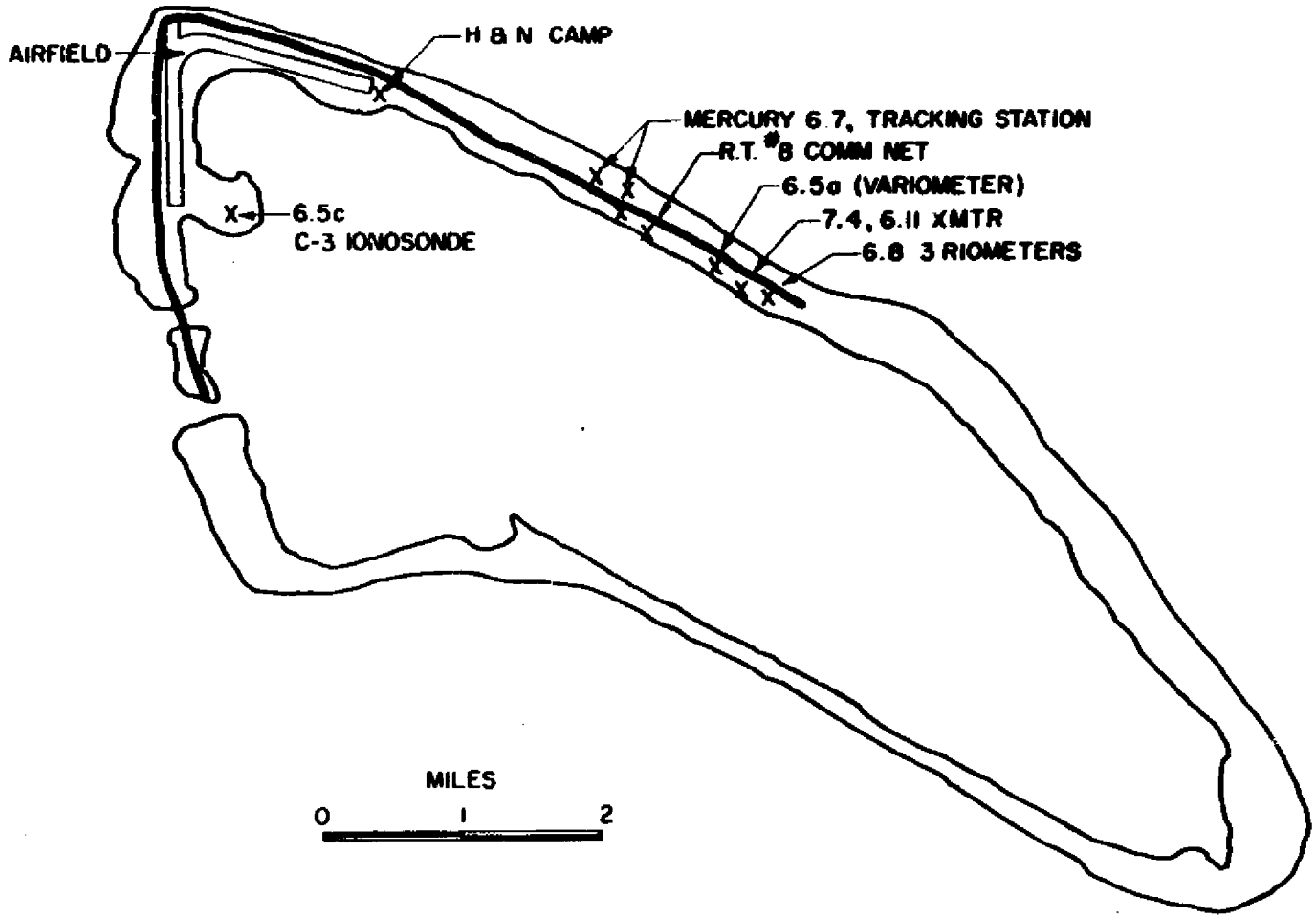


Figure B.9 Canton.

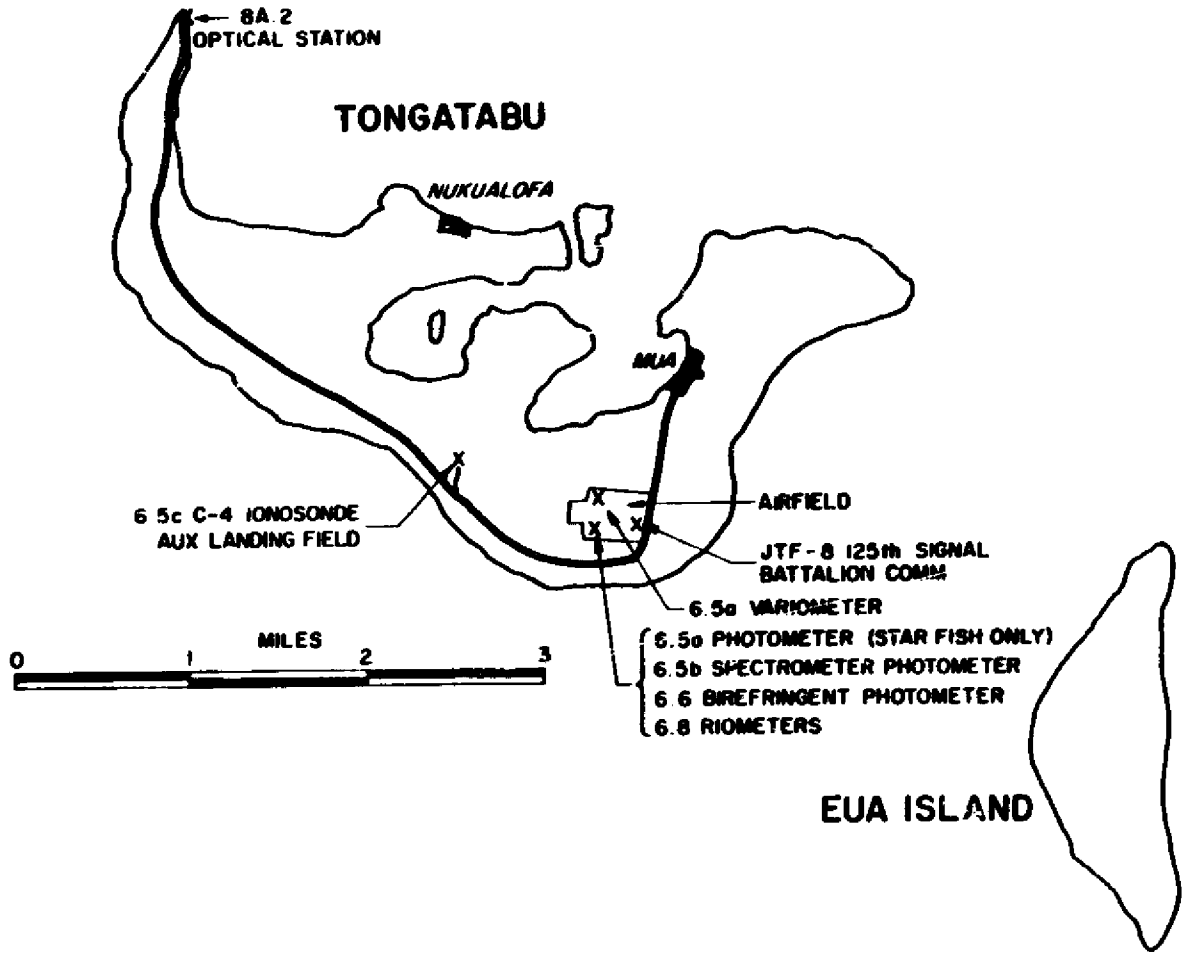


Figure B.10 Tongatabu.

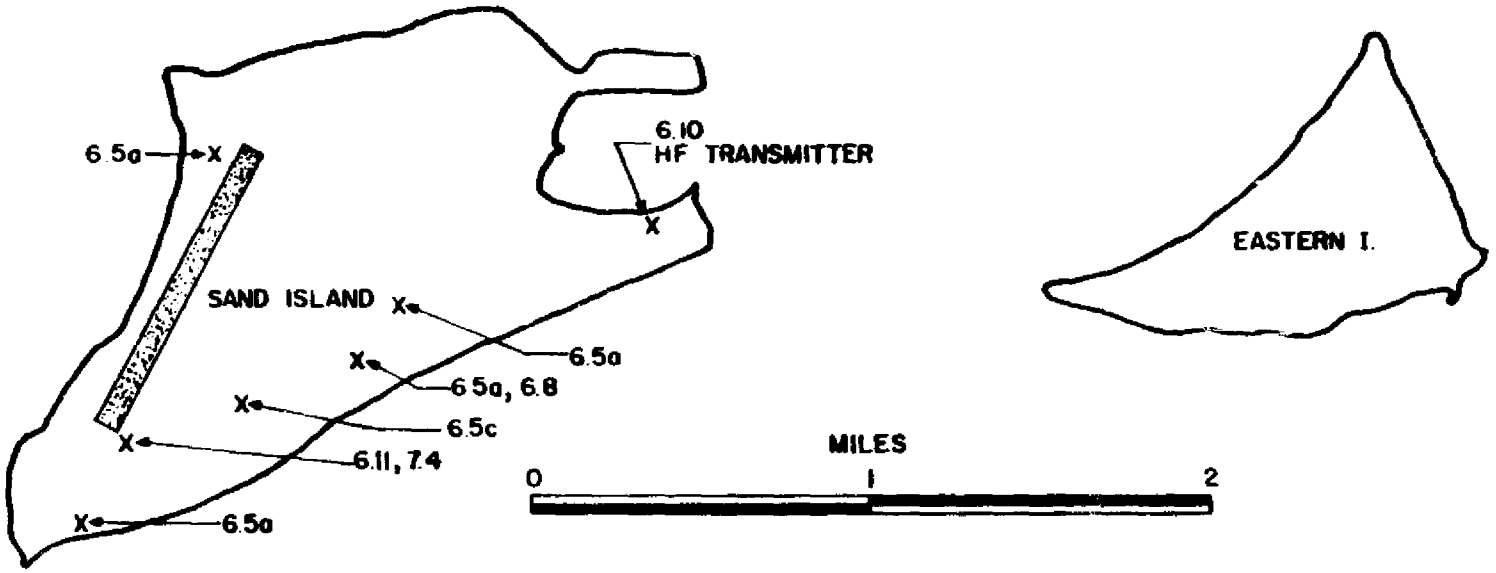


Figure B.11 Midway.

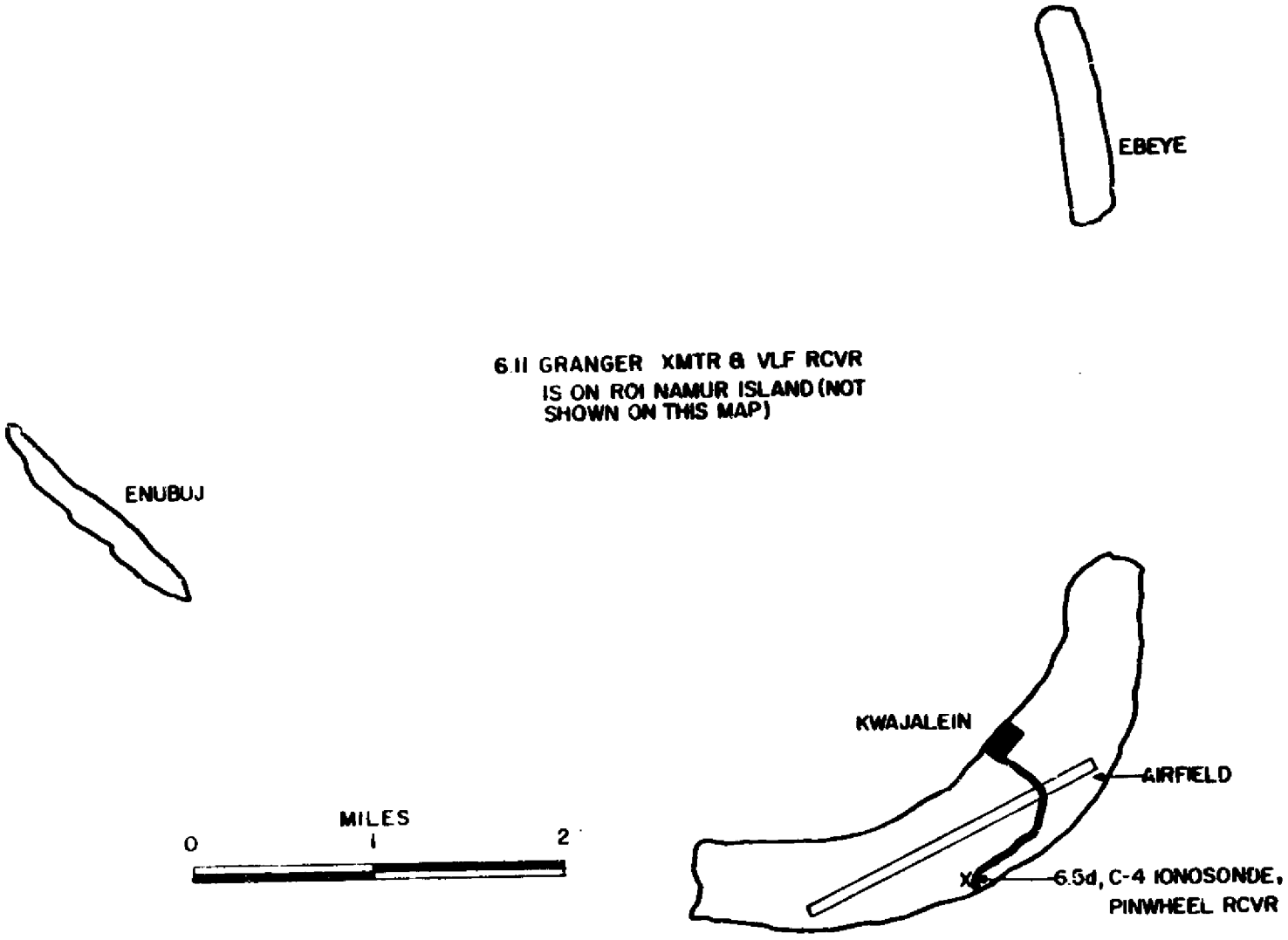


Figure B.12 Kwajalein Atoll.

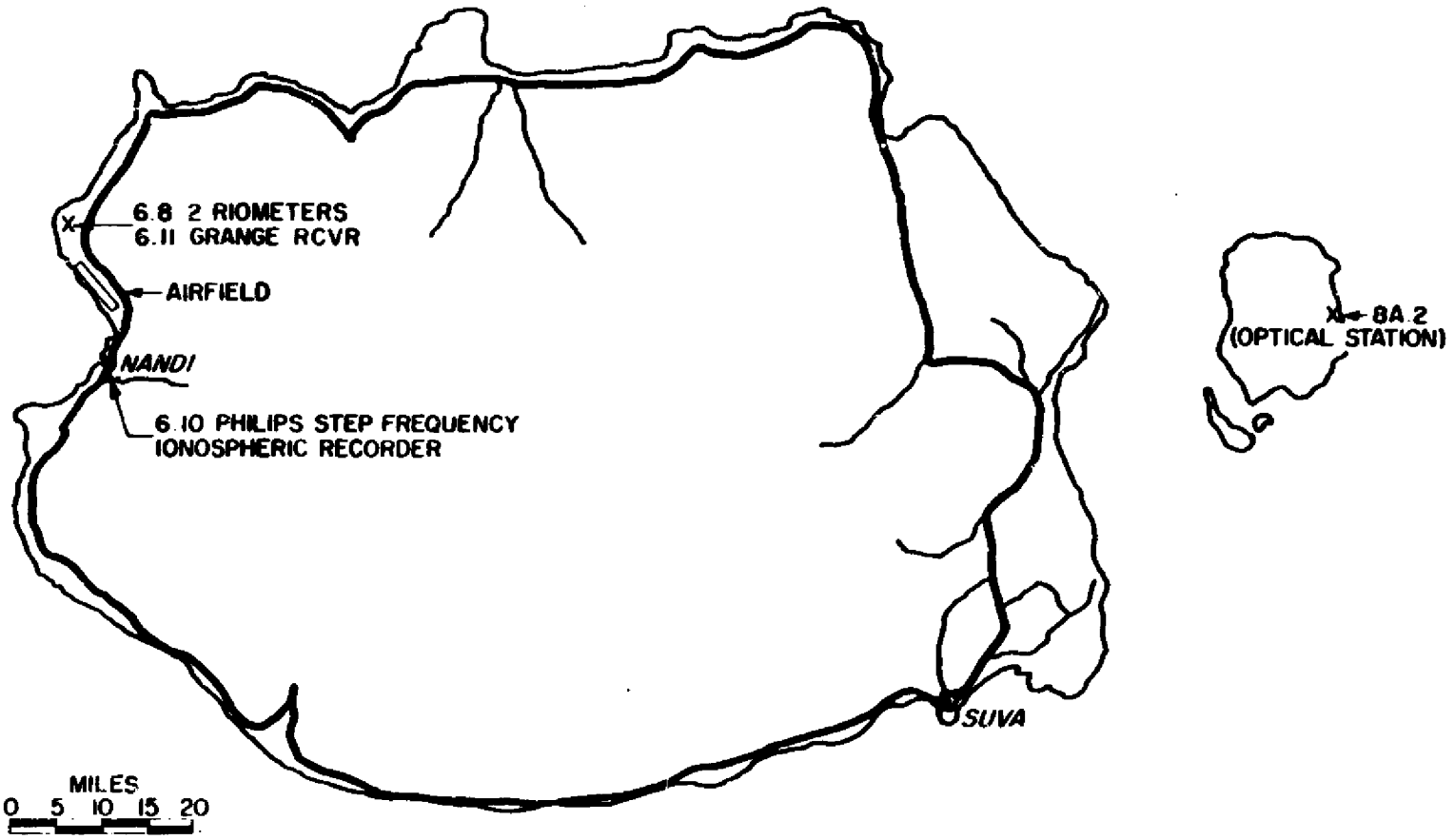


Figure B.13 Viti Levu.

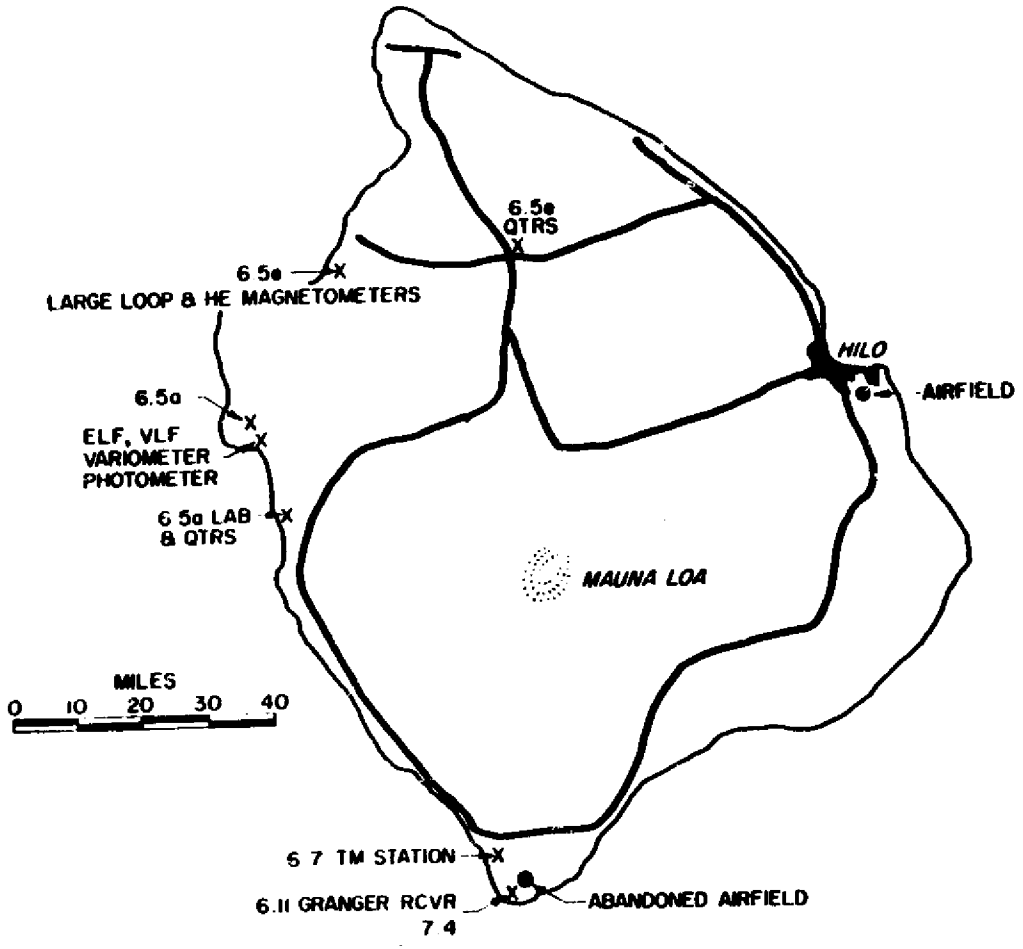


Figure B.14 Hawaii.

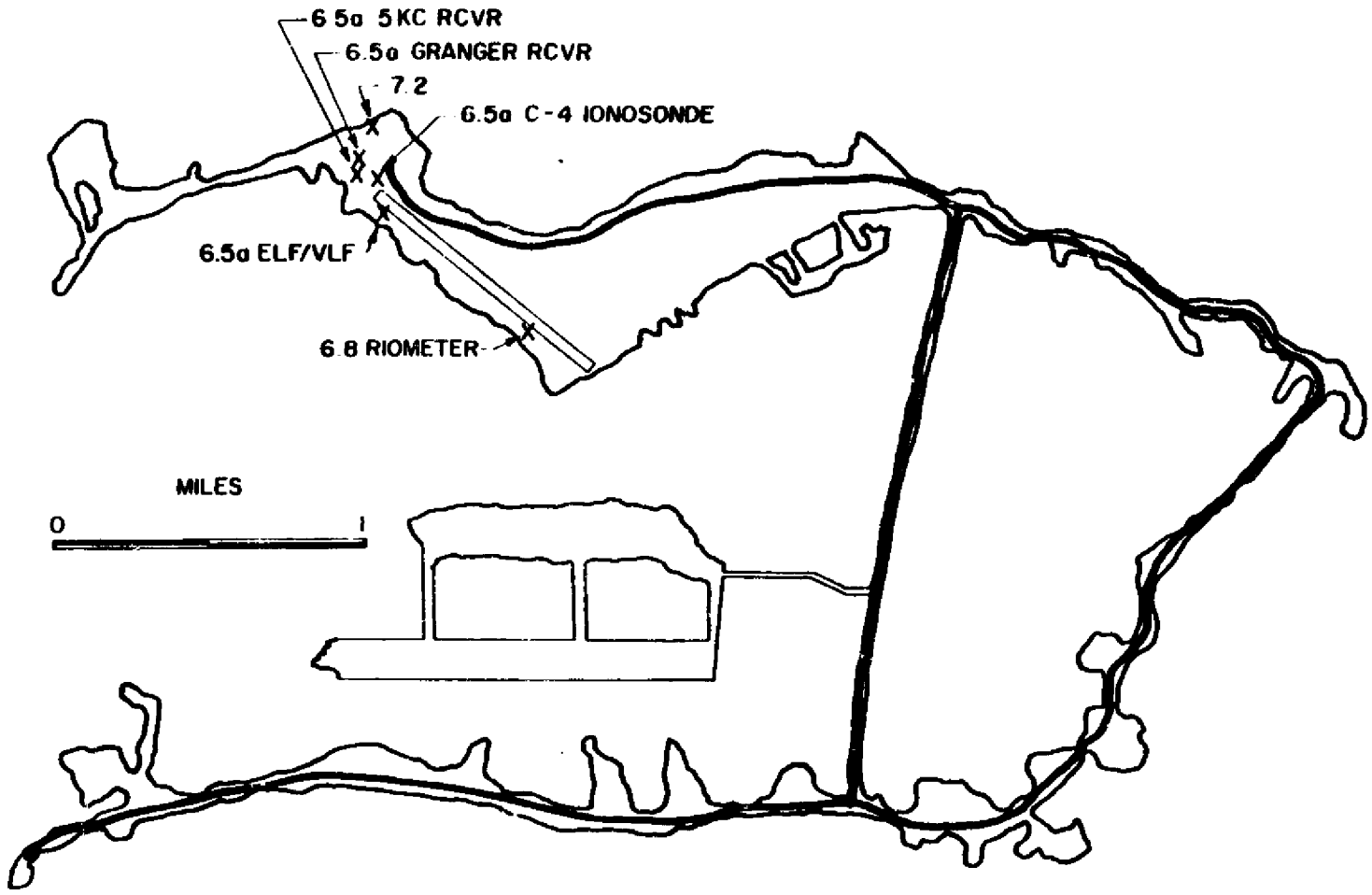


Figure B.15 Palmyra.

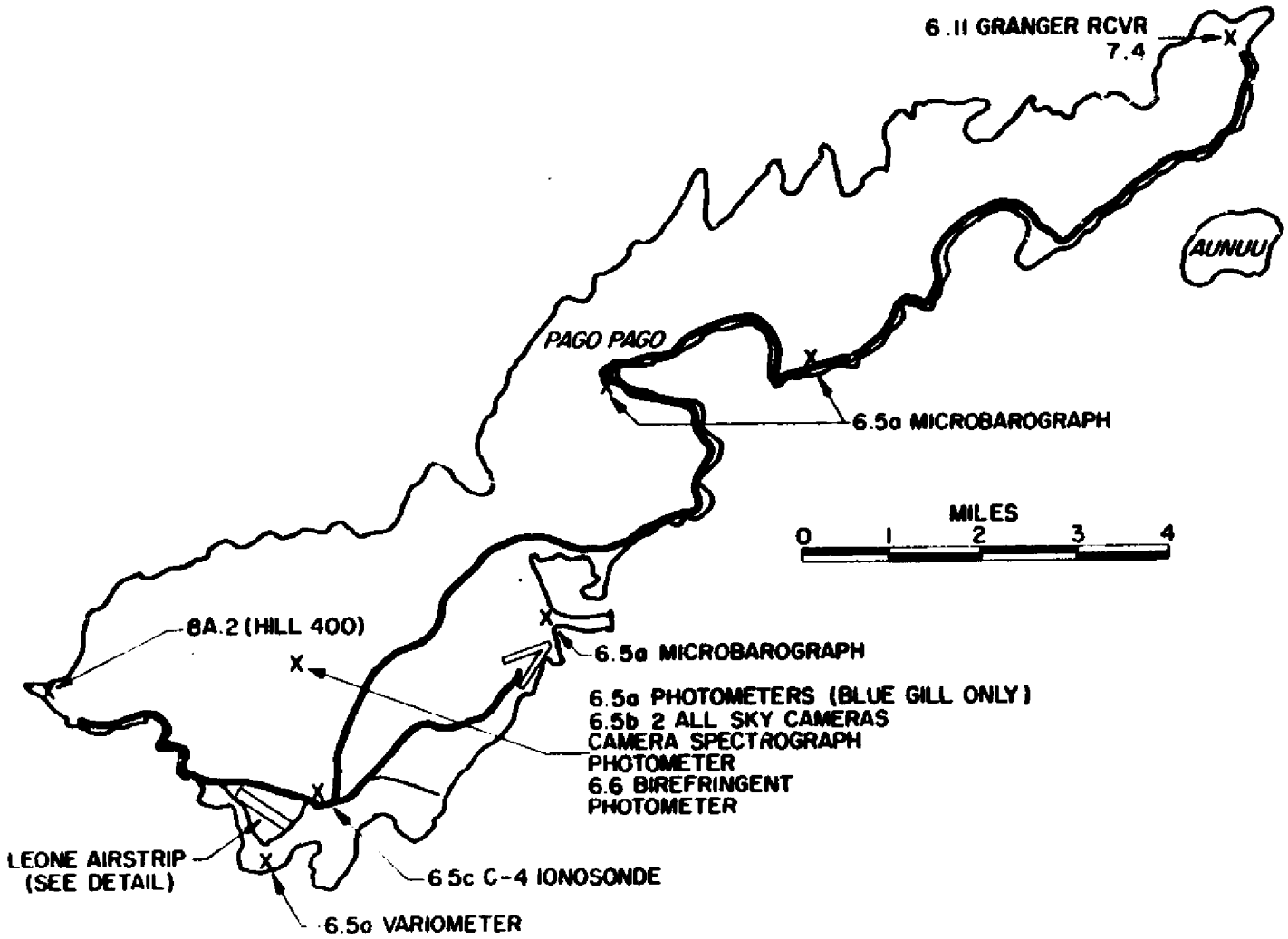


Figure B.16 Tutuila.

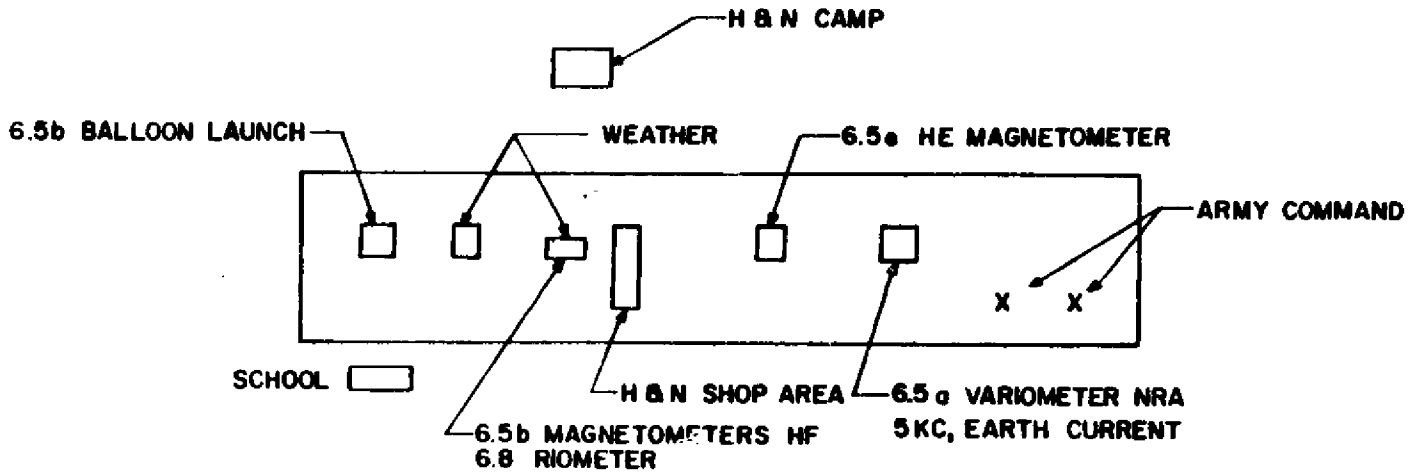


Figure B.17 Tutuila, Leone Airstrip detail.

## APPENDIX C TYPICAL WEATHER SOUNDING SCHEDULE

18 June 1962

Star Fish RAWINSONDE and PIBALL Schedule

| Release Time | | Type of Release |
|---|---|---|
| D–DAY: | 0100 | RAWINSONDE sounding. |
| | 0700 | RAWINSONDE sounding. |
| | 1300 | RAWINSONDE sounding. |
| | 1600 | RAWINSONDE sounding with double-theodolite trackout. |
| | 1645 | Double-theodolite PIBALL sounding. |
| | 1730 | Double-theodolite PIBALL sounding. |
| | 1815 | Double-theodolite PIBALL sounding. |
| | 1900 | RAWINSONDE sounding with double-theodolite trackout. |
| | 1940 | Double-theodolite PIBALL sounding. |
| | 2045 | Double-theodolite PIBALL sounding. |
| | 2110 | Double-theodolite PIBALL sounding. |
| | 2140 | Double-theodolite PIBALL sounding. |
| | 2210 | RAWINSONDE sounding with double-theodolite trackout. |
| | 2225 | Weather station evacuated. |
| D + 1 DAY: | | |
| | 0100 | RAWINSONDE sounding with double-theodolite trackout. |
| | 0400 | RAWINSONDE sounding with double-theodolite trackout. |
| | 0445 | Double-theodolite PIBALL sounding. |
| | 0530 | Double-theodolite PIBALL sounding |
| | 0700 | RAWINSONDE sounding with double-theodolite trackout. |
| | 1000 | RAWINSONDE sounding. |
| | | End of Special Star Fish meteorological soundings. |

Appendix D

SHIP POSITION DATA

TABLE D.1 SHIP PARTICIPATION

| Phase I | | Phase II | |
|---|---|---|---|
| Station | Ship | Station | Ship |
| S-1 | USS Oak Hill (LSD-7) | S-1 | USS Summit County (LST-1146) |
| S-2 | USS Fort Marion (LSD-22) | S-2 | USS Henry County (LST-824) |
| S-3 | USS Polk County (LST-1084) | S-3 | USNS Harris County (T-LST-822) |
| S-4 | USNS Point Barrow (T-AKD-1) | S-4 | USNS Point Barrow (T-AKD-1) |
| S-5 | USS Taylor (DDE-468) | S-5 | USS Takelma (ATF-113) |
| DAMP | USAS American Mariner | S-6 | USS Hassayampa (AO-145) |
| | M/V Acania | S-7 | USS Hitchiti (ATF-103) |
| | SS Mauna Tele | S-8 | USNS Petrarca (T-AK-250) |
| | | DAMP | USAS American Mariner |
| | | | M/V Acania |
| | | | SS Hifofua |

TABLE D.2 SHIP POSITION DATA, SHOT STAR FISH

Shot Data: Date and Time: 9 July 1962, 090009.0290 (Zulu); Yield: 1.15 Mt; Latitude N 16° 28′ 06.32″; Longitude W 169° 37′ 48.27″; Altitude, 400.09 km, 1,312,639 feet.
Johnston Island (Point John): Latitude N 16° 44′ 03.3″; Longitude W 169° 31′ 41.48″.

| | | H-Hour Positions | | Johnston Island | | Shot | |
|---|---|---|---|---|---|---|---|
| Station | Ship * | Latitude North | Longitude West | Range km | Bearing °True | Range km | Bearing °True |
| S-1 | Oak Hill | 10° 28.5′ | 171° 28.5′ | 735 | 196.7 | 704 | 196.6 |
| S-2 | Fort Marion | 13° 57.5′ | 169° 06.5′ | 253 | 010 | 285 | 011 |
| S-3 | Polk County | 17° 57′ | 164° 24′ | 566 | 076 | 581 | 073.5 |
| S-4 | Point Barrow | 16° 53′ | 172° 12′ | 289 | 273 | 283 | 279.3 |
| S-5 | Taylor | 21° 33.0′ | 168° 50′ | 540 | 007.8 | 576 | 008.4 |
| DAMP | American Mariner | 13° 52.5′ | 168° 58.5′ | 357 | 009.5 | 390 | 010 |

| | |
|---|---|
| Line-of-Sight and Burst Point Data: | |
| Azimuth from north | 200° 17′ 28.74″ |
| Elevation angle with refraction correction | 85° 14′ 12.37″ |
| Elevation angle without refraction correction | 85° 14′ 07.91″ |
| Slant range | 1,316,906.5 feet |
| Slant range | 401,394 meters |
| R/V Position: | |
| X (minus) | 37,933 ± 132 feet |
| Y (minus) | 102,594 ± 132 feet |
| Z (plus) | 1,312,420 ± 50 feet |

* H-hour position for M/V Acania in the Southern Conjugate Area: Latitude S 15° 35.2′
Longitude W 175° 40.3′

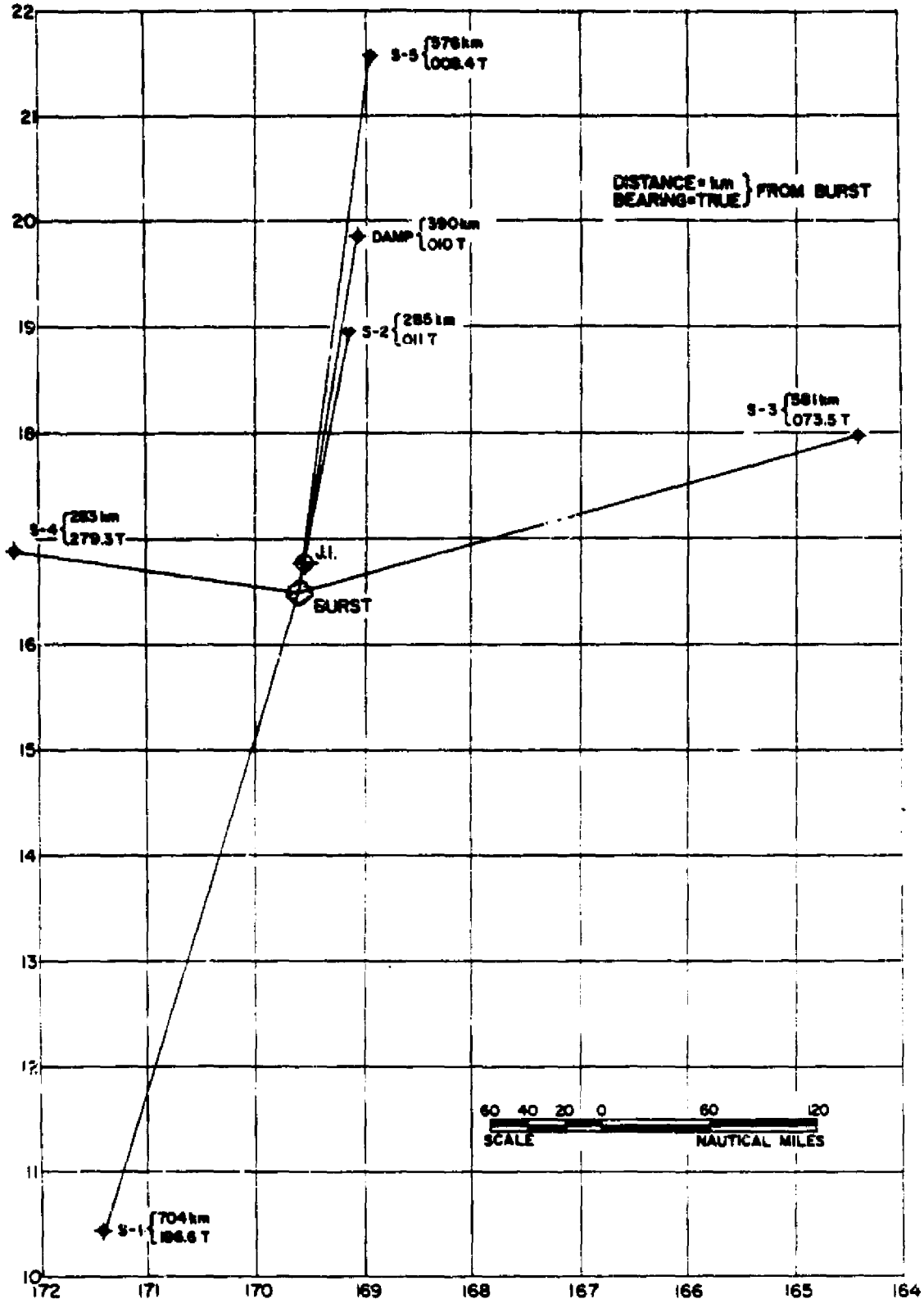


Figure D.1 Ship array, Shot Star Fish.

TABLE D.3 SHIP POSITION DATA, SHOT CHECK MATE

Shot Data: Date and Time: 20 October 1962, 083000.003 (Zulu); Latitude N 16° 04′ 20.57″; Longitude W 169° 36′ 35.95″;
Johnston Island (Point John): Latitude N 16° 44′ 03.3″; Longitude W 169° 31′ 41.48″.

| Station | Ship* | H-Hour Positions | | Johnston Island | |
|---|---|---|---|---|---|
| | | Latitude North | Longitude West | Range km | Bearing °True |
| S-1 | Summit County | 12° 36′ | 170° 19′ | Not computed | |
| S-2 | Henry County | 16° 05.5′ | 171° 01.5′ | Not computed | |
| S-3 | Harris County | 15° 36′ | 168° 23.3′ | Not computed | |
| S-4 | Point Barrow | 17° 37′ | 169° 21′ | Not computed | |
| S-5 | Takelma | 22° 20.5′ | 168° 32.4′ | Not computed | |
| S-6 | Hassayampa | 17° 33.5′ | 167° 59′ | Not computed | |
| S-7 | Hitchiti | 19° 24.8′ | 169° 00.8′ | Not computed | |
| S-8 | Petrarca | 17° 51′ | 170° 46′ | Not computed | |
| DAMP | American Mariner | 18° 27′ | 169° 11.2′ | Not computed | |

* H-hour position for M/V Acania in the Southern Conjugate Area: Latitude S 12° 27′
Longitude W 174° 56′

Page 229 deleted.

TABLE D.4 SHIP POSITION DATA, SHOT BLUE GILL

Shot Data: Date and Time: 26 October 1962, 095948.4753 (Zulu); Latitude N 16° 24' 57.03"; Longitude W 169° 36' 11.15";
Johnston Island (Point John): Latitude N 16° 44' 03.3"; Longitude W 169° 31' 41.48".

| | | H-Hour Positions | | Johnston Island | |
|---|---|---|---|---|---|
| Station | Ship* | Latitude North | Longitude West | Range km | Bearing °True |
| S-1 | Summit County | 16° 12.55' | 169° 40.20' | 60.15 | 195 |
| S-2 | Henry County | 16° 12.15' | 169° 37.45' | 59.80 | 190 |
| S-3 | Harris County | 16° 10.45' | 169° 41.00' | 64.30 | 195.3 |
| S-4 | Point Barrow | 16° 09.50' | 169° 37.65' | 64.60 | 189.7 |
| S-5 | Takelma | 20° 45.5' | 168° 48.0' | 487 | 010.0 |
| S-6 | Hassayampa | 18° 43' | 167° 42.0' | 326 | 038 |
| S-7 | Hitchiti | 18° 57' | 169° 08.1' | 281 | 010 |
| S-8 | Petrarca | 19° 13' | 170° 30' | 314 | 340.6 |
| DAMP | American Mariner | 17° 41' | 169° 21' | 135 | 010 |

* H-hour position for M/V Acania in the Southern Conjugate Area: Latitude S 13° 01'
Longitude W 175°

Page 231 deleted.

TABLE D.8 SHIP POSITION DATA, SHOT KING FISH

Shot Data: Date and Time: 1 November 1962, 121006.1263 (Zulu); Latitude N 16° 06' 48.61"; Longitude W 169° 40' 56.02";
Johnston Island (Point John): Latitude N 16° 44' 03.3"; Longitude W 169° 31' 41.48"

| Station | Ship* | H-Hour Positions | | Johnston Island | |
|---|---|---|---|---|---|
| | | Latitude North | Longitude West | Range km | Bearing °True |
| S-1 | Summit County | 15° 27.7' | 169° 59' | 146.41 | 196 |
| S-2 | Henry County | 16° 49' | 169° 31.5' | 9.27 | 002 |
| S-3 | Harris County | 15° 27.1' | 169° 41.5' | 143.63 | 187 |
| S-4 | Point Barrow | 15° 33.2' | 169° 45.5' | 134.73 | 191 |
| S-5 | Takelma | 30° 03.75' | 166° 42.35' | Not computed | |
| S-6 | Hassayampa | 21° 11' | 168° 36' | Not computed | |
| S-7 | Hitchiti | 18° 57' | 169° 09.7' | Not computed | |
| S-8 | Petrarca | 16° 40' | 172° 10' | Not computed | |
| DAMP | American Mariner | 17° 35' | 169° 21' | Not computed | |

* H-hour position for M/V Acania in the Southern Conjugate Area: Latitude S 12° 08'
Longitude W 174° 50'

Page 233 deleted.

TABLE D.6 LOCATIONS OF SHIPS AFTER SHOT KING FISH

Date: 1 November 1962 W. Range and bearing were computed from shot ground zero.

| Station | Time | Range | Bearing | Latitude | Longitude |
|---|---|---|---|---|---|
| | W | km | °True | North | West |
| S-1 | 0800 | 207 | 200 | 15° 06′ | 170° 09′ |
| | 1200 | 268 | 193 | 14° 26′ | 170° 05′ |
| | 2000 | 337.3 | 190 | 13° 47′ | 170° 3.5′ |
| S-2 | 0600 | 94.5 | 337 | 16° 54′ | 170° 01.5′ |
| | 1900 | 237 | 299.5 | 17° 09′ | 171° 38.5′ |
| S-3 | No significant changes subsequent to H-hour before returning to Johnston Island. | | | | |
| S-4 | 0800 | 101.93 | 142 | 15° 24′ | 169° 06′ |
| | 1200 | 153.83 | 126 | 15° 18′ | 168° 31′ |
| | 2000 | 266.8 | 116 | 15° 03′ | 167° 26′ |
| S-5 | No significant change from H-hour through second twilight. | | | | |
| S-6 | 0800 | 544.9 | 10.5 | 20° 54′ | 168° 45′ |
| | 1200 | 574.5 | 12 | 21° 08′ | 168° 33′ |
| | 2000 | 586.6 | 10 | 21° 13′ | 168° 44′ |
| S-7 | No significant change from H-hour through second twilight. | | | | |
| S-8 | 0800 | 352 | 283 | 16° 50′ | 172° 52′ |
| | 1200 | 354 | 279 | 16° 37′ | 172° 55′ |
| | 2000 | 430 | 280 | 16° 49′ | 173° 37′ |
| DAMP | Ship remained at H-hour position. | | | | |

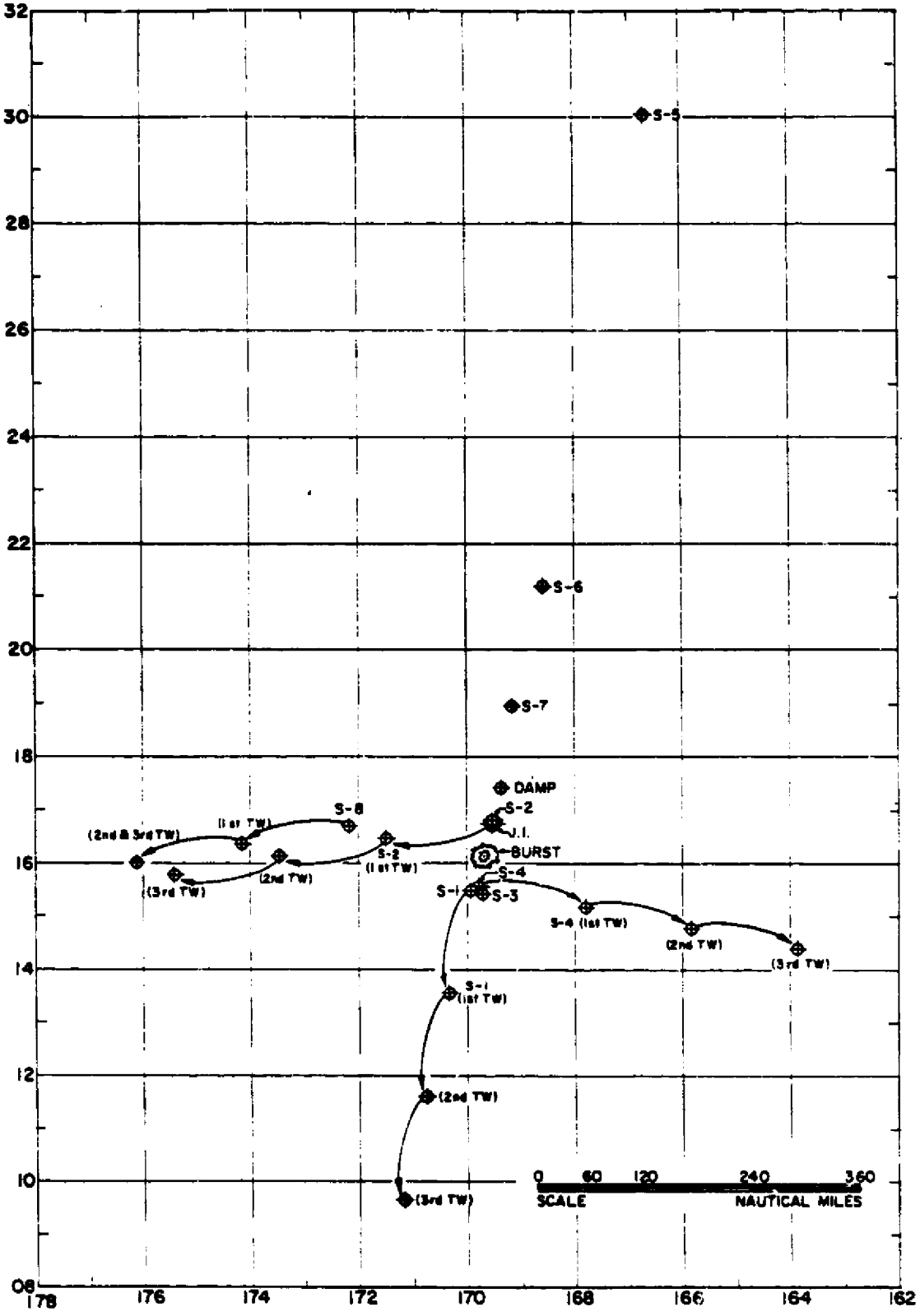


Figure D 5 Ship array, post H-hour, Shot King Fish.

TABLE D.7 SHIP POSITION DATA, SHOT TIGHT ROPE

**Shot Data: Date and Time: 4 November 1962, 073000.0678 (Zulu); Latitude N 16° 42′ 26.71″; Longitude W 169° 32′ 32.66″;**
Johnston Island (Point John): Latitude N 16° 44′ 03.3″; Longitude W 169° 31′ 41.48″.

| | H-Hour Positions | | | Johnston Island | |
|---|---|---|---|---|---|
| Station | Ship * | Latitude North | Longitude West | Range km | Bearing °True |
| S-1 | Summit County | 16° 44′ 25″ | 169° 31′ 43″ | 0.493 | 359 |
| S-2 | Henry County | 16° 47′ 42″ | 169° 30′ 36″ | 7.0 | 011 |
| S-3 | Harris County | 16° 44′ 30″ | 169° 31′ 35″ | 0.72 | 017 |
| S-4 | Point Barrow | 16° 48′ 36″ | 169° 29′ 42″ | 9.1 | 023 |
| S-5 | Did not participate in Shot Tight Rope | | | | |
| S-6 | Hassayampa | 18° 30′ | 169° 10′ | 196.4 | 010 |
| S-7 | Hitchiti | 17° 38.5′ | 169° 22′ | 100.5 | 010 |
| S-8 | Petrarca | 16° 54′ | 170° 27′ | 100 | 280 |
| DAMP | American Mariner | 16° 49′ | 169° 30′ 31″ | 9.4 | 013 |

* H-hour position for M/V Acania in the Southern Conjugate Area: Latitude S 13°
Longitude W 175°

Page 237 deleted.

TABLE D.8 LOCATIONS OF SHIPS AFTER SHOT BLUE GILL

Range and bearing were computed from shot ground zero.
Stations S-5 through S-8 and DAMP ship remained at H-hour position.

| Station | Time | Range | Bearing | Latitude | Longitude |
|---|---|---|---|---|---|
| | W | km | °True | North | West |
| S-1 | 26 October 1962 W | | | | |
| | 0800 | 124 | 195 | 15° 20.8′ | 169° 54.5′ |
| | 1200 | 114 | 185 | 15° 24′ | 169° 42.7′ |
| | 2000 | 120 | 196 | 15° 22.4′ | 169° 55.0′ |
| | 27 October 1962 W | | | | |
| | 0800 | 126.5 | 193 | 15° 18.5′ | 169° 52′ |
| | 1200 | Returned to Johnston Island anchorage. | | | |
| S-2 | 26 October 1962 W | | | | |
| | 0800 | 28 | 197 | 16° 10.8′ | 169° 40.6′ |
| | 1200 | 24 | 173 | 16° 12.1′ | 169° 34.2′ |
| | 2000 | 23 | 183 | 16° 13.6′ | 169° 36.6′ |
| | 27 October 1962 W | | | | |
| | 0800 | 25.5 | 181 | 16° 11.1′ | 169° 36.1′ |
| S-3 | 26 October 1962 W | | | | |
| | 0800 | 102 | 084 | 16° 31′ | 168° 39′ |
| | 1200 | 134 | 078 | 16° 40′ | 168° 22′ |
| | 2000 | 107 | 080 | 16° 35.5′ | 168° 36.6′ |
| | 27 October 1962 W | | | | |
| | 0800 | 96 | 075 | 16° 38′ | 168° 43.5′ |
| | 1200 | 137 | 079 | 16° 38.7′ | 169° 20.1′ |
| | 2000 | Returned to Johnston Island anchorage. | | | |
| S-4 | 26 October 1962 W | | | | |
| | 0800 | 103.5 | 302 | 16° 55′ | 170° 25′ |
| | 1200 | 107 | 305 | 16° 58′ | 170° 25′ |
| | 2000 | 92 | 295 | 16° 46′ | 170° 23′ |
| | 27 October 1962 W | | | | |
| | 0800 | 35 | 294 | 16° 43′ | 170° 20′ |
| | 1200 | 70 | 230 | 16° 00′ | 170° 07′ |
| | 2000 | 81 | 005 | 17° 05′ | 169° 34′ |

TABLE D.9 LOCATIONS OF SHIPS AFTER SHOT TIGHT ROPE

Date: 4 November 1962 W. Range and bearing were computed from shot ground zero.
Stations S-1 through S-4 and S-7: No significant position changes through second twilight. Station S-5 did not participate in Shot Tight Rope. Station DAMP ship remained at H-hour position.

| Station | Time | Range | Bearing | Latitude | Longitude |
|---|---|---|---|---|---|
| | W | km | °True | North | West |
| S-6 | 0800 | 209.4 | 004 | 18° 33′ | 169° 25′ |
| | 1200 | 207.6 | 009 | 18° 32′ | 169° 15′ |
| | 2000 | 218.7 | 011 | 18° 35′ | 168° 55′ |
| S-8 | 0800 | 92.7 | 287 | 16° 58′ | 170° 22′ |
| | 1200 | 105.6 | 282 | 16° 55′ | 170° 30′ |
| | 2000 | 126 | 293 | 17° 10′ | 170° 37′ |



Pages 239 through 244
deleted.

## APPENDIX F SMALL-ROCKET LAUNCH DATA

### TABLE F.1 SMALL-ROCKET LAUNCH DATA, SHOT STAR FISH

Rockets launched from Johnston Island (total: 27). All data based on preshot planning and therefore approximate.

| Time of Launch | Pad No. | Project ID | Rocket Type | Azimuth True | Elevation Apogee | | Last Stage Impact Point | Type of Measurement |
|---|---|---|---|---|---|---|---|---|
| | | | | deg | deg | nauti mi | | |
| H−2¾ hr | 21 | 9.1 | Nike-Cajun | 155 | 85 | 74 | 33 naut mi | Winds with Na vapor |
| H−30 min | 20 | 9.1 | Nike-Cajun | 155 | 85 | 74 | 33 naut mi | Winds with Na vapor |
| H−600 sec | 19 | 6.4 | Javelin | 90 | 83 | 270 | 16.48°N, 162.48°W | X-, beta- and gamma-rays, ionization |
| H−510 sec | 25 | 6.7 | XM 33 | 198 | 78 | 555 | 0.3° S, 172.6° W | Magnetic field and debris expansion |
| H−500 sec | 1 | 6.7 | XM 33 | 10 | 85 | 715 | 24.4°N, 169.6°W | Magnetic field and debris expansion |
| H−280 sec | 2 | 6.7 | XM 33 | 10 | 85 | 715 | 24.4°N, 169.6° W | Magnetic field and debris expansion |
| H−206 sec | 14 | SJI 152 | Nike-Apache | 195 | 88 | 93 | 18 naut mi | X-ray |
| H−201 sec | 10 | SJI 152 | Nike-Apache | 195 | 88 | 86 | 17 naut mi | X- and beta-rays |
| H−200 sec | 7 | SJI 111 | Nike-Apache | 195 | 88 | 86 | 17 naut mi | X-ray, radiochemical sampler |
| H−199 sec | 9 | SJI 151 | Nike-Apache | 195 | 88 | 86 | 17 naut mi | X-ray, radiochemical sampler |
| H−196 sec | 8 | SJI 112 | Nike-Apache | 195 | 88 | 86 | 17 naut mi | X-ray, radiochemical sampler |
| H−160 sec | 24 | 6.7 | XM 33 | 198 | 93 | — | 5.8°N, 172.2°W | Magnetic field and debris expansion |
| H−140 sec | 23 | 6.7 | XM 33 | 198 | 78 | 555 | 0.3°S, 172.6°W | Magnetic field and debris expansion |
| H−132.5 sec | 13 | SJS 151 | Nike-Apache | 195 | 86.5 | 95 | 33 naut mi | Radiochemical sampler |
| H−90 sec | 6 | 6.3 | Honest John-Nike | 120 | 85 | 48 | 25 naut mi | X-, beta-, and gamma-rays, ionization |
| H−60 sec | 16 | 6.3 | Nike-Cajun | 90 | 85 | 64 | 29 naut mi | Mass spectrometry |
| H − 220 sec | 3 | 6.13 | Speedball | 10 | 84 | 124 | 75 naut mi | Radar jitter |
| H − 420 sec | 18 | 6.3 | Honest John-Nike | 90 | 85 | 48 | 25 naut mi | X-, beta-, and gamma-rays, ionization |
| H + 420 sec | 22 | 6.4 | Javelin | 120 | 80 | 237 | 11.47°N, 161.36°W | X-, beta-, and gamma-rays, ionization |
| H + 480 sec | 15 | 6.3 | Nike-Cajun | 90 | 85 | 64 | 29 naut mi | Mass spectrometry |
| H + 710 sec | 26 | 6.13 | Speedball | 190 | 82 | 124 | 98 naut mi | Radar jitter |
| H + 960 sec | 17 | 6.4 | Javelin | 90 | 83 | 270 | 16.48°N, 162.3° W | X-, beta-, and gamma-rays, ionization |
| H − 1,200 sec | 5 | 6.2 | Javelin | 15 | 80 | 345 | 27.09°N, 167.9°W | Gamma- and beta-photometry |
| H + 1,860 sec | 7 | 6.13 | Speedball | 180 | 82 | 121 | 98 naut mi | Radar jitter |
| H − 2,400 sec | 4 | 6.2 | Javelin | 15 | 80 | 345 | 27.09°N, 167.9°W | Gamma- and beta-photometry |
| H + 3,540 sec | 11 | SJS 152 | Nike-Apache | 195 | 86.5 | 95.4 | 33 naut mi | Radiochemical sampler |
| 0549, D + 1 | 21 | 9.1 | Nike-Cajun | 155 | 85 | 74 | 33 naut mi | Winds with Na vapor |

TABLE F.2 SMALL-ROCKET LAUNCH DATA, SHOT CHECK MATE

Rockets launched from Johnston Island (total: 10).

| Time of Launch | Pad No. | Project | Rocket Type | Azimuth True | Elevation | Apogee, Time after Launch | | Last Stage Impact Distance, Time after Launch | | Type of Measurement |
|---|---|---|---|---|---|---|---|---|---|---|
| sec | | | | deg | deg | km | sec | km | time | |
| −139 | 7 | LRL SJI-121 | Nike-Apache | 190 | 78.3 | 165 | 368 | 77 | 188 sec | X-ray, radiochemical sampler |
| −137 | 8 | LRL SJI-122 | Nike-Apache | 190 | 78.3 | 165 | 368 | 77 | 188 sec | X-ray, radiochemical sampler |
| −128 | 2 | 6.7 | X-M33/254 | 187 | 83 | 1,060 | 588 | 1,230 | 18.3 min | Debris tracking |
| −123 | 1 | 6.7 | XM-33/254 | 191 | 75 | 794 | 588 | 2,160 | 15.5 min | Debris tracking |
| −74 | 10 | Sandia SJS-161 | Nike-Apache | 190 | 86 | 163 | 202 | 35 | 394 sec | Radiochemical sampler |
| −71 | 9 | Sandia SJI-192 | Nike-Apache | 190 | 86 | 172 | 207 | 37 | 405 sec | Betas and gammas |
| −70 | 27 | 6.13 | Nike-Apache | 191 | 82 | 200 | 230 | 172 | 450 sec | Radar tracking |
| +500 | 28 | 6.13 | Nike-Apache | 191 | 82 | 200 | 230 | 172 | 450 sec | Radar tracking |
| +600 | 20 | 9.1a | Nike-Cajun | 170 | 85 | 149 | 190 | 68.3 | 372 sec | Atmospheric drag |
| +1,020 | 29 | 6.13 | Nike-Apache | 191 | 82 | 200 | 230 | 172 | 450 sec | Radar tracking |

TABLE F.3 SMALL ROCKET LAUNCH DATA, SHOT BLUE GILL

Rockets launched from Johnston Island (total: 28).

| Time of Launch | Pad No. | Project | Rocket Type | Azimuth True | Elevation | Apogee, Time After Launch | | Last Stage Impact Distance, Time After Launch | | Type of Measurements |
|---|---|---|---|---|---|---|---|---|---|---|
| sec | | | | deg | deg | km | sec | km | sec | |
| 1915 to 1925W | 21 | 9.1b | Nike-Cajun | 155 | 85 | 137 | 180 | 61.4 | 354 | Winds by Na vapor |
| −312 | 3 | 6.13 | Nike-Apache | 199 | 82 | 234 | 230 | 204 | 470 | Radar tracking |
| −195 | 22 | 6.1a | Nike-Cajun | 191 | 83 | 122 | 170 | 76 | 336 | Radar propagation |
| −190 | 23 | 6.1a | Nike-Cajun | 191 | 83 | 122 | 170 | 76 | 336 | Radar propagation |
| −180 | 26 | 6.13 | Nike-Apache | 190 | 82 | 234 | 230 | 204 | 470 | Radar tracking |
| −120 | 19 | 6.3 | Honest John-Nike | 090 | 80 | 81.4 | 140 | 89 | 270 | Gamma-, beta-, and X-ray, ion trap, impedance probe |
| −112 | 24 | 6.1a | Nike-Cajun | 191 | 87 | 126 | 170 | 33.4 | 340 | Radar propagation |
| −108 | 25 | 6.1a | Nike-Cajun | 191 | 87 | 126 | 170 | 33.4 | 340 | Radar propagation |
| −60 | 16 | 6.3 | Nike-Cajun | 100 | 80 | 109 | 150 | 104 | 287 | Mass spectrometer |
| −40 | 9 | SC | Nike-Apache | 205 | 87.7 | 94 | 205 | 21.4 | 406.5 | Beta- and gamma-flux |
| −28 | 8 | SC | Nike-Apache | 205 | 87.6 | 89.5 | 202 | 21.2 | 396 | Radiochemical sampler |
| + 166 | 10 | SC | Nike-Apache | 214 | 87.3 | 94 | 205 | 25.1 | 406 | Beta- and gamma-flux |
| + 178 | 7 | SC | Nike-Apache | 214 | 87 | 89 | 202 | 26.4 | 395 | Radiochemical sampler |
| + 180 | 27 | 6.13 | Nike-Apache | 190 | 82 | 126 | 241 | 110 | 470 | Radar tracking |
| + 290 | 1 | 6.1a | Nike-Cajun | 191 | 87 | 126 | 170 | 33.4 | 340 | Radar propagation |
| + 300 | 6 | 6.3 | Honest John-Nike | 028 | 85 | 89 | 150 | 47 | 294 | Gamma-, beta-, RF-impedance, ion trap |
| + 360 | 15 | 6.3 | Nike-Cajun | 090 | 85 | 118 | 150 | 53.7 | 295 | Mass spectrometer |
| + 670 | 18 | 6.3 | Honest John-Nike | 090 | 85 | 89 | 150 | 47 | 294 | Gamma-, beta-, and RF-impedance, ion trap |
| + 900 | 5 | 6.2 | Honest John-Nike-Nike | 025 | 83 | 142 | 190 | 86 | 367 | Gamma-scanner, Langmuir probe, photometer, 3-freq. beacon |
| + 900 | — | 6.1a | Nike-Cajun | 191 | 87 | 126 | 170 | 33.4 | 340 | Radar propagation |
| + 900 | 20 | 9.1a | Nike-Cajun | 165 | 85 | 149 | 190 | 68.3 | 372 | Atmospheric drag |
| + 1,320 | 17 | 6.3 | Honest John-Nike | 120 | 80 | 81.4 | 140 | 89 | 270 | Gamma-, beta-, and RF-impedance, ion trap |
| + 1,320 | 28 | 6.13 | Nike-Apache | 190 | 82 | 234 | 230 | 204 | 470 | Radar tracking |
| + 1,860 | 4 | 6.2 | Honest John-Nike-Nike | 025 | 83 | 142 | 190 | 86 | 367 | Same as + 900 |
| + 2,640 | 11 | SC | Nike-Apache | 145 | 88 | 82 | 193 | 16 | 378 | Atmospheric density |
| + 3,540 | 12 | SC | Nike-Apache | 145 | 88 | 82 | 193 | 16.1 | 378 | Atmospheric density |
| 0625 to 0635W | 21 | 9.1b | Nike-Cajun | 155 | 85 | 137 | 180 | 61.4 | 354 | Winds by Na vapor |
| + 13 hours | 13 | SC | Nike-Apache | 145 | 88 | 82 | 193 | 16 | 378 | Same as + 3,540 |

TABLE F.4 SMALL-ROCKET LAUNCH DATA, SHOT KING FISH

Rockets launched from Johnston Island (total: 29).

| Time of Launch | Pad No. | Project | Rocket Type | Azimuth True | Elevation | Apogee, Time After Launch | | Last Stage Impact Distance, Time After Launch | | Type of Measurements |
|---|---|---|---|---|---|---|---|---|---|---|
| sec | | | | deg | deg | km | sec | km | sec | |
| 1905 to 1915W | 21 | 9.1b | Nike-Cajun | 155 | 85 | 137 | 180 | 61.4 | 354 | Na vapor (winds) |
| −350 | 26 | 6.13 | Nike-Apache | 191 | 82 | 202 | 224 | 164 | 436 | Radar tracking |
| −160 | 25 | 6.1 | Nike-Apache | 191 | 83 | 143 | 191 | 100 | 370 | Radar propagation |
| −155 | 24 | 6.1 | Nike-Apache | 191 | 83 | 143 | 191 | 100 | 370 | Radar propagation |
| −123 | 8 | SC | Nike-Apache | 191 | 70 | 118 | 172 | 248 | 340 | X-ray |
| −120 | 1 | 6.2 | Honest John-Nike-Nike | 120 | 85 | 195 | 230 | 101 | 432 | Gamma-ray |
| −120 | 17 | 6.3 | Honest John-Nike-Nike | 100 | 85 | 180 | 230 | 92 | 414 | D-region physical chemistry |
| −101 | 7 | SC | Nike-Apache | 191 | 86 | 135 | 183 | 48 | 378 | X-ray |
| −93 | 9 | SC | Nike-Apache | 191 | 70 | 117 | 170 | 241 | 335 | Radiochemical sampler |
| −85 | 23 | 6.1 | Nike-Apache | 191 | 86 | 152 | 196 | 54.2 | 375 | Radar propagation |
| −84 | 13 | SC | Nike-Apache | 191 | 86 | 172 | 205 | 69 | 403 | X-ray |
| −84 | 10 | SC | Nike-Apache | 191 | 70 | 117 | 170 | 241 | 335 | Radiochemical sampler |
| −80 | 3 | 6.1 | Nike-Apache | 191 | 86 | 152 | 196 | 54.2 | 375 | Radar propagation |
| −60 | 19 | 6.4 | Javelin | 100 | 83 | 500 | 425 | 772 | 798 | Beta- and gamma-rays |
| −39 | 12 | SC | Nike-Apache | 191 | 83 | 159 | 199 | 111 | 389 | D-region characteristics |
| −0− | 15 | 6.3 | Nike-Apache | 100 | 85 | 120 | 155 | 55 | 285 | |
| + 200 | 28 | 6.13 | Nike-Apache | 191 | 82 | 202 | 224 | 164 | 436 | Radar tracking |
| + 210 | 14 | SC | Nike-Apache | 191 | 80 | 174 | 195 | 35 | 407 | Beta- and gamma-rays |
| + 360 | 16 | 6.3 | Nike-Cajun | 090 | 85 | 120 | 155 | 55 | 282 | D-region characteristics |
| + 360 | 5 | 6.3 | Honest John-Nike-Nike | 021 | 85 | 184 | 230 | 94 | 419 | D-region characteristics |
| + 540 | 22 | 6.4 | Javelin | 145 | 83 | 488 | 425 | 784 | 790 | F-region characteristics |
| + 600 | 20 | 9.1a | Nike-Cajun | 170 | 83 | 145 | 190 | 72 | 372 | Atmospheric density |
| + 780 | 2 | 6.2 | Honest John-Nike-Nike | 120 | 85 | 195 | 230 | 101 | 432 | Gamma-ray |
| + 810 | 18 | 6.3 | Honest John-Nike-Nike | 100 | 85 | 184 | 230 | 94 | 419 | D-region characteristics |
| + 1,010 | 29 | 6.13 | Nike-Apache | 191 | 82 | 202 | 224 | 164 | 436 | Radar tracking |
| + 1,500 | 4 | 6.2 | Honest John-Nike-Nike | 120 | 85 | 195 | 230 | 101 | 432 | Gamma-ray |
| + 1,960 | 27 | 6.13 | Nike-Apache | 191 | 78 | 216 | 232 | 226 | 452 | Radar tracking |
| + 2,400 | 6 | 6.3 | Honest John-Nike-Nike | 020 | 85 | 180 | 230 | 92 | 414 | D-region characteristics |
| 0630 to 0640W (postshot) | 21 | 9.1b | Nike-Cajun | 155 | 85 | 137 | 180 | 61.4 | 354 | Na vapor (winds) |

TABLE F.5 SMALL-ROCKET LAUNCH DATA, SHOT TIGHT ROPE

Rockets launched from Johnston Island (total: 7).

| Time of Launch | Pad No. | Project | Rocket Type | Azimuth True | Elevation | Apogee, Time After Launch | | Last Stage Impact Distance, Time After Launch | | Type of Measurements |
|---|---|---|---|---|---|---|---|---|---|---|
| sec | | | | deg | deg | km | sec | km | sec | |
| 1902 to 1912W | 21 | 9.1b | Nike-Cajun | 155 | 85 | 137 | 180 | 61.4 | 354 | Winds by Na vapor |
| −50 | 1 | 6.1 | Nike-Cajun | 203 | 84 | 107 | 160 | 57.4 | 317 | Radar transmission |
| −50 | 24 | 6.1 | Nike-Cajun | 203 | 84 | 107 | 160 | 57.4 | 317 | Radar transmission |
| −40 | 23 | 6.1 | Nike-Cajun | 200 | 81 | 104 | 157 | 85 | 314 | Radar transmission |
| −40 | 25 | 6.1 | Nike-Cajun | 200 | 81 | 104 | 157 | 85 | 314 | Radar transmission |
| + 240 | 20 | 9.1a | Nike-Cajun | 175 | 86 | 147 | 190 | 69 | 372 | Atmospheric density |
| 0635 to 0645W (postshot) | 21 | 9.1b | Nike-Cajun | 155 | 85 | No second stage ignition | | | | Winds by Na vapor |

Appendix G

TECHNICAL OPERATIONS REPORTING PROCEDURES

HEADQUARTERS TASK UNIT 8.1.3 (FORWARD)
FIELD COMMAND, DEFENSE ATOMIC SUPPORT AGENCY
APO 105, San Francisco, California

30 September 1962

TEST DIRECTOR
MEMORANDUM 2-62

TECHNICAL OPERATIONS REPORTING PROCEDURES

1. General. The Technical Operations Center (TOC) on Johnston Island is the DOD Scientific Task Unit Headquarters (CTU 8.1.3). All scientific project status reports are received and evaluated in the TOC. Because of the many remote locations involved, a reporting procedure which will provide the required clarity, speed, and economy of effort is needed by the Task Unit and Commander in order to evaluate the status of assigned projects.

2. Purpose. This memorandum establishes guide lines for the implementation of this reporting procedure. The Scientific Reporting Network and the SUNSHINE Reporting System are the means whereby each project can maintain quick, direct, and unclassified communication with its Task Element Commander.

3. Applicability and Implementation. The reporting procedures are applicable to all scientific projects of this Task Unit. They are effective immediately.

4. TU 8.1.3 Scientific Reporting Network. The Scientific Reporting Network will consist of three separate and distinct loops. One loop comprises the northern and western Pacific stations, the second loop encompasses the southern Pacific stations, and the third loop will serve the immediate Johnston Island area.

a. The northern and western loops will consist of the following stations and associated projects:

| LOCATION | PROJECTS |
|---|---|
| Adak | 6.5d |
| Fairbanks | 6.11 |
| Hawaii | 6.5a, 6.5e, 6.7, 6.11, 7.4, 8A.2 |
| Kauai | 6.5a, 6.5d, 6.11 |
| Kwajalein | 6.5d, 6.11, 7.4 |
| Maui | 6.5c, 6.10, 8A.1, 9.5a |
| Midway | 6.5a, 6.5c, 6.8, 6.10, 6.11, 7.4 |
| Oahu | 1.1, 4.1, 6.7, 6.8, 6.10, 6.11, 7.4, 8A.1, 8A.2, 9.3, 9.5a |
| Okinawa | 6.5a, 6.5d, 6.11 |
| Palo Alto | 6.5d, 6.11 |
| Wake | 6.5a, 6.8, 6.11, 7.4 |

Projects of this loop will report to the TU 8.1.3 Hickam Air Force Base Headquarters. Those projects located within the State of Hawaii will report over existing commercial facilities provided by the Honolulu Office of Holmes and Narver, Inc. The projects on Okinawa will utilize the facilities of one of the three military communications centers there (one Air Force and one Navy center at Naha AFB; one Air Force center at Kadena AFB). Projects located on Midway, Wake, Kwajalein, and at Adak will utilize the facilities of the existing military communication centers at each site. The 6.11 site at Fairbanks and the 6.5d and 6.11 sites at Palo Alto will channel their reports over the 6.11 HF radio network to one of their 6.11 Hawaiian stations for retransmission to the TU 8.1.3 Hickam AFB Headquarters. The Officer-In-Charge, Task Element 8.1.3.2, will evaluate all of these reports, summarize them, and then send a brief analysis to Commander, TU 8.1.3 on Johnston Island.

b. The southern Pacific loop will consist of the following stations and associated projects:

| LOCATION | PROJECTS |
|---|---|
| Aircraft from Samoa | 6.9 |
| Aircraft from Nandi | 6.10 |
| Acania | 6.8, 6.9 |
| Canton | 6.5a, 6.5c, 6.8, 6.11, 7.4 |
| Palmyra | 6.5a, 6.8. 7.2 |
| Rarotonga | 6.8, 6.11 |
| Tongatabu | 6.5b, 6.5c, 6.6, 6.8, 8A.2, 6.5a |
| Tutuila | 6.5a, 6.5b, 6.5c, 6.5e, 6.6, 6.8, 6.11, 8A.2, 7.4 |
| Viti Levu | 6.8, 6.10, 6.11, 8A.2, 7.4 |
| Christmas | 6.8 |

The projects located on Canton, Palmyra, Tongatabu, and Viti Levu will report to the Officer-in-Charge, Task Element 8.1.3.4 at Tutuila over the established AN/GRC-26D radios operated by Army Communications Teams. The remaining projects of the southern Pacific loop will utilize radios inherent to their scientific equipment. Net control will be exercised at Tutuila. The TU 8.1.3 South Conjugate Coordinations Officer (OIC TE 8 1.3.4) has the responsibility for receiving, evaluating, and summarizing these reports and retransmitting a brief analysis to CTU 8.1.3 on Johnston Island.

c. The Johnston Island area loop will consist of the following stations and associated projects:

| LOCATION | PROJECTS |
|---|---|
| Air Array: | |
| A-1 | 8A.1, 8A.2 |
| A-2 | 8A.1, 8A.2 |
| A-3 | 6.9 |
| A-4 | 6.9 |
| A-5 thru A-9 | 4.1 |
| A-10 thru A-12 | 7.4 |
| Ship Array: | |
| S-1 | 6.1a, 6.6, 6.8, 9.1b |
| S-2 | 6.1a, 6.6, 6.8, 9.1b |
| S-3 | 6.1a, 6.8 |
| S-4 | 1.1, 6.1a, 6.6, 6.8, 9.1b |
| S-5 thru S-8 | 6.5a, 6.8 |

| | |
|---|---|
| DAMP Ship | 6.8, 6.13 |
| Johnston | 1.1, 2.1, 2.2, 6.1a, 6.1c, 6.2, 4.1, 6.3, 6.4, 6.5a, 6.5d, 6.6, 6.7, 6.8, 6.9, 6.13, 7.2, 7.4, 8A.1, 8A.2, 8A.3, 8B, 9.1a, 9.1b, 9.4b, 9.5a, 9.6 |
| French Frigate Shoals (Tern) | 6.5c, 6.6, 6.8 |

(1) Shipboard projects will report over ship-to-shore radio net directly to CTU 8.1.3 on Johnston Island; French Frigate Shoals is included on this net.

(2) Projects aboard aircraft will report via the control aircraft (ABUSIVE), who in turn will report to the Johnston Island JCP. The TU 8.1.3 representative in the JCP will pass information to the TOC via hot line.

(3) Projects on Johnston Island will report over the island hard-wire communications system.

(4) This proposed breakdown of the TU 8.1.3 Scientific Reporting Net provides the optimum in speed and reliability. Communications centers have been notified to expect message requirements from the projects co-located with them. These centers can send and receive both classified and unclassified traffic.

5. SUNSHINE Reporting System.

a. Each project of TU 8.1.3 will be required to give periodic reports to CTU 8.1.3 on Johnston Island concerning the status of its particular scientific effort. Such reports are of extreme necessity to the Commander in order for him to make quick, intelligent, and knowledgeable decisions concerning the overall Task Unit's readiness to achieve the scientific objective of Operation FISHBOWL. To facilitate the transmission, handling, receipt, analysis, and comparison of these reports from many projects, this memorandum describes a uniform procedure to be followed by all agencies of Task Unit 8.1.3 using the scientific reporting net.

b. All operational readiness reports from each project are hereby designated SUNSHINE Reports. These reports will be transmitted to CTU 8.1.3 Johnston Island as directed by the appropriate Task Element Commander. Initial complete report will be submitted at times filter center communications are established with changes submitted as they occur and when requested by CTU 8.1.3. At H minus 6 hours reports will be submitted hourly indicating change in status. If no change occurs negative reports will be submitted.

c. All SUNSHINE reports will consist of four items. Item One will be the phrase SUNSHINE. Item Two will be the project number. Item Three will be the project status, using the reporting code outlined in paragraph 5d. Item Four, if needed, will be any necessary clarification of the report. SUNSHINE Reports will be UNCLASSIFIED in their entirety. Any necessary classified information will be transmitted via separate message.

d. To utilize the SUNSHINE Reporting System, the following code will be used to describe each project's degree of readiness (Item Three of the report):

(1) Status ALPHA. Project completely ready. This status report indicates that the station anticipates excellent results should the test occur at the scheduled time.

(2) Status BRAVO. Equipment and personnel in readiness, but local weather conditions will degenerate the results of this experiment approximately 25 percent.

(3) Status CHARLIE. Equipment and personnel in readiness, but local weather conditions will degenerate the results of this experiment approximately 50 percent.

(4) Status DELTA. Equipment and personnel in readiness, but local weather conditions prohibit this particular experiment from collecting any worthwhile data.

(5) Status ECHO. Equipment trouble, but only minor repairs are required that can be performed locally within six hours.

(6) Status FOXTROT. Equipment trouble, but only minor repairs are required that can be performed locally within six to twelve hours.

(7) Status GOLF. Equipment trouble, but only minor repairs are required that can be performed locally within 12 to 24 hours.

(8) Status HOTEL. Equipment trouble, but the repairs required can be performed locally in ____ days (this report will include the expected number of days until equipment will be back in operation).

(9) Status JULIETT. Major trouble with squipment, which will require parts and/or services from a rear area. This status report will include the piece of equipment involved, the parts and/or services required, the name of the rear area from which help is expected, and the name of the responsible person in that rear area.

(10) Status KILO. Personnel trouble. This status report indicates that some of the site's personnel are ill. However, sufficient knowledgeable persons are available to perform the work necessary to complete a valid experiment. This report will include the number of persons affected against the total number of knowledgeable persons assigned to the site, together with a brief description of the illness.

(11) Status LIMA. Personnel trouble. This status report indicates that sufficient illness exists at the site such that no valid data can be gathered. This is an emergency report and will include the same additional data as the KILO report plus all other pertinent details.

(12) Status MIKE. Indicates a lack of necessary support items, i.e., a power generator, an antenna stand, a reel of wire, etc., that will reduce the efficiency of the station. This status report will include a brief description of the item, when the item was scheduled to arrive, steps already taken to locate the item, and any other pertinent unclassified information.

(13) Status NOVEMBER. Indicates a situation that is not listed in the other SUNSHINE reports. This report will also require clarification, but only to the extent that unclassified information will be transmitted.

e. To make this reporting procedure more readily understandable, sample SUNSHINE Reports are as follows:

(1) SUNSHINE Project 8A.2 Status BRAVO.

(2) SUNSHINE Project 6.8 Status HOTEL 3 days.

(3) SUNSHINE Project 6.7 Status JULIETT. Tape recorder. Complete replacement required. Hickam AFB. J.J. Jones.

(4) SUNSHINE Project 6.6 Status KILO, 3 out of 10. Diarrhea.

(5) SUNSHINE Project 6.10 Status LIMA, 6 out of 7. Extreme skin infections. Locally hospitalized. Recovery two weeks. Replacement crew requested immediately.

(6) SUNSHINE Project 6.11 Status MIKE. 30 KW generator, 20 April. Wired to Lt Col Jones at Sandia Base 30 April. No reply.

(7) SUNSHINE Project 6.5c Status NOVEMBER. All food has spoiled. Request emergency shipment.

(8) SUNSHINE Project 6.5a Status NOVEMBER. Suspected sabotage in area. Details follow via classified message 252230Z.

(9) SUNSHINE Project 6.10 Status CHARLIE AND KILO, 3 out of 9. Extreme sunburn.

f. Normally, these messages will be transmitted with a priority precedence. A higher priority may be assigned if necessary. ALL SUNSHINE Reports sent subsequent to H−6 hours for an event will be given a precedence of Operational Immediate.

g. This reporting system is in effect upon receipt by each project. Queries concerning its implementation should be directed to the appropriate Task Element Commander.

Appendix H

REPORTS ON STATUS OF TECHNICAL AIRCRAFT

1. Test Director Memorandum 1-62 will be used to report aircraft status until the aircraft has become airborne for rehearsal or an actual event. A SUNSHINE report will be made for each participating aircraft, individually if other than Status ABLE, and collectively by projects if Status ABLE. Aircraft status (other than technical or scientific equipment) will be reported under Status MIKE. (TD 1-62)

2. Following takeoff, status reports will be submitted to the Aircraft Commander for transmittal to the Task Group 8.4 Air Operations Center in accordance with the following schedule:

a. As soon after takeoff as possible.

b. H-1 hour.

c. H-30 minutes.

d. On an "as necessary" basis when conditions change from the last report.

e. When any condition not provided for will affect the TU 8.1.3 scientific effort.

f. The degree of success will be indicated after event time (Status ABLE).

g. When aircraft departs station for landing point.

3. Status reports for airborne aircraft will be in accordance with the Attachment hereto. The reporting procedure will be as follows:

a. From the technical representative aboard the aircraft to the Aircraft Commander (AC).

b. From the AC via radio link to the TG 8.4 Air Operations Center (AOC).

c. From the AOC to TU 8.1.3 representative on the Iwo Jima (IJ).

d. From the IJ via radio link to the Technical Operations Center (TOC) in Bunker 405.

4. Reports will be unclassified and will consist of four items:

a. ITEM 1 - Aircraft call sign.

b. ITEM 2 - SUNSHINE.

c. ITEM 3 - Project status.

d. ITEM 4 - Clarification information.

NOTE: The only exception to the above will be for Project 8A.1 and 8A.2 aircraft. For these two aircraft, the words "point one or point two" will be used immediately following the aircraft call sign to identify whether the report concerns 8A.1 or 8A.2. The aircraft call sign, without this exception, will indicate both projects fall under the same report. Examples are:

Kettle One Point One. SUNSHINE ALPHA (8A.1).

Kettle Two Point Two. SUNSHINE CHARLIE (8A.2).

Kettle Two. SUNSHINE ALPHA (both 8A.1 and 8A.2).

5. It will not be necessary to identify the type report (H-1 hour, H-30 minutes, etc.) since time phasing of reports should indicate the type of report being submitted. Several status codes may be used in one report when necessary to adequately explain the conditions. In addition, two or more codes may be used, if necessary, to give the proper number. Examples are:

BRAVO CHARLIE adds to 75%.

ECHO FOXTROT adds to 30%.

VICTOR WHISKEY adds to 1 hour 30 minutes, etc.

6. To aid in clarification of the above procedures, the following examples are given (aircraft numbers and call signs may not be correct):

a. Inertia Two SUNSHINE ALPHA

Meaning: Project 7.4 on KC-135, #0341, ready to go and the aircraft is on the prescribed flight plan.

b. Kettle One Point One SUNSHINE CHARLIE

Meaning: Weather will degrade Project 8A.1 on KC-135, #3144, by about 50%.

c. Inertia Three SUNSHINE ECHO FOXTROT WHISKEY

Meaning: Project 6.10 on KC-135, #3131, is having equipment trouble so as to degrade data by 30%. Will require 60 minutes to remedy

d. Lambkin One SUNSHINE SIERRA ZEBRA

Meaning: Project 4.1 on RC-121, #0547, is having aircraft difficulties so as to degrade data by 25%. Will be unable to remedy while airborne.

e. Caboodle One One SUNSHINE ABLE 5

Meaning: Project 4.1 on C-118, #07651, obtained approximately 50% of their data.

ATTACHMENT TO REPORTS ON STATUS OF TECHNICAL AIRCRAFT

AIRBORNE SUNSHINE REPORTS

| Condition | Status Code | Criteria |
|---|---|---|
| Ready | ALPHA | Project is ready to go, to include positioning of the aircraft in accordance with flight plan. |
| Weather | | Weather will degrade data by: |
| | BRAVO | 25% |
| | CHARLIE | 50% |
| | DELTA | No worthwhile data will be collected. |
| Technical and scientific equipment | | Trouble with technical and scientific equipment will degrade data by approximately: |
| | ECHO | 10% |
| | FOXTROT | 20% |
| | GOLF | 40% |
| | HOTEL | 60% |
| | JULIETT | No worthwhile data will be collected. |
| Personnel | | Personnel are incapacitated so as to reduce data by: |
| | KILO | 25% |
| | LIMA | 50% |
| | MIKE | No worthwhile data will be collected. |
| Unique situation | NOVEMBER | Indicates a situation not covered in this report. Briefly describe trouble. This will cause a reduction in data of: |
| | OSCAR | 15% |
| | PAPA | 30% |
| | QUEBEC | 50% |
| Aircraft | | Aircraft trouble will cause the project data to be degraded by: |
| | ROMEO | 10% |
| | SIERRA | 25% |
| | TANGO | 50% |
| | UNIFORM | No worthwhile data will be collected. |
| Time required to repair or remedy the condition | | The time required to repair or remedy the situation so that essentially all data can be obtained will be: |
| | VICTOR | 30 min. |
| | WHISKEY | 1 hour |
| | X-RAY | 2 hours |
| | YANKEE | 4 hours |
| | ZEBRA | Unable to repair or remedy the situation while airborne. |
| Success of mission | | The approximate percentage of data obtained is as follows: |
| | ABLE 1 | 10% |
| | ABLE 2 | 20% |
| | ABLE 3 | 30% |
| | ABLE 4 | 40% |
| | ABLE 5 | 50% |
| | ABLE 6 | 60% |
| | ABLE 7 | 70% |
| | ABLE 8 | 80% |
| | ABLE 9 | 90% |
| | ABLE 10 | 100% |

Appendix 1

MINIMUM GO-NO-GO CRITERIA, SHOT BLUE GILL

This material was published by TU 8.1.3, 9 October 1962.

WEATHER

1. Cloud Cover.

a. Excellent "seeing" conditions are desired for Johnston Island photo station and the two KC-135 photo aircraft for the period shot time to about H + 30 minutes. At Johnston Island, recommend BLUE GILL be attempted only on days when no more than light high clouds and $^3/_{10}$ or less low and medium clouds are predicted during the firing window. This would provide good chance for success for Johnston Island surface optical stations. Aircraft should have little high cloud above their operating altitude (about 35,000).

b. DAMP ship, Project 6.13, need optical line of sight to flares expelled from their rockets. This requires a condition of very few clouds essentially along the line between the ship and shot point at elevation angles of 20 to 70° from the horizon. Fulfillment of DAMP ship requirement is not mandatory.

2. Ballistic Wind.

a. Launchers are adjusted based on ballistic wind reports available at H-75 minutes. If subsequent reports show ballistic wind changes greater than 5 knots or 15 degrees, holds as follows are necessary to adjust launchers for safety reasons: (1) at H-45 min - - - - Hold 30 Minutes. (2) at H-35 minutes - - - - Hold 30 minutes. (60 minutes if weather Pibal crews not permitted to stay out until H-30 minutes.)

b. There are infrequent wind conditions which would prevent Project 6.1a rockets from following desired trajectories. This could be a no-go condition. These conditions are described in a separate paper.

3. Magnetic Storms.

Project 6.9 (SRI) will obtain and provide forecast of magnetic storms. If major storm predicted, this is a no-go condition.

PODS

4. Tracking. Must have Sandia Corporation and Cubic on B-3. Check made at H - 30 minutes and H - 17 minutes.

5. Stabilization. Must have 2 of 3 pods. Check at H - 17 minutes.

6. Recovery. The two pods with stabilization OK must have recovery packages OK. Check pod recovery unit pressure at H-4 hr.

ROCKETS

7. 6.1A Radar Blackout. Project uses six rockets fired essentially in pairs (-195 and -190 seconds; -112 and -108 seconds; + 290 and + 900 seconds). One rocket of each pair must be in an operating condition and this will be known by H-5½ hours. Cubic tracking must be go on these rockets as well. Final check at H-45 minutes. In addition, a minimum of three of the four ships, the JI x-band receiver, and the JI L and C band interferometers must be operating.

8. 6.2, 6.3 Gamma Scanners and D-region Physical Chemistry.

a. Project has 8 rockets:

| | Primary Experiment |
|---|---|
| 2 Nike-Cajun | Mass spectrometer |
| 4 HJ-Nike | Electron density radiation measure |
| 2 HJ-Nike-Nike | Gamma scanner |

b. Project needs six rockets, one HJ-N-N and five others, with experiment essentially ready. These six rockets need one telemetry and one tracking system in order. Honest John-Nike rocket experiments are considered go as long as one measurement of electron density and one of radiation are ready. Operation of every instrument is checked at H−8 hours and again between H−90 minutes and H−65 minutes. Correction of problems inside bird take at least 24 hours.

9. 6.13 Radar Refraction Jitter (H−4 hours).

Three of the four Nike Apaches must have C-band beacons operating and must be tracked by DAMP Ship radar (5700 Mc). Optical track of rockets from DAMP Ship is desirable. (See weather.)

COMMUNICATIONS

10. 3 of 4 Granger transmitters, Kauai, Okinawa, Kwajalein, and Canton must be going, and 6 of 8 receivers should be operable and synchronized.

RADAR CLUTTER

11. 88-foot SRI dish must be operable. One each RC-121 aircraft and equipment must be in position and ready in the Northern and Southern Conjugate Areas.

12. Sufficient ionosondes, riometers, photometers, etc., exist so that no particular go-no-go criteria is applicable here.

AIRBORNE IONOSPHERIC MEASUREMENTS

13. Readiness of 6.10 aircraft and equipment is desirable but not mandatory.

PHOTOGRAPHY-SPECTROSCOPY

14. Surface Stations. Appropriate cloud conditions necessary (see weather). Sufficient backup in surface stations measurements exists between LASL and DOD so that go-no-go are based on cloud conditions alone, except for major catastrophes affecting both LASL and DOD surface stations.

15. Aircraft. At least one DASA KC-135 must be in position and ready to record.

Appendix J

## OPERATION EXPERIENCE SUMMARY, ENGINEERING AND CONSTRUCTION

(This report was prepared by an officer in the E&C Branch, TU 8.1.3.)

This report concerns areas of responsibility including: (1) criteria developments and design of facilities for Johnston Island and all other sites, and (2) construction at all other sites. All other areas are summarized by those primarily responsible.

As soon as construction and facility requirements could be determined, site selection on Johnston Island was coordinated with representatives from all users, AEC, H&N, and JTF-8. H&N acted as the overall coordinator and provided all members with a current scientific plot plan. This system was satisfactory because it funneled all requirements to a single point where scientific requirements, interference, restrictions, and construction feasibility could be analyzed. Later, TG 8.6 insisted on having this responsibility, but the larger portion of siting was completed and only minor consequences developed. Since Johnston Island is so small, the limited real estate available required maximum utilization of existing facilities, minor degradation on some experiments because of interference, and calculated safety risks.

It was necessary to make many long-distance telephone calls, trips, and inquiries to extract the details from the scientific agencies to insure that each facility was in the best possible location. Concurrently, construction criteria were being developed at a rapid pace and submitted to AEC, (TG 8.5) for H&N action.

In many cases where construction lead time was critical, design was started before the project submitted an E&R plan. Criteria were developed from Annex E of the E&R plan and from revisions, conferences, and telephone calls. The criteria for rocket launch pads were written in general terms, and the design details were resolved by meeting with the launcher manufacturers and the H&N Project Engineer. This procedure was highly satisfactory and proved itself in the timely construction and dual use of launchers by more than one project agency.

Requirements for sites other than Johnston Island were late and frequently changed because of: (1) late diplomatic approval on the use of foreign owned islands, (2) scientific and logistic suitability of available islands, (3) lack of the project's decision to request H&N support because of funding problems (to be explained later), (4) lack of firm control over projects to force timely decisions on requirements, or (5) lack of information concerning construction and logistic capabilities locally available at selected islands.

Project and TU 8.1.3 representatives made a survey trip to sites under consideration. The results varied from firm commitments and plans by some projects to indecision by other projects. Because of limited time and costs, every attempt was made to minimize H&N construction and support. Construction by local sources was arranged at Rarotonga, Viti Levu, Tongatabu, Tutuila, Canton, Wake, Midway, Kwajalein, Okinawa, Kauai, Maui, and Hawaii. If all requirements had been placed on H&N, the costs would have been prohibitive and the readiness time would have been extremely doubtful. Furthermore, the local governments preferred not to have outside contractors, so that their own economy could benefit. There was also a concern about inflation, which would have been quite harmful to the small communities.

Generators proved to be the most troublesome items. Projects that originally planned to furnish their own power later required generators at remote locations on a crash basis. Many generators malfunctioned because of improper maintenance, improper switching on of the load before warmup, lack of load banks on generators with loads that were too small, and inferior design. Time would not permit major repairs, so replacements were used. Most projects had backup generators toward the end of the operation.

Land leases were the responsibility of TG 8.5; however, it was necessary in most cases to anticipate TG 8.5 negotiations and to make preliminary agreements for consummation by TG 8.5 at a later date. Land leases at Tutuila, Samoa were the most difficult to handle, because the property is jointly owned by the natives. In one case, 42 owners were involved at the Olotele Hill site without adequate land survey and descriptions. This was handled through the American Samoa Government Attorney General who negotiated through a "talking chief" who represented all of the owners. Leases in the future should be easier to obtain on Samoa because of the experience gained by all parties.

Construction activities at remote sites involved access roads, land clearance, instrument shelters, placement of vans, generators and fuel storage, and antenna erection. In camps, the activities involved walk-in reefers, water distillation plants, powerplants, septic tanks, tent messhalls, kitchens, latrines, and quarters.

On-site surveillance was essential during the construction, to meet readiness dates. Off-site H&N construction was late in the field, because user requirements were late as were consequently, the criteria. Field trips disclosed major deficiencies such as working crews in place without materials and tools or vice versa. The deficiencies were itemized and given to the H&N and AEC, Honolulu manager for crash action. Followup field trips were still necessary to insure that corrective action had been taken.

In future operations, a completely mobile concept for islands, other than Johnston, should be adopted, and construction should be held to a minimum. The support contractor could design and procure trailers to serve all test needs at any test site. The trailers should be four-wheeled types and have simple-tongue hitch, leveling jacks, and dimensions compatible to C-124, C-133, and other transport aircraft. The trailers should be of the following types: water distillation, powerplant, maintenance (generator, plumbing, carpenter), living, kitchen, messing, laundry, and scientific.

In future operations, more time should be allowed for criteria development and construction. Strong program management should be exercised to insure timely submission of requirements and to minimize change. Local resources should be used for construction in remote areas.

Appendix K

## EXPERIENCE REPORT, PROJECT 9.2, SHIP MODIFICATION

(This report was prepared by an officer in the E&C Branch, TU 8.1.3.)

TU 8.1.3 received the Fish Bowl program from CHDASA in late December 1961. Included in the Fish Bowl instrument locations were five positions on the high seas to be occupied by surface ships. The E&C Branch was assigned the responsibility of modifying these ships to receive the scientific instrumentation.

Since this ship modification project was a somewhat new E&C responsibility and because very little history and data from previous ship modification projects (premoratorium) was on record in WET, this experience report is submitted to document the background, procedures, and problems encountered in the Fish Bowl project. It is hoped that this information together with recommendations based on experience from this project will enable personnel assigned to any future operations to conduct the project more efficiently and smoothly. In addition to improving the next operation and aiding the personnel assigned to it, the information contained in this report may serve as a guide for picking qualified personnel for assignment to any future project.

The body of this experience report consists of a history of the ship modification program with emphasis on problems encountered, the solutions thereto, and/or recommendations for future operations. It should be noted that this report alone cannot possibly give a complete chronological history of Project 9.2. Anyone desiring to study the project in detail should use this report in conjunction with the complete E&C Project 9.2 files.

Early in January 1962, E&C called a meeting in Washington to discuss general policy and to get the first indication of what the projects required. Representatives of BUSHIPS, MSTS, JTF-8, FCDASA, NAVY OPS, H&N, and the projects were present. At that time it was decided that all technical construction requirements of the projects would be submitted to the E&C Branch, which would review, coordinate, and consolidate them for later submission to either BUSHIPS or COMSTS, depending upon the ships involved. (Five belonged to US Navy and one to MSTS.) BUSHIPS would decide in which yard the modifications were to be performed and authorize the yards to proceed. Thus, WET dealt with BUSHIPS rather than the yards during the early planning stages. COMSTS turned its portion over to MSTS PACAREA, which performed the design work and then let a contract to a civilian yard for the actual modifications. H&N was acting as architect-engineer for LASL and LRL for some modification work (later canceled when Christmas Island became available). H&N was represented at the first meeting at the request of WET. During this meeting, after the general scope of the program became known, WET decided that it would deal directly with the Navy and MSTS and would not require the services of an outside architect-engineer.

Shortly after the first meeting, six ships were assigned as the Fish Bowl instrument platforms. Assignment of ships was worked out between JTF-8 and the Navy with DASA supplying only technical recommendations.

The scope of work to be done was finally determined to be installation of antennas, photography equipment, and associated recording instrumentation on three LSD's, one LST, and two DDE's. LSD's were selected because of their relative stability. Original plans called for launching of small instrument rockets from the ships. This plan was dropped, but the stable platforms were still required by the Project 6.1a tracking antennas.

Following the first meeting in Washington, the E&C Branch started the all-out effort to obtain final criteria from the project agencies. After weeks of meetings, personal contact, telephone calls, TWX's and shipboard and shipyard visits, enough data was obtained to write a formal criteria letter to BUSHIPS and MSTS setting forth the details of work to be accomplished. It should be noted that the E&C staff must take the initiative of calling such meetings, and making trips, especially if a short time frame is involved. The person assigned to ship modification cannot expect information to come rolling in without doing a lot of coordinating, traveling, and inspecting. Shipboard trips and meetings with the design personnel of shipyards proved extremely profitable. Most of the projects had not been associated with ships at all so every chance to get aboard was most valuable to them. E&C did all coordinating of these inspections. During the planning stages, the shipboard visits were the most important single item for determining instrumentation location and mounting.

Following criteria collection, a comprehensive criteria letter was sent to BUSHIPS and COMSTS. This letter was all-inclusive, contained all known requirements, and was supplemented with numerous drawings and sketches. E&C stated the requirements, but left all design work and finish blueprints to the shipyard design staff. The shipyards were extremely happy with the criteria letter because of its completeness. In any future operation, every effort should be made to give all requirements under one cover, and all agencies involved should receive information copies.

Funding for the modifications was through BUSHIPS and COMSTS. They received estimates and bills from their respective yards and submitted a final bill to FCDASA.

Upon receipt of the FCDASA criteria letter, BUSHIPS assigned yards to perform the work. Two LSD's were modified at the Naval Repair Facility, San Diego, and the LST and two DDE's were modified in Pearl Harbor. MSTS let a contract to a civilian yard in San Francisco for modification of one LSD. The various yards did their own design work; thus, three separate, different sets of designs and plans resulted. The E&C project officer approved all plans and coordinated them with the project agencies. During the actual modification period at the shipyard, the E&C officer acted as coordinator between ship, shipyard, JTF-8, project agency, and TU 8.1.3. He also inspected all work, directed shipyard effort, and acted as a pusher to get things moving faster. In this area, more rank (LCDR or higher) would be very helpful. Although everyone cooperated, the author believes it would have been beneficial if a Navy captain from TU 8.1.3 had met with the directors of the yards concerned and discussed the program and explained the tight time schedule and the built-in uncertainties of the testing game.

Since the work was performed at three different installations, it meant the E&C man had to move between them to supervise all the jobs. This arrangement worked satisfactorily, because the Pearl Harbor work was scheduled after the West Coast work; however, if the program had been any larger, one man could not have handled it alone. It is highly desirable to have all the work done at one location, and in the future, every effort should be made to have one set of drawings and one yard do the work.

Shipyards are very complex and highly subdivided organizations. It is impossible to find one individual who can handle all problems that arise. Design people will not touch anything after it leaves the drawing board; workers blame design, destroyer planning people will not have anything to do with LST's, etc. Three identical stations have three separate work orders written if they happen to be on different types of ships. Since the yard is so complex, it is the author's belief that the ranking man at the shipyard should be approached by comparable rank in TU 8.1.3 and request that a yardman be assigned to the test modification work only. The officers in the shipyards are generally overworked and by necessity cannot devote enough time to the out-of-the-ordinary work required by the test program. This is especially true of the ship's superintendent. All were most helpful and cooperative, but the additional work imposed on them over and above their regular duties worked a hardship on them. It is realized people are hard to get, but proper high-level meetings should result in getting a man from the yard assigned to the special task of test modification.

During the planning, design, and actual shipboard modification work period, the E&C project officer was the only man connected with the testing program who came in contact with the yard or ship's personnel. There was a definite lack of communication or contact between JTF-8 (The Navy Task Unit) and the yard or ship's force. The personnel of the yard and the ship were naturally concerned with basic questions and operational matters. The captains of the ships were kept in complete darkness until the last moment. They were quite concerned about this lack of information and continually hounded the only one they knew from the test organization, the E&C man. Thus, the E&C man spent considerable valuable time trying to assist the skippers in getting answers to operational and logistic questions. Lack of answers to these questions also delayed modification work. For example, antennas could not be placed until it was determined if areas must be left clear for helicopters, etc. In any future operation, an effort should be made to have more lower level coordination between WET Operations Branch and the ship's company. Also, the Navy Task Unit and JTF-8 should keep the ships better informed. The E&C man cannot properly watch out for his modification work if he spends 50 percent of his time doing operational work.

One major problem concerned generation of power for the instrumentation. Since the ships had dc and the test equipment required ac, diesel generators were provided to supply power. This was acceptable because the operation, as originally planned, was to last only 6 to 8 weeks. As it turned out, the generators were operated and exposed to the elements for 6 to 8 months. They finally began to break down. In future operations, motor generators working off ship's power should be used if possible because of the unpredictable time duration of the tests.

Recording instrumentation was installed in both ship's compartments and in fabricated wooden structures fixed to the deck. The fixed wooden shacks proved to be far superior to the ship's compartments. They are easier to build, easier to alter for equipment mounts, easier to air condition, and cause less trouble to the ship. In the long run, it is much cheaper to build a wooden shack to the required design than to try to alter a steel compartment.

Rollup or removal of scientific instrumentation poses no problem, because the yard can simply be told to remove everything previously installed and return the ship to its original configuration. The projects will look out for their gear, and the ship's officers will naturally make sure their ship returns to its original condition, if not better.

Although there were numerous minor problems and a lot of crash efforts involved, all of the ships were instrumented satisfactorily and on schedule.

The following recommendations are based on the experience during Fish Bowl:

(1) In the task unit, a Navy officer should be in charge of ship modification.

(2) The officer should be a LCDR if the modification program is any larger than that for Fish Bowl.

(3) Submit good final criteria to the designers. Whenever practicable, delay submission until all criteria are compiled.

(4) To establish criteria, the officer should visit ships and yards to get information about instrument placement and location.

(5) Do everything possible to have all design and modification work done by one yard, not several.

(6) Wherever possible, avoid using ship's compartments for recording spaces. Use deck-mounted trailers or wooden shacks.

(7) Have one designer and one ship superintendent from the yard assigned to the test program work only.

(8) Have operations personnel maintain better liaison with the ships to avoid time-consuming questioning by skippers.

(9) Avoid use of portable diesel power generators whenever possible.

Appendix L

## EXPERIENCE REPORT, ENGINEERING AND CONSTRUCTION, JOHNSTON ISLAND

(This report was prepared by an officer in the E&C Branch, TU 8.1.3.)

### Preliminary Operations.

(1) The E&C representative should become familiar with project operations in general prior to arriving at site.

(2) The E&C job-site representative must know space requirements in detail. Stated space requirements from Annex E of E&R Plans proved invalid in most cases; some were too large, others too small. In general, projects require more space than allocated.

(3) In preliminary planning, avoid user-furnished material whenever practicable. Define clearly who is to furnish material—especially, the electrical instrument, timing, and similar cable.

(4) Have E&C representatives at jobsite in advance of starting construction. This helps establish good relationship with the architect-engineer (A-E) representatives and allows E&C personnel to become familiar with A-E personnel and their methods of operation.

(5) Avoid being overly austere on headquarters and similar facilities. Items such as soundproofing and air conditioning may prove to be necessities and must then be installed later. This later method is expensive and not completely effective.

(6) Try to establish realistic beneficial occupancy data (BOD's). During this series, no event was delayed because of construction; however, many BOD's were exceeded by 2 weeks or more.

(7) Plan to place all buried cable (cable trenches) in a conduit to protect them from corrosion, shrinkage, and coral wear.

(8) Plan to have a small-sized ozalid machine for E&C use.

### Construction Operations.

#### Prior to arrival of projects.

(1) Periodic visits by a representative of programs is helpful during this period.

(2) Without exception, power requirements stated in E&R plans for Fish Bowl were understated. Power facilities should be designed to handle at least 50 percent more load than is requested for the primary sites, e.g., Johnston Island.

(3) Junction boxes and wiring for trailers at the primary site should not be installed until arrival of trailers. In most cases during Fish Bowl, users wanted to change positions, and the stated power requirements differed from what was required.

(4) On all major construction items, a user representative should be at each jobsite when construction begins.

(5) Have the A-E send copies of all drawings, sent for approval, to the E&C representative at the job site. These drawings should be marked "For Approval".

#### After arrival of projects.

(1) Expect numerous changes and/or new requirements. All of these can be expected to be accomplished on a crash basis.

(2) Modifications and repair of user-furnished material will consume a disproportionate amount of time and effort.

(3) At the primary site, provide a pool of portable power units ranging from 10 to 100 kw. Recommend numbers and types as follows: six 10-kw, four 15-kw, ten 30-kw, six 60-kw, and two 100-kw. At other sites, provide 100-percent backup power.

(4) At the primary site, provide a pool of construction equipment and operators for field support purposes. Types and amounts must be based on stated requirements for field support but should include at least five forklifts.

(5) At the primary site and AEC contractor locations only, provide a means of easy communication on details of user requirements developed at jobsite. Use of mail-order catalogs or similar documents is recommended.

Appendix M

## INSTRUMENTATION FOR MEASURING COMMUNICATIONS EFFECTS

TABLE M.1 VLF PROPAGATION INSTRUMENTATION

| Frequency kc | Transmitter | Project/Sponsor | Receiver Sites |
|---|---|---|---|
| 6 | Noise | 6.11 | Hawaii, Wake, Viti Levu, Canton, Tutuila, Johnston, Kwajalein |
| 6 | Noise | NOL, Corona (7.5) | Corona |
| 10.0 | Noise | NOL, Corona (7.5) | Corona |
| 10.2 | Balboa, C.Z. | 6.11 | Kwajalein |
| 10.2 | Balboa, C.Z. | NEL, San Diego (7.5) | San Diego, Pt. Barrow, Forrest Port, N.Y., Thule (omega navigation system) |
| 10.2/14.2 | Oahu | 6.11 | Kwajalein |
| 13.0 | Arizona | NEL, San Diego (7.5) | GU Komelik, Castle Dome, Somerton, (13-kc ionospheric sounder system) |
| 14.7 | NAA (Maine) | NOL/NEL (7.5) | Corona/San Diego |
| 15.0 | Noise | NOL, Corona (7.5) | Corona |
| 16.0 | GBR (England) | 6.5b | Tutuila, Tongatabu |
| 16.0 | GBR (England) | NBS, Boulder | College Alaska |
| 17.4 | NDT (Japan) | NOL, Corona (7.5) | Corona |
| 18.0 | NBA (Canal Zone) | 6.5b | Tutuila, Tongatabu |
| 18.0 | NBA (Canal Zone) | 6.11 | Maui, Fairbanks, Hawaii, Palo Alto, Rarotonga, Okinawa, Tutuila, Viti Levu, Wake, Kwajalein, Midway, Canton |
| 18.0 | NBA (Canal Zone) | NBS/NEL (7.5) | Boulder, College Alaska, Maui/San Diego |
| 18.6 | NPG (Seattle) | NBS, Boulder | Boulder, College Alaska |
| 18.6 | NPG (Seattle) | NOL/NEL (7.5) | Corona/San Diego |
| 19.8 | NPM (Hawaii) | 6.10/6.11/7.4 | Palo Alto, Wake, Tutuila, Maui |
| 19.8 | NPM (Hawaii) | NBS, Boulder | Boulder, College Alaska, Midway |
| 19.8 | NPM (Hawaii) | 6.5b | Tutuila, Tongatabu |
| 19.8 | NPM (Hawaii) | NOL/NEL (7.5) | Corona/San Diego |
| 21.0 | WWVL (Boulder) | NBS, Boulder | Fort Collins, Colorado (one-hop vertical path) |
| 21.0 | Noise | NOL, Corona (7.5) | Corona |
| 22.3 | NSS (Annapolis) | NBS/NEL (7.5) | Boulder/San Diego |
| 27.0 | Noise | 6.11 | Hawaii, Wake, Viti Levu, Canton, Tutuila, Johnston, Kwajalein |

TABLE M.2 LF PROPAGATION INSTRUMENTATION

| Frequency kc | Transmitter | Project/Sponsor | Receiver Site |
|---|---|---|---|
| 46 | 10-kw airborne (KC-135) vicinity Johnston Island, 9000-foot antenna | 7.4 | Kwajalein, Canton, Viti Levu, Tutuila, Palo Alto, Fairbanks, Auburn, Wichita, Dayton, Midway, Wake, Hawaii, Johnston |
| 46 | 10-kw airborne (KC-135) vicinity Johnston Island, 9,000-foot antenna | 6.11 | Kwajalein, Canton, Viti Levu, Tutuila, Palo Alto, Midway, Wake |
| 49 | Noise | 7.4 | Hawaii, Auburn, Dayton (BG and CM only) |
| 51 | Noise | 6.11 | Hawaii, Wake, Viti Levu |
| 76 | Johnston Island | USN | Hickam (balloonborne antenna at Johnston) |
| 100 | Loran-C | 6.10 | Oahu, Palmyra, Maui, Kauai, southern conjugate aircraft |
| 120 | Noise | 6.11 | Hawaii, Wake, Viti Levu |
| 155 | Guam (Ratt) | 7.6 | Hawaii, Japan, Ships |
| 185 | Honolulu (Ratt) | 7.6 | Guam, Adak, Ships |
| 200 | Noise | 6.11 | Hawaii, Wake, Viti Levu |

TABLE M.3 HF PROPAGATION INSTRUMENTATION

| Frequency Mc | Transmitter | Project/Sponsor | Receiver Site |
|---|---|---|---|
| 4 to 64 | Granger (Okinawa) | 6.11 | Viti Levu, Tutuila, Rarotonga, Hawaii, Palo Alto, Fairbanks |
| 4 to 64 | Granger (Kwajalein) | 6.11 | Viti Levu, Tutuila, Rarotonga, Hawaii, Palo Alto, Fairbanks, Midway, Wake |
| 4 to 64 | Granger (Canton) | 6.11 | Viti Levu, Tutuila, Rarotonga, Hawaii, Palo Alto, Fairbanks, Midway, Wake |
| 4 to 64 | Granger (Kauai) | 6.11 | Rarotonga, Wake, Midway, Fairbanks, Palo Alto, Kwajalein, Tutuila |
| 4 to 64 | Granger (Midway) | 6.5a | Palmyra (one-hop reflection point over Johnston) |
| HF Operational Circuit | Melbourne | DCA/ACSD/USASRDL | Camp Davis |
| | Okinawa | DCA/ACSD/USASRDL | Hawaii |
| | Tokyo | DCA/ACSD/USASRDL | Hawaii, Camp Davis, Anchorage |
| | Anchorage | DCA/ACSD/USASRDL | Hawaii, Camp Davis |
| | Seattle | DCA/ACSD/USASRDL | Anchorage |
| | Australia, Canton, Wake | 7.4 | Hawaii |
| | Kwajalein, USA | 7.4 | Hawaii |
| 4.7, 9, 15, 23 | March AFB | 7.4 | Hawaii, Johnston, Kwajalein, two aircraft vicinity Johnston |
| 4, 6, 9 | Tongatabu | 6.5b | Samoa (3-frequency phase-stable link) |
| 12, 18, 30 | Pinwheel (Kauai) | 6.5c | Okinawa, Adak, Palo Alto |
| HF operational Ratt | Fleet broadcast | 7.6 | Selected US Navy ships |
| 10, 15, 20 | Midway | 6.10 | Southern conjugate KC-135 aircraft, Palmyra, Fiji |

TABLE M.4 HF SOUNDERS

| Frequency Mc | Project/Sponsor | Equipment | Location |
|---|---|---|---|
| 5 to 26.5 | USAF | Backscatter | Australia, Alaska, Puerto Rico, Roswell, Hawaii, Maryland, Pakistan |
| 9.8 and 12.6 | ARPA | Backscatter | Palo Alto |
| 1 to 25 | 6.5d | Vertical ionosonde | Johnston, Kwajalein |
| 0.25 to 20 | 6.5c | Vertical ionosonde | Maui, French Frigate Shoals, Tutuila, Wake, Canton |
| 1 to 25 | 6.5c | Vertical ionosonde | Midway, Tongatabu |
| 1 to 25 | 6.5a | Vertical ionosonde | Palmyra, Trinidad |
| 1 to 25 | 6.10 | Ionosonde | KC-135, Fiji |
| 3 to 30 | 6.9 | 7-frequency HF-sounding radar | M/V Acania |
| 3.3 to 50 | 6.9 | 7-frequency phase-path sounder | Johnston |

Appendix N

## INSTRUMENTATION FOR MEASURING RADAR EFFECTS

### TABLE N.1 RADAR NOISE INSTRUMENTATION

| Instrument | Project | Frequency | Antenna | Sensitivity | Location |
|---|---|---|---|---|---|
| | | Mc | | | |
| Radiometer | 7.2 | 35,000 | Parabolic 0.6° beam | T = 1°K | Johnston Island |
| Radiometer | 7.2 | S-band | Parabolic 3° beam | T = 3°K | Johnston Island |
| Radiometer | 7.2 | L-band | Array 10° × 20° beam | T = 5°K | Johnston Island |
| Radiometer | 6.13 | 442 | Parabolic 6° beam | NF = 5 db | USAS American Mariner |
| Radar | 6.9 | 1210 | Parabolic 0.7° beam | NF = 5 db | Johnston Island |
| Radar | 6.9 | 850 | Parabolic 1° beam | NF = 3 db | Johnston Island |
| Radar | 6.9 | 398 | Parabolic 2° beam | NF = 3 db | Johnston Island |

### TABLE N.2 RADAR CLUTTER INSTRUMENTATION

| Frequency* | Project | Peak Power | Antenna Beam Width | Band Width | PRF | Location |
|---|---|---|---|---|---|---|
| Mc | | kw | deg | | | |
| 5825 | 6.13 | 3,000 | 0.8 | 2 Mc | 285 | USAS American Mariner |
| 1300 | 6.13 | 2,000 | 2 | 1.2 Mc | 285 | USAS American Mariner |
| 1210 | 6.9 | 30 | 0.7 | 6 Mc | 75 | Johnston Island |
| 850 | 6.9 | 35 | 1 | 6 kc | 75 | Johnston Island |
| 530 | 6.13 | 5,000 | 1 by 4 | — | 150 | Kwajalein (ZAR) |
| 425 | 6.13 | 5,000 | 2 | — | 1100 to 1500 | Roi Namur (Tradex) |
| 432 | 6.13 | 2,000 | 6 | 1.2 Mc | 285 | USAS American Mariner |
| 426 to 443 | 6.9 | 1,500 | 10 by 18 | 200 kc | 250 | Five RC-121-D aircraft |
| 398 | 6.9 | 35 | 2 | 6 kc | 75 | Johnston Island |
| 370 | 6.9 | 20 | 5 | 6 kc | 30 | M/V Acania |
| 140 | 6.9 | 50 | 13.5 | 6 kc | 30 | M/V Acania |
| 32.5 | 6.9 | 100 | 45 | 6 kc | 30 | M/V Acania |
| 3 to 19.5 | 6.9 | 7 to 30 | 60 to 90 | 10 kc | 8.6 to 30 | M/V Acania |
| 3.3 to 50 | 6.9 | 7-frequency phase-path sounder | — | — | — | Johnston Island |
| 27 | 6.9 | 1.8 | Sensitivity 9.5 mv | — | 12.5 to 50 | Canton Island |

* Approximate or nominal.

TABLE N.3 RADAR REFRACTION INSTRUMENTATION

| Frequency * Mc | Project | Transmitter | Receiver |
|---|---|---|---|
| 5775 | 6.13 | Nike-Apache rocketborne 400-watt peak power transponder. 5700-Mc receiver. | AN/FPQ-4 precision monopulse tracking radar on DAMP ship. |
| 4750 | 6.1 | Nike-Cajun (Blue Gill and Tight Rope) Nike-Apache (King Fish) rocketborne 5-watt CW transmitter. | Interferometer array on Johnston Island. |
| 950 | 6.1 | Nike-Cajun (Blue Gill and Tight Rope) Nike-Apache (King Fish) rocketborne 5-watt CW transmitter | Interferometer array on Johnston Island |

* Approximate or nominal.

TABLE N.4 DIRECT ATTENUATION MEASUREMENTS

| Frequency * Mc | Project | Shot Participation | Transmitter | Receiver |
|---|---|---|---|---|
| 9500 | 6.1 | Blue Gill, King Fish, Tight Rope | Rocketborne 5-watt CW (4 to 6 per event) | Johnston Island and Ships S-1 through S-4 |
| 5775 | 6.13 | All | Rocketborne 400-watt peak power transponder (1 to 7 per event) | AN/FPQ-4 precision Monopulse tracking radar on DAMP ship |
| 4750 | 6.1 | Blue Gill, King Fish, Tight Rope | Rocketborne 5-watt CW (4 to 6 per event) | Johnston Island and Ships S-1 through S-4 |
| 950 | 6.1 | Blue Gill, King Fish, Tight Rope | Rocketborne 5-watt CW (4 to 6 per event) | Johnston Island and Ships S-1 through S-4 |
| TM band | 6.2, 6.3, 6.4 | Star Fish, Blue Gill, King Fish | Satellite and rocketborne telemetry including GMD (1660 to 1690 Mc) and 137.148- and 388-Mc beacon) | Amplitude of these signals measured by receivers on Johnston Island |

* Approximate or nominal.

TABLE N.5 INDIRECT ATTENUATION MEASUREMENTS

| Frequency* | Project | Shot Participation | Data |
|---|---|---|---|
| Mc | | | |
| 150<br>400 | 6.13 | All | Electron line density from doppler measurements on signal from transit satellite. Approximately 20 passes recorded per event on Damp ship. |
| 54<br>324<br>(phase coherent) | 6.2 | All | Electron line density from doppler, dispersive doppler and faraday rotation on signals from Transit IIA, Transit IVA, and Anna. Data recorded at Johnston Island and Aberdeen Proving Ground. |
| 37<br>148<br>888<br>(phase coherent) | 6.2, 6.3 | Star Fish, Blue Gill, King Fish | Electron line density from doppler, dispersive doppler, and faraday rotation on signals from rocketborne 3-frequency phase-coherent beacon. Six rockets per event were monitored from Johnston Island. |
| 3<br>12 | 6.3 | Star Fish, Blue Gill, King Fish | Electron density from measurement of RF impedance of rocketborne antennas. Two to four rockets per event, monitored from Johnston Island. |

* Approximate or nominal